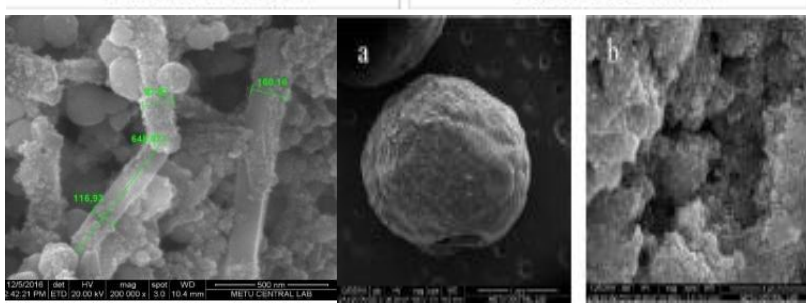
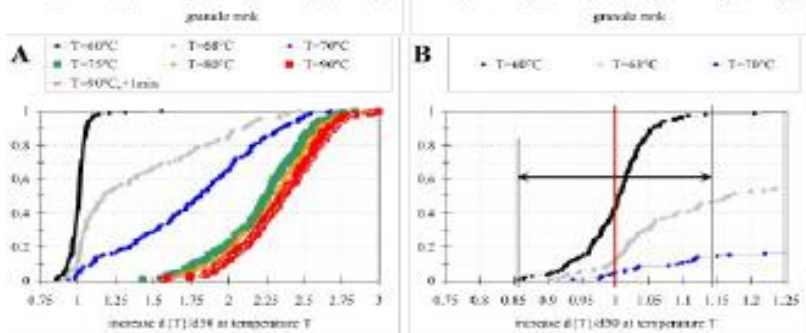
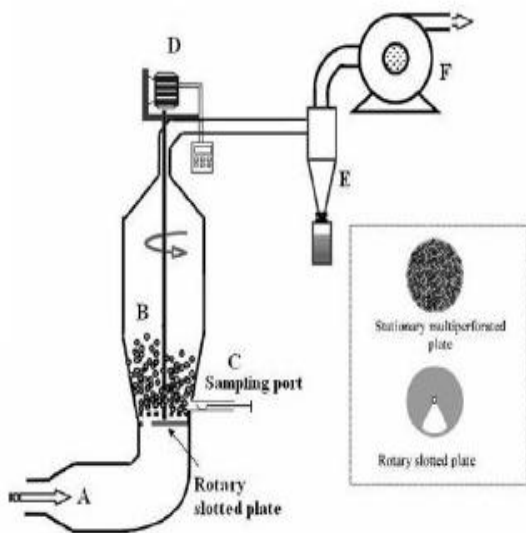
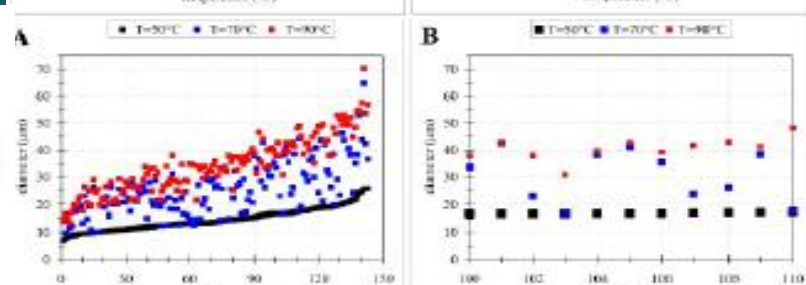
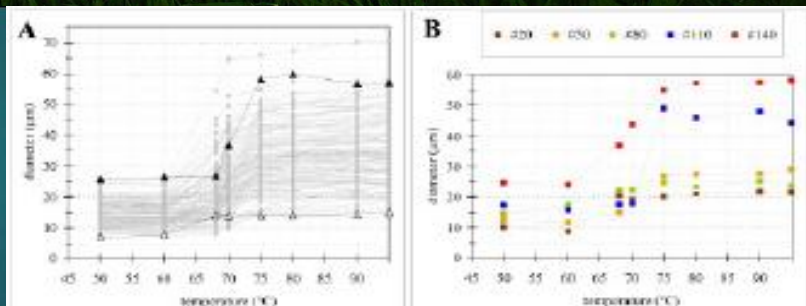
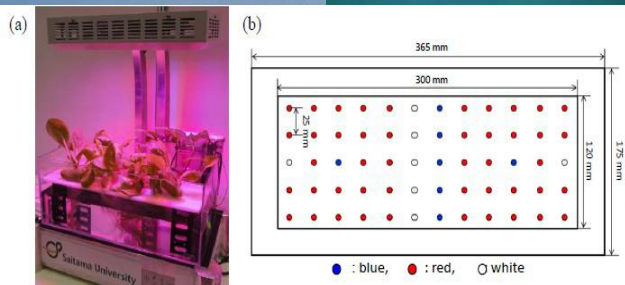
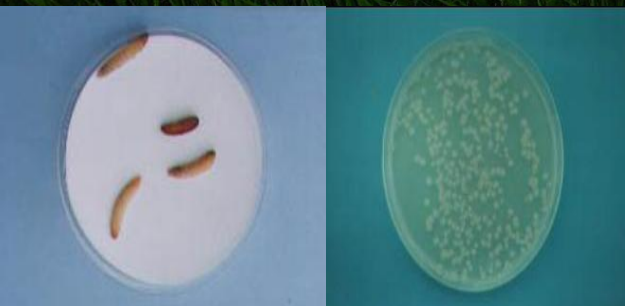


International Journal of Food and Biosystems Engineering

Volume 5, Number 1, August 2017



INTERNATIONAL JOURNAL OF FOOD and BIOSYSTEMS ENGINEERING

Volume 5, Number 1, August 2017

Supported by

Technological Educational Institute of Thessaly,
Technological Research Center of Thessaly
and the
Laboratory of the Food and Biosystems Engineering of TEI of Thessaly



website: <http://www.fabe.gr/en/journal>

Publication information:

International Journal of Food and Biosystems Engineering, ISSN 2408-0675 is published every two months as an electronic and hard copy Journal by the laboratory of Foods and Biosystems Engineering which is incorporated in the structure of Biosystems Engineering Dept. of the School of Agricultural Technology of Technological Educational Institute (TEI) of Thessaly. The laboratory is located at TEI of Thessaly at peripheral road Larissa-Trikala, 411 10, Larissa, Greece.

Aims and Scope:

The *International Journal of Food and Biosystems Engineering* has broad and scientifically interesting topics on: ‘Environmental Sustainability and innovation of Food and Biosystems Engineering in an “Ever Changing World”’. The journal offering a platform where knowledge, innovative ideas, experiences and research achievements of people involved in the field of Food and Biosystems Engineering found a step of expression and dissemination. *International Journal of Food and Biosystems Engineering* is a professional Academic journal particularly emphasizes new research results and innovations in topics such as:

- Advances in Food Process Engineering.
- Engineering of Novel Food Process.
- Food Product Engineering and Functional Foods.
- Food and Agricultural Waste & Byproducts.
- Advances in Food Packaging and Preservation.
- Modeling and Control of Food Process.
- C.F.D. applications in Food Engineering.
- Novel Aspects of Food Safety and Quality
- Nano and microencapsulation in Food and Agriculture.
- Engineering and Mechanical Properties of Food.
- Sustainability aspects in food and agricultural engineering.
- Extraction Technology for natural antioxidants and Phytochemical.
- Industrial Fermentations and Biotechnology.
- Advanced Greenhouse Technologies.
- Precision Agriculture and Variable Rate Irrigation.
- Water and Wastewater Management and Irrigation Engineering.
- Novel Bioremediation Technologies
- Automation –Robotics and Geo-information novelty in Bio-systems Engineering.
- Multi Criteria Decision Analysis, Remote Sensing, GIS and Fuzzy Logic Modeling.
- Biosensors Engineering and Applications.
- Wastewater and Sludge Reuse from Food, Agricultural and other Industries.
- Pollution of natural resources Ecotoxicology.
- Biomass, Photovoltaic (solar cell) and Aeolian (Wind) Energy engineering

Editorial Board Members:

Prof., A Gálvez (Spain)	Assistant Prof., E. Hatzidimitriou (Greece)
Associate Prof., Adrian Asanica (Romania)	Dr. Efi Alexopoulou (Greece)
Associate Prof., Aicha Nancib (Algeria)	Assoc Prof., Esra Capanoglu (Turkey)
Dr. Aleksandra Djukić-Vuković (Serbia)	Dr. Estela de Oliveira Nunes (Brazil)
Prof., Alexander Jaeger (Austria)	Prof., Fabio Marcelo Breunig (Brazil)
Prof., Alexandrina Sîrbu (Romania)	Dr. Fernando D. Ramos (Argentina)
Prof., Ali Zazoua (Algeria)	Dr. Ferruh Erdogan (Turkey)
Prof., Alina Catrinel Ion (Romania)	Prof., Figen Ertekin (Turkey)
Associate Prof., Alina Kunicka-Styczyńska (Poland)	Prof., Francis Butler (Ireland)
Dr. Amin Mousavi Khaneghah (Brazil;Iran)	Assist. Prof., Francisco Javier Deive (Spain)
Dr. Ana B. Baranda (Spain)	Prof., Gil Fraqueza (Portugal)
Dr. Ana María Díez Pascual (Spain)	Prof., Gustavo V. Barbosa-Cánovas (USA)
Dr. Ana Sanches Silva (Portugal)	Prof., Idlimam Ali (Morocco)
Prof., Anand Y. Joshi (India)	Prof., Ingrid Bauman (Croatia)
Dr. András Kovács (Hungary)	Assistant Prof., Ioannis Giavasis (Greece)
Emeritus Prof., Andree Voilley (France)	Dr. Iuliana Diana Barbulescu (Romania)
Prof., Andrzej Skulimowski (Poland)	Prof., Jan W. Dobrowolski (Poland)
Prof., Angelica Marquetotti Salcedo Vieira (Brazil)	Prof., Jiri Blahovec (Czech Republic)
Dr. Angelo Algieri (Italy)	Dr. Jorge Welti-Chanes (México)
Dr., Annamaria Costa (Italy)	Dr. K. Alagusundaram (India)

- Dr. Artur Wiktor (Poland)
Associate Prof., Ayse Handan Baysal (Turkey)
Prof., B.H. Chen (Taiwan)
Prof., Baghdad Ouddane (France)
Dr. Benmeziane Farida (Algeria)
Prof., Bharathi Raja (India)
Prof., Branka Levaj (Croatia)
Prof., Brett Pletschke (South Africa)
Prof., Cornelia Vasile (Romania)
Prof., Célia Quintas (Portugal)
Associate Prof., Celile O. Dolekoglu (Turkey)
Assistant Prof., Cheima Fersi (Tunisia)
Prof., Chuan-He Tang (China)
Prof., Constantina Tzia (Greece)
Prof., Constantine Sfomlos (Greece)
Prof., Costas Stathopoulos (UK)
Dr. Cristina Castillo (Spain)
Prof., Cristina L.M. Silva (Portugal)
Dr. Dagbjorn Skipnes (Norway)
Assoc. Prof., Dainius Steponavičius (Lithuania)
Prof., Dan Scarpete (Romania)
Dr. Daniel Hill (Spain)
Assistant Prof., Daniel Abugri (USA)
Assistant Prof., Deborah Panepinto (Italy)
Prof. Dimitrios Fessas (Italy)
Dr. Douglas Wilson (UK)
Prof., Dritan Topi (Albania)
Assistant Prof., Dubravka Novotni (Croatia)
- Prof., Keshavan Niranjan (UK)
Assistant Prof., K. Dermentzis (Greece)
Prof., Laura Piazza (Italy)
Prof., M. Chandrasekaran (Saudi Arabia)
Prof., Marco Dalla Rosa (Italy)
Prof., Marek Kowalczyk (UK)
Prof., Maria Turtoi (Romania)
Dr. Mihaela Begea (Romania)
Associate Prof., Minh Nguyen (Australia)
Prof., Miriam Hubinger (Brazil)
Prof., Miroljub Barać (Serbia)
Prof., Muhammad Subhan Qureshi (Pakistan)
Dr. Navin K Rastogi (India)
Dr. Ourania Gouseti (UK)
Assoc. Prof., Olga Gortzi (Greece)
Prof., Paula Pires-Cabral (Portugal)
Prof., Ruta Galoburda (Latvia)
Dr. Sara Canas (Portugal)
Prof., Stavros Yanniotis (Greece)
Prof., Stefanos Zaoutsos (Greece)
Prof., Tawfik Benabdallah (Algeria)
Dr. Ursula A. Gonzales-Barron (Portugal)
Prof., V. Aslihan Nasir (Turkey)
Dr. Veronica Chedea (Romania)
Assoc. Prof., Yacoub Idriss Halawlaw (Chad)
Prof., Yen-Con Hung (USA)
Assoc. Prof., Yesim Ekinci (Turkey)
Emeritus Prof., Zeki Berk (Israel)
Associate Prof., Oguz Gursoy (Turkey)

Manuscripts and correspondence are invited for publication. You can submit your paper via we submission or e-mail to: ifbe-journal@fabe.gr. Submission guidelines and web submission system are available at: <http://www.fabe.gr/en/journal>

Editorial office:

Editor: Associate Professor Konstantinos Petrotos
Editorial team members: Dr. Stefanos Leontopoulos, Sotiria Tsilfoglou, Maria Papakosta, Zoi Papathanasiou, Marios Chalaris, Fani Karkanta, Tatiana Androulaki, Giorgos Kefalakis and Christos Mantas

TEI of Thessaly, Periferial road Larissa-Trikala, 411 10, Larissa, Greece
Tel: +30 2410 684524 and +30 6944 191500 (mobile) (Associate Professor, Konstantinos Petrotos)
E-mail: petrotos@teilar.gr and ifbe-journal@fabe.gr

Copyright©2016 by the head of *FABElab* TEI of Thessaly. All rights reserved. *International Journal of Food and Biosystems Engineering* editor holds the exclusive copyright of all the contents of this journal. In accordance with the international convention, no part of this journal may be reproduced or transmitted in any form or by any means, electronic, mechanical, photocopying, and recording without the written permission of the copyright holder. Otherwise any conduct would be considered as the violation of the copyright. The contents of this journal are available for any citation. However, all the citations should be clearly indicated with the title of this journal, serial number and the name of the author.

Journal web site: <http://www.fabe.gr/en/journal>

*Food and Biosystems Engineering Laboratory,
Technological Educational Institute of Thessaly
(TEI of Thessaly),
Perifereiaki Odos Larissa-Trikala,
Larissa, TK 41110, Greece*



International Journal of Food and Biosystems Engineering

Volume 5, Number 1, August 2017

Contents

- 1 **Assessment of Ammonia and Carbon Dioxide Concentrations in a Breeding Hen Building Under Portuguese Winter**
Jose L.S. Pereira, Silvia Ferreira, Carla S.P. Garcia, Andre Conde, Pedro Ferreira, Victor Pinheiro, Henrique Trindade
- 7 **Chromium (VI) Removal By A Novel Magnetic Halloysite-Chitosan Nanocomposite From Aqueous Solutions**
Ezgi Turkes, Yesim Sag Acikel
- 15 **Synthesis of Magnetic Halloysite Nanotube-Alginate Hybrid Beads: Use in the Removal of Methylene Blue from Aqueous Media**
Gorkem Polat, Yesim Sag Acikel
- 23 **An Experimental Study of the Swelling Behavior of Starch Granules Under Heat Treatment**
Plana-Fattori, A., Almeida, G., Moulin, G., Doursat, Ch., Flick, D.
- 31 **Application of Ultrasound to Extraction of Biologically Active Substances of Some *Serratula* Species**
Larisa Zibareva, Anan Athipornchai, Orawan Wonganan, Apichart Suksamrarn
- 38 **Effect of the Drying Conditions in a Pulsed Fluidized Bed Dryer on the Sulforaphane Content of Broccoli**
Andrea Mahn, Carmen Perez, Alejandro Reyes
- 44 **Development of Agriculture Support System Using Plant Bioelectric Potential Responses and Gas Sensor**
Yuki Hasegawa, Donatella Puglisi, Anita Lloyd Spetz
- 52 **Recovery and Analysis of the Biological Activity of Lycopene Produced by *Rhodotorula glutinis* P4M422**
Ayerim Hernandez-Almanza, Jae Kweon Park, Nallely E. Carlos-Interrial, Jose G. Fuentes-Aviles, Cristobal N. Aguilar
- 60 **High Pressure Processing of Raw and Marinated Mackerel Fillets. Study on the Inactivation of Anisakidae Larvae and Some Quality Aspects**
Anna G. Fiore, Luigi Palmieri, Andrea Lo Voi, Ivana Orlando, Giovanni Normanno, Antonio Derossi, Carla Severini
- 68 **A Study on the Enrichment of Olive Oil with Natural Olive Fruit Polyphenols**
Tsilfoglou Sotiria, Petrotos Kostantinos, Leontopoulos Stefanos, Hadjichristodoulou Christos, Tsakalof Andreas
- 75 **Chemotactic Responses of *Pseudomonas oryzihabitans* and Second Stage Juveniles of *Meloidogyne javanica* on Tomato Root Tip Exudates**
Stefanos Leontopoulos, Kostantinos Petrotos, Vassiliki Anatolioti, Prodromos Skenderidis, Sotiria Tsilfoglou, Ioannis Vagelas

Assessment of Ammonia and Carbon Dioxide Concentrations in a Breeding Hen Building Under Portuguese Winter

Jose L.S. Pereira^{1,2*}, Silvia Ferreira², Carla S.P. Garcia¹,
Andre Conde³, Pedro Ferreira³, Victor Pinheiro², Henrique Trindade²

¹Polytechnic Institute of Viseu, Agrarian School of Viseu, CI&DETS,
Quinta da Alagoa, 3500-606 Viseu, Portugal

²University of Trás-os-Montes and Alto Douro, CITAB, CECAV,
Quinta de Prados, 5000-801 Vila Real, Portugal

³LUSIAVES, Marinha das Ondas, 3090-485 Figueira da Foz, Portugal

Abstract

Excessive ammonia (NH₃) and carbon dioxide (CO₂) in the housing of breeding hens can cause various negative effects on the health of hens and the welfare of the workers who care for them. The aim of this study was to evaluate the NH₃ and CO₂ concentrations in the first month of housing the breeding hens during Portuguese winter. The study was conducted on a commercial hen breeding farm located in central Portugal. One modern building equipped with climate control system, automatic feeding and drinking systems and minimum transitional tunnel ridge system was selected. New litter material made with rice hulls was used in the building, and the breeding sample comprised five months old 6864 female and 720 male birds housed in the building on 7 November 2016. The outdoor and indoor environmental conditions and indoor gas concentrations were measured continuously from 10 November to 30 November 2016. (NH₃) and CO₂ concentrations were measured with a photoacoustic field gas monitor and air samples collected through 4 sampling points located indoor, by a multipoint sampler. Results showed that the CO₂ concentrations did not exceed 3000 ppm during the first month of housing the breeding hens and under winter environment. However, the NH₃ concentrations exceed 20 ppm on most measurement days. For a good indoor air quality, the study suggests the use of mitigating measures for maintaining NH₃ concentration below 10 ppm

Keywords: Breeding hens, CO₂, Gas concentration, Mediterranean Portugal, NH₃, Poultry husbandry, Winter environment.

*Corresponding author e-mail: jlpereira@esav.ipv.pt

I. INTRODUCTION

Excessive ammonia (NH_3) and carbon dioxide (CO_2) in the housing of breeding hens can cause various negative effects on the health of hens and the welfare of the workers who care for them. International and national regulations have been published in order to protect animals and workers health, with short period exposure limits of 20 and 3000 parts per million (ppm) for NH_3 and CO_2 , respectively (CIGR, 1992; 1994; Kilic and Yaslioglu, 2014). Ammonia and CO_2 coming from the decomposition and fermentation of the litter and excreta can damage indoor air quality. The nitrogen compounds (uric acid and urea) of excreta are hydrolysed into NH_3 and CO_2 and consequently the concentrations of these gases are increased at in-house (Wathes et al., 1997; Pereira and Trindade, 2014; Alberdi et al., 2016; Lin et al., 2017). In addition, the hens' respiration as well as the aerobic and anaerobic decomposition of the litter material enhances the CO_2 levels at in-house (Sommer et al., 2006; Ni et al., 2012). High NH_3 concentrations (>20 ppm) in hen buildings are related with negative health and welfare concerns (Portejoie et al., 2002). A decrease in egg production, feed intake and growth rate has been reported due the presence of NH_3 (Kristensen and Whates, 2000, Xin et al., 2011; Costa et al., 2012). In terms of health, NH_3 causes damage in the respiratory tract and increases the incidence of respiratory diseases (Nahm, 2005). Also,

high NH_3 levels have also been associated with the increase of pathogens concentrations in the litter material and the increase of morbidity and mortality (Kristensen and Whates, 2000; Miles et al., 2004). It could be hypothesised that breeding hens have high nitrogen excretion rates and NH_3 and CO_2 concentrations are particularly damaging to the hens during periods of minimum ventilation like winter. Thus, the aim of this study was to evaluate the NH_3 and CO_2 concentrations in the first month of housing the breeding hens during Portuguese winter.

II. MATERIAL AND METHODS

The study was conducted in the commercial breeding hen farm Quinta da Cruz (latitude: 40.024176° , longitude: -8.629285°) located in central Portugal (Soure, Portugal) (Figure 1). The selected building (length = 80 m, width = 16 m, ridge = 4.0 m and sidewall height = 2.7 m) is a steel construction with insulation, equipped with climate control system (model F37, Fancom), automatic feeding and drinking systems (Roxell). Ventilation was made by minimum transitional tunnel ridge system being controlled with one differential pressure (0-100 Pa, Fancom), and two sensors of temperature (model SF7, Fancom) and two sensors of relative humidity (model RHM.17 for inside and model RHO.17 for outside, Fancom) located indoor and outdoor the building.



Figure 1. Location of the hen building where measurements were made (photo taken in 2016; latitude: 40.024176° , longitude: -8.629285° ; <https://www.google.pt/maps/place>, accessed: 18-01-2017) (no scale).

New litter material made with rice hulls was used in the building, and the breeding sample comprised five months old 6864 female and 720 male birds housed in the building on 7 November 2016.

The NH₃ and CO₂ concentrations at indoor building were measured continuously from 10 November to 30 November 2016. The concentrations of these two gases were measured with a photoacoustic field gas monitor (model INNOVA 1412i-5, Lumasense Technologies) and air samples collected, in sequence (2 minute intervals), through 4 sampling points located indoor, by a multipoint sampler (model INNOVA 1409-12, Lumasense Technologies). Sampling points were made using Teflon tubes (3 mm internal diameter) equipped with PTFE-filters (0.001 mm pore size, Whatman) to protect from dust.

The outdoor and indoor temperatures and levels of relative humidity were taken from the climate control system of the building. The average NH₃ and CO₂ concentrations were defined as the average of the hourly mean concentrations measured. All data obtained from the monitored building were analysed by Excel spreadsheet using descriptive statistics.

III. RESULTS AND DISCUSSION

The climate data as well as the NH₃ and CO₂ concentrations are shown in Figure 2. During measurement, the outdoor temperature ranged from 4 °C to 15 °C whereas indoor temperature was higher and varied between 17 °C and 20 °C (Figure 2A). The indoor relative humidity varied between 64% and 78%, being observed lower values in almost all measurement relative to indoor relative humidity (Figure 2A).

The NH₃ concentration increased from 10 November to 16 November 2016, with maximum values lower than 13 ppm (Figure 2B). Up this date (16 November 2016), NH₃ con-

centration increased continuously and reached values higher than 20 ppm until the end of the measurement, with maximum values that ranged from 20 ppm to 35 ppm except in 10 November 2016 (Figure 2B).

The CO₂ concentration had a similar evolution than NH₃ concentration, with maximum values always lower than 3000 ppm during whole measurement (Figure 2C).

The negative effects of NH₃ on hens and farm workers themselves begin at 25 ppm and become very serious at 50 ppm, being more deleterious a short period exposure rather than a continuously exposition (CIGR, 1992, 1994). Humans can generally smell NH₃ at concentrations between 20 ppm and 30 ppm, being an irritant to mucous membranes (cilia and epithelium) of the respiratory tract and causes conjunctivitis and damages the cornea of the eyes (CIGR, 1994; Kristensen and Whates, 2000). The damage of the mucous membranes of the respiratory system increases the susceptibility of hens to respiration infection by *Escherichia coli* (Kristensen and Whates, 2000; Miles et al., 2004). The severity of damage depends on the concentration of NH₃ and duration of exposure (Miles et al., 2004).

The indoor air humidity and temperature could affect the NH₃ concentration. The principal factors affecting indoor NH₃ concentration in hen houses are litter conditions and airflow rate (Wathes et al., 1997; Ni et al., 2012; Lin et al., 2017). Therefore, outdoor air humidity and temperature affect indoor environmental conditions. Thus, the increase of indoor air humidity and temperature will increase the moisture and temperature of the litter material and consequently will enhance the NH₃ volatilisation (Sommer et al., 2006; Pereira et al., 2010, 2012; Alberdi et al., 2016). Previous studies recommend a limit of 20 ppm of NH₃ but in some European countries such as Sweden the exposure limit for hens is 10 ppm (Ni et al., 2012; Kilic and Yaslioglu, 2014).

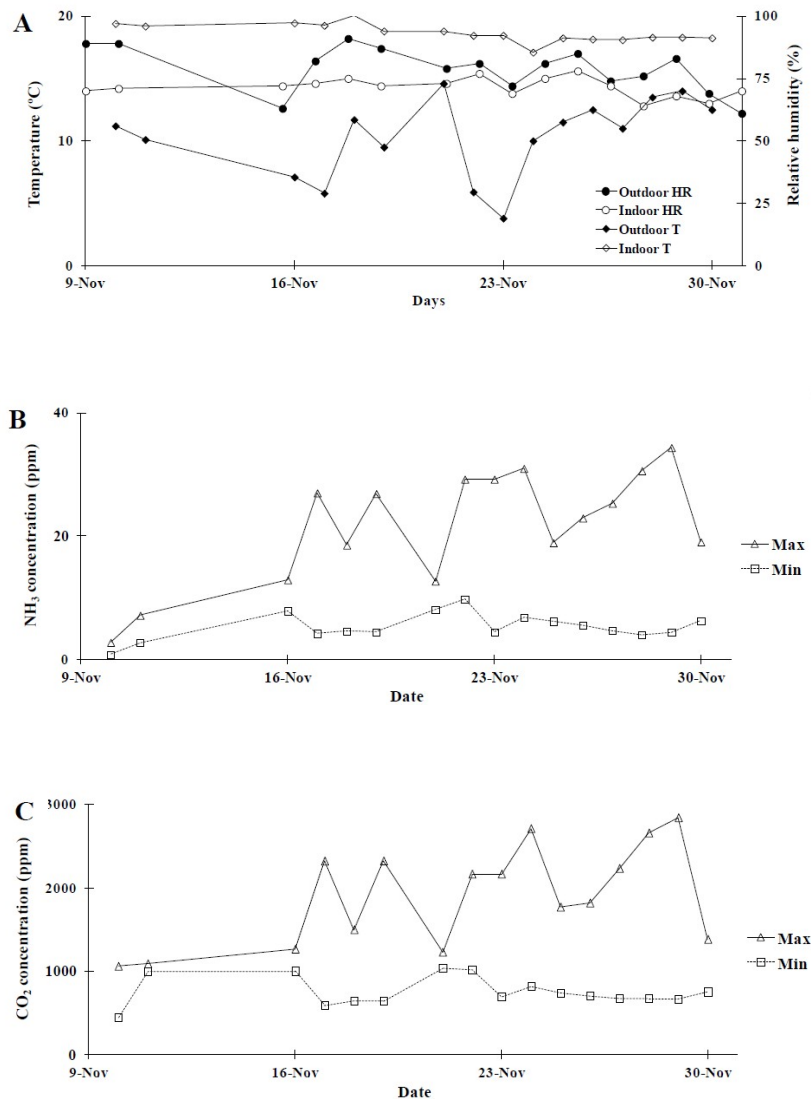


Figure 2. Outdoor and indoor temperature and relative humidity (A) and ammonia (B) and carbon dioxide (C) concentrations during the measurement in the hen building.

The harmful effects of NH₃ on hens have direct consequences on the health and welfare, and indirectly in the economic result of the activity, especially in the cold season. In order to obtain fertile eggs, the breeding of hens should begin when they are 20 weeks old and end when they are 40 weeks old. The breeding hens should have high excretion rates and larger amounts of bedding material will be accumulated on the concrete floor of the build-

ings. Hence, high amounts of NH₃ and CO₂ should be emitted from manure until 40 weeks old. More studies are needed to fully evaluate NH₃ and CO₂ concentrations during the whole cycle, and are recommended the use of mitigating measures for maintaining NH₃ concentration below 10 ppm. This needs additional research.

IV. CONCLUSIONS

The NH₃ concentrations exceed 20 ppm during the first month of housing the breeding hens and under winter environment, leading to potential negative effects on the health of hens and the welfare of the farm workers. How-

ever, long term studies are required to properly assess the NH₃ and CO₂ concentrations during whole cycle. In addition, further research is needed in order to evaluate additives such as clinoptilolite or aluminium sulphate as mitigating measures for maintaining NH₃ concentration below 10 ppm.

V. ACKNOWLEDGEMENTS

This work was supported by European Investment Funds by FEDER/COMPETE/POCI-Operational Competitiveness and Internationalisation Programme, under project POCI-01-0145-FEDER-006958, project Ovislab ICT-2013-05-004-5314 ID-64757, project POCI-01-0247-FEDER-003430 AMONIAVE and National Funds by FCT-Portuguese Foundation for Science and Technology, under the project UID/AGR/04033/2013 and Portugal 2020.

REFERENCES

- [1] Alberdi, O., Arriaga, H., Calvet, S., Estelles, F., and Merino, P., 2016. Ammonia and greenhouse gas emissions from an enriched cage laying hen facility. *Biosystems Engineering*, 144: 1-12.
- [2] CIGR, 1992. Climatization of animal houses. Second Report of the Working Group on Climatization of Animal Houses. International Commission of Agricultural Engineering (CIGR), Ghent, Belgium, 147 pp.
- [3] CIGR, 1994. Aerial environment in animal housing. Working Group Report Series No 94.1. International Commission of Agricultural Engineering (CIGR) and CEMAGREF, Rennes, France, 116 pp.
- [4] Costa, A., Ferrari, S., and Guarino, M., 2012. Yearly emission factors of ammonia and particulate matter from three laying-hen housing systems. *Animal Production Science*, 52: 1089-1098.
- [5] Lin, X., Zhang, R., Jiang, S., El-Mashad, H., and Xin, H., 2017. Emissions of ammonia, carbon dioxide and particulate matter from cage-free layer houses in California, *Atmospheric Environment*, 152: 246-255.
- [6] Kilic, I., and Yaslioglu, E., 2014. Ammonia and carbon dioxide concentrations in a layer house. *Asian-Australasian Journal of Animal Sciences*, 27: 1211-1218.
- [7] Kristensen, H.H., and Wathes, C.M., 2000. Ammonia and poultry welfare: a review. *World's Poultry Science Journal*, 56: 235-245.
- [8] Miles, D.M., Branton, S.L., and Lott, B.D., 2004. Atmospheric ammonia is detrimental to the performance of modern commercial broilers. *Poultry Science*, 83: 1650-1654.
- [9] Nahm, K.H., 2005. Environment effects of chemical additives used in poultry litter and swine manure. *Critical Reviews in Environment Science and Technology*, 34: 487-513.
- [10] Ni, J.-Q., Chai, L., Chen, L., Bogan, B.W., Wang, K., Cortus, E.L., Heber, A.J., Lim, T.-T., and Diehl, C.A., 2012. Characteristics of ammonia, hydrogen sulfide, carbon dioxide, and particulate matter concentrations in high-rise and manure-belt layer hen houses. *Atmospheric Environment*, 57: 165-174.

- [11] Pereira, J., and Trindade, H., 2014. Control of ammonia emissions in naturally ventilated dairy cattle facilities in Portugal. *Engenharia Agricola*, 34: 600-609.
- [12] Pereira, J., Misselbrook, T.H., Chadwick, D.R., Coutinho, J., and Trindade, H., 2010. Ammonia emissions from naturally ventilated dairy cattle buildings and outdoor concrete yards in Portugal. *Atmospheric Environment*, 44: 3413-3421.
- [13] Pereira, J., Misselbrook, T.H., Chadwick, D.R., Coutinho, J., and Trindade, H., 2012. Effects of temperature and dairy cattle excreta characteristics on potential ammonia and greenhouse gas emissions from housing: A laboratory study. *Biosystems Engineering*, 112: 138-150.
- [14] Portejoie, S., Martinez, J., and Landmann, G., 2002. L'ammoniac d'origine agricole: impacts sur la sant  humaine et animale et sur le milieu naturel. *Productions Animales*, 15: 151-160.
- [15] Sommer, S.G., Zhang, G.Q., Bannink, A., Chadwick, D., Misselbrook, T., Harrison, R., Hutchings, N.J., Menzi, H., Monteny, G.J., Ni, J.-Q., Oenema, O., and Webb, J., 2006. Algorithms determining ammonia emission from buildings housing cattle and pigs and from manure stores. *Advances in Agronomy*, 89: 261-335.
- [16] Wathes, C.M., Holden, M.R., Sneath, R.W., White, R.P., and Phillips, V.R., 1997. Concentrations and emission rates of aerial ammonia, nitrous oxide, methane, carbon dioxide, dust and endotoxin in UK broiler and layer houses. *British Poultry Science*, 38: 14-28.
- [17] Xin, H., Gates, R.S., Green, A.R., Mitloehner, F.M., Moore Jr., P.A., and Wathes, C.M., 2011. Environmental impacts and sustainability of egg production systems. *Poultry Science*, 90: 263-277.

Chromium (VI) Removal By A Novel Magnetic Halloysite-Chitosan Nanocomposite From Aqueous Solutions

EZGI TURKES, YESIM SAG ACIKEL*

Hacettepe University, 06800 Beytepe Campus,
Department of Chemical Engineering, Ankara, Turkey

Abstract

A novel magnetic nanocomposite composed of halloysite nanotube (HNT) and chitosan (CTN) was prepared for recovery of Cr (VI). Magnetic halloysite (MHNT) nanotubes were synthesized by co-precipitation method. Magnetic halloysite-chitosan (MHNT-CTN) nanocomposites were synthesized through the adsorption of CTN onto magnetic halloysite nanotubes (MHNTs). The Cr (VI) adsorption behaviour on the prepared MHNT-CTN nanocomposites was studied under various conditions of different pH values, mass ratio of HNT to CTN, amount of nanocomposite and initial Cr (VI) concentrations. The optimum pH, mass ratio of HNT to CTN, amount of nanocomposite, and initial Cr (VI) concentration were found as pH 5.0, 1:2, 6.0 g/L, and 100-150 mg/L. At these conditions the initial adsorption rate, the amount of adsorbed Cr(VI) per unit weight of MHNT-CTN and the adsorption efficiency were found as 0.55 mg/g-min, 2.29 mg/g, 16.94%, respectively.

Keywords: Wastewater treatment, adsorption, chromium, magnetic HNT-CTN nanocomposite

I. INTRODUCTION

REMOVAL of chromium pollution has been received great attention in recent years because of the toxicity and carcinogenic nature of its to the ecosystem and human health (Jinhua et al., 2010). For that reason, wastewaters containing Cr(VI) ions must be treated before discharging to the environment. Chromium has two different valencies in aqueous media, namely Cr(VI) and Cr(III) (Krishna Kumar et al., 2015).

Cr(VI) is highly soluble in aqueous media and also more toxic and carcinogenic even at low concentrations over a wide range of pH values according to Cr(III). Cr(VI) accumulation and direct contact cause serious health problems for human included lung cancer as well as liver, kidney and gastric damage, and skin irritation (Duranoglu et al., 2012).

The discharge standard of Cr(VI) to surface water was given as 0.1 mg L^{-1} for total chromium by the United States-Environmental

*Corresponding author e-mail: yesims@hacettepe.edu.tr

Protection Agency (US EPA). This includes all forms of chromium, including Cr(VI)(Yang et al., 2016).

Waste waters containing both Cr(VI) and Cr(III) in concentrations ranging from tens to hundreds of milligrams per liter come from various industrial processes, such as electroplating, textile and leather industry, manufacturing of dyes, paint industries and petroleum refining processes (Krishna Kumar et al., 2015). Conventional Cr(VI) treatment methods from contaminated water comprise precipitation, reduction, electrolytic removal, ion exchange, reverse osmosis, and adsorption. Adsorption seems to be the best removal method for Cr(VI) removal in terms of basic design and operation using chemical or natural biological origin materials. A wide range of adsorbents, such as carbonaceous material (biocharc, active carbon), natural oxides (aluminum oxide, ferric oxide), clays (kaolin, sepiolite, clinoptilolite), zeolites, microorganisms, biopolymers (alginate, chitin, chitosan, K-carrageenan), agricultural wastes have been reported for Cr(VI) removal (Yang et al., 2016).

The polymer of CTN is a natural hydrophilic cationic polysaccharide, which is a deacetylated biopolymer of chitin, the second most abundant natural polymer on earth. CTN is composed of randomly distributed β -(1,4)-linked-D-glucosamine and N-acetyl-D-glucosamine. Due to its outstanding properties like non-toxicity, biodegradability, biocompatibility and low cost, CTN is widely used in the fields of cosmetics, water engineering, paper and textile industries, food processing, photography, chromatographic separations and biomedical applications (Yao et al., 2015). CTN contains reactive amino and hydroxyl groups available, which generates strong adsorption and complexation interactions and chelates with many transitional metal ions and dyes. The hydrogen bonding, electrostatic attractions, ion exchange and weak van der Waals forces are responsible for heavy metal and dye binding of CTN (Peng et al., 2015).

CTN can be easily chemically modified or physically blended to produce CTN compos-

ites via reactive amino and hydroxyl groups. In this manner, mechanical properties of CTN can be strengthened and chemical stability of its under acidic media can be improved (Choo et al., 2016). Nanosized inorganic materials such as hydroxyapatite, nanoclay, carbon nanotubes, titanium dioxide, and graphene have been incorporated into CTN to improve the mechanical properties. HNT ($\text{Al}_2\text{Si}_2\text{O}_2(\text{OH})_4 \cdot 2\text{H}_2\text{O}$) is a aluminosilicate clay with a predominantly hollow nanotube structure(Zhang et al., 2016). As HNTs can be mined from the corresponding deposit as a raw mineral, they are abundant in nature. Since HNTs have some superior characteristics, such as large surface area, good mechanical and thermal properties, large surface/volume ratio, rich reactive groups, they are widely used in catalytic conversions, electronics, drug delivery and the removal of hazardous species(Zhai et al., 2013). To combine the advantages of both inorganic and organic materials, a novel, environmentally friendly and cheap CTN-HNT hybrid materials are designed. Protonated CTN under acid condition can bind effectively to the negatively charged outer surface of the HNTs. Recently, magnetic separation technology (MST) is gaining growing attention. Applying an external magnetic force, magnetic particles can be separated from the medium easily. In this study, firstly, magnetic HNT nanoparticles were synthesized according to co-precipitation method on the surface of HNT; secondly, magnetic HNT-CTN (MHNT-CTN) nanocomposites were prepared through the adsorption of CTN onto surface of the negatively charged magnetic HNT nanoparticles. The effects of various experimental conditions like different pH values, mass ratio of HNT to CTN, amount of nanocomposite and initial Cr (VI) concentrations on Cr(VI) adsorption by MHNT-CTN nanocomposites were studied.

II. MATERIALS AND METHODS

Materials

HNTs were obtained from Sigma-Aldrich. The characteristic dimensions of the HNTs

range from about 1-1.3 μm in length, 30-70 nm in diameter. Chitosan powder (75-85% deacetylated) was also obtained from Sigma-Aldrich. Deionized (DI) water obtained from Thermo Scientific Smart2Pure water purification system, with resistivity of 18.2 M Ω cm was used for preparation of all solutions. Iron(II) chloride tetrahydrate ($\text{FeCl}_2 \cdot 4\text{H}_2\text{O}$), iron(III) chloride hexahydrate ($\text{FeCl}_3 \cdot 6\text{H}_2\text{O}$) were supplied from Sigma-Aldrich. Ammonium hydroxide solution (NH_4OH) (32% NH_3 extra pure), potassium dichromate ($\text{K}_2\text{Cr}_2\text{O}_7$) and 1,5-diphenylcarbazid ($\text{C}_{13}\text{H}_{14}\text{N}_4\text{O}$) were purchased from MERCK.

Synthesis of magnetic halloysite nanotubes (MHNT)

MHNT nanoparticles were prepared by a modification of co-precipitation method (Owoseni et al, 2016). Firstly, 0.50 g of HNTs was dispersed in 200 ml of deionized water in a 500 ml five necked glass reactor under vigorous stirring. The HNTs suspension was purged with N_2 atmosphere for 20 min, to remove dissolved oxygen. Secondly, appropriate amounts of $\text{FeCl}_3 \cdot 6\text{H}_2\text{O}$ and $\text{FeCl}_2 \cdot 4\text{H}_2\text{O}$ were then added to the reactor to give a molar ratio of Fe^{2+} to Fe^{3+} of 1:2. The mixture was further purged with N_2 atmosphere for 20 min. The temperature of the mixture was then increased to 80 °C. Then, 0.5 M NH_4OH was added to the suspension using a syringe pump by slow addition. Then, the mixture was kept waiting at 80 °C under N_2 atmosphere with strong stirring for 1 h. The nanoparticles were separated by magnetic decantation and then washed 4 times with deionized water. After the magnetic separation stage, the nanoparticles were dried in a freeze-dryer at 24 h.

Synthesis of magnetic HNT-CTN nanocomposites (MHNT-CTN)

Previously prepared MHNT nanoparticles were dispersed in deionized water. CTN was dissolved in acetic acid solution at different ratios and then was added to MHNT suspension by a syringe pump slowly. Magnetic HNT-CTN nanocomposites were prepared with different mass ratios of MHNT to CTN of 1:1, 1:2, 2:1,

1:3 and 3:1. To obtain magnetic HNT-CTN nanocomposites, the final mixture was mixed vigorously using a mechanical stirrer for 24 hours. The final product was separated from the solution by means of a magnetic force and then washed by deionized water several times to remove the excess CTN and acetic acid. After washing step, MHNT-CTN nanocomposites were dried in a freeze-dryer at 24 h.

Adsorption experiments

All the adsorption experiments were performed in 50 mL tubes filled with 25 mL aqueous Cr(VI) solution and after the pH of Cr(VI) solutions was adjusted to the required values, certain amounts of MHNT-CTN nanocomposites were added to the solution. The tubes were placed in rotator with circular motion and shaken for 24 h at 25 °C. At certain time intervals ($t = 0, 5, 10, 15, 30, 60, 120, 180, 1440$ mins), samples were taken from the media and then the remained MHNT-CTN nanocomposites in the samples were separated using an external magnetic force. The unadsorbed Cr(VI) concentrations in the supernatant were determined by UV-visible spectrophotometer using 1,5-diphenylcarbazid as the complexing agent at 540 nm.

III. RESULTS AND DISCUSSION

The morphology of the MHNT-CTN nanocomposites was observed by scanning electron microscopy (SEM). The image of SEM shows that HNT-CTN nanocomposites have a tubular structure covered with CTN and iron oxide nanoparticles on HNTs. Diameters of MHNT-CTN nanocomposites show a distribution between 97.7 nm and 160.18 nm, while lengths of tubes generally range from 404 nm to 649 nm (Fig. 1). Tube walls of MHNT nanotubes formed nanocomposites with CTN become more rough, compared with natural HNTs. Tube walls of MHNT-CTN nanocomposites seem to be thicker than those of HNTs because its inner lumen and pores are filled with iron oxide nanoparticles and its surface is covered with iron oxide nanoparticles and CTN.

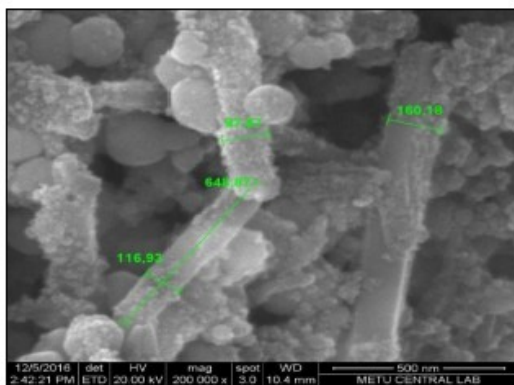


Figure 1. The SEM images of the MHNT-CTN nanocomposites

Effect of pH

HNTs consist of gibbsite octahedral sheet (Al-OH) groups on the internal surface and siloxane groups (Si-O-Si) on the external surface. For that reason, outer surface of HNTs has negative charge and inner lumen of HNTs has positive charge in the pH range 2-8. On the other hand, the pKa of CTN is around 6.20, below pH 5.0 almost 90% of active sites are protonated. For that reason, outer surface of MHNT locally coating with positively charged CTN may have positive and negative charged centers depending on success of CTN coating. Cr(VI) anion in aqueous solutions can be found in a series of chromate anions such as H_2CrO_4 , HCrO_4^- , CrO_4^{2-} and $\text{Cr}_2\text{O}_7^{2-}$ depending upon the pH of the solution. Although the HCrO_4^- is the predominant form between pH 2.0 and 6.0, HCrO_4^- and $\text{Cr}_2\text{O}_7^{2-}$ are in equilibrium. If pH is increased, CrO_4^{2-} form shifts to $\text{Cr}_2\text{O}_7^{2-}$.

At lower pH values, the outer surface of MHNT-CTN become positively charged due to strong protonation of CTN. Electrostatic force between the positively-charged surface and the negatively-charged HCrO_4^- and $\text{Cr}_2\text{O}_7^{2-}$, as well as the interaction between positively charged inner sides of MHNTs and HCrO_4^- and $\text{Cr}_2\text{O}_7^{2-}$, will increase the Cr(VI) adsorption.

The initial adsorption rates of Cr(VI) ions by MHNT-CTN nanocomposites increased when the solution pH was increased from 2.0 to 5.0.

A bell-shaped pH dependence with highest equilibrium Cr(VI) adsorption capacity around pH 5.0 was obtained. At pH values lower than 2.0, HCrO_4^- and $\text{Cr}_2\text{O}_7^{2-}$ can convert H_2CrO_7 and binding with the electrostatic interaction will decrease conveniently. At pH values higher than 6.0, the degree of protonation of the CTN on outer surface of MHNT decreases and the adsorption capacity of Cr(VI) reduces.

The maximum amount of Cr(VI) adsorbed per unit weight of MHNT-CTN and initial adsorption rate at 30 mg/L initial Cr(VI) concentration, at 2:1 ratio of MHNT to CTN were obtained as 1.887 mg/g and 0.298 mg/g-min, respectively at pH 5.0 (Fig. 2).

Effect of amount of MHNT-CTN nanocomposites

An increase in MHNT-CTN nanocomposite concentration from 0.5 g/L to 10 g/L enhanced the adsorbed Cr(VI) concentration and efficiency (Fig. 3). The adsorbed Cr(VI) quantity q_{eq} per unit weight of MHNT-CTN and initial adsorption rate increased by increasing the MHNT-CTN concentration upto 4 g/L, then began to decrease because of decreasing active surface area. The tendency for MHNT-CTN nanocomposite aggregates to form at higher nanocomposite concentrations results in a decrease in active sorption area. The initial rate of adsorption was also reduced from 0.29 mg/g-min (at 4 g/L MHNT-CTN nanocom-

posite concentration) to 0.23 mg/g-min (at 10 g/L MHNT-CTN nanocomposite concentration) and hence more time is needed to reach equilibrium. The adsorbed Cr(VI) quantity q_{eq} per unit weight of MHNT-CTN and adsorption efficiency were obtained as 1.60 mg/g

and 36.07%, respectively at 6 g/L nanocomposite concentration, and this concentration was assumed the most feasible, the adsorption experiments were continued at this quantity of nanocomposite.

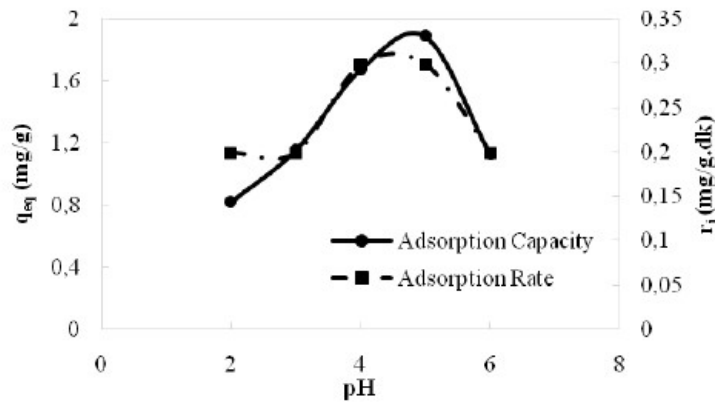


Figure 2. Effect of pH on Cr(VI) adsorption capacity and initial adsorption rate

[Experimental Parameters: $V=25$ mL; Concentration of MHNT-CTN = 4 g/L; Initial Cr(VI) concentration= 30 mg/L; Mass ratio of MHNT to CTN= 2:1; Contact time = 24 h, Temperature = 25°C]

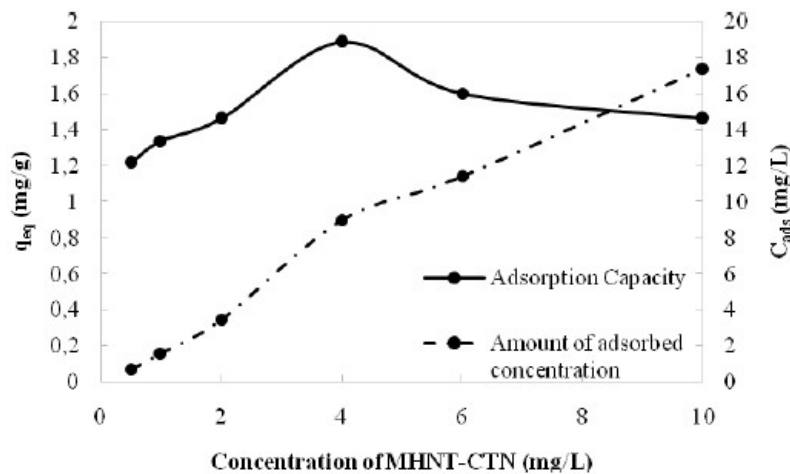


Figure 3. Effect of concentration of MHNT-CTN on Cr(VI) adsorption capacity and adsorbed concentration

[Experimental Parameters: $V=25$ mL; Initial Cr(VI) concentration= 30 mg/L; Mass ratio of MHNT to CTN= 2:1; Contact time = 24 h; Temperature = 25°C; pH= 5.0]

Effect of mass ratio of MHNT to CTN

To investigate the mass ratio of MHNT to CTN on Cr(VI) removal, MHNT-CTN ratios were chosen as 1:1, 1:2, 2:1, 1:3 and 3:1. When CTN was added to MHNT, the Cr(VI) adsorption capacity and efficiency of MHNT-CTN nanocomposite were significantly higher than those of MHNT alone. It is suggested that Cr(VI) adsorption increases with an increasing mass ratio of cationic chitosan in the nanocomposite. When the mass ratio of CTN to MHNT increased from 1:1 to 1:2, the amount of Cr(VI) adsorbed per unit weight of MHNT-CTN and adsorption efficiency increased from 1.38 mg/g to 1.56 mg/g and from 30.49% to 35.0%, respectively (Fig. 4). When the mass ratio of

MHNT to CTN was chosen as 2:1 and 1:2, the adsorbed amount of Cr(VI) did not change significantly. It can be explained that inner lumens of HNTs with positively charged (Al-OH) groups are effective in Cr(VI) adsorption as well as CTN coated positive surface of HNTs. When the amount of CTN is three times higher than HNT the initial adsorption rates, equilibrium removal and efficiency began to decrease slightly. Deterioration of MHNT-CTN nanocomposite structure was observed. When the mass ratio of MHNT to CTN reached 3:1, the amount of Cr(VI) adsorbed per unit weight of MHNT-CTN and adsorption efficiency decreased to 1.12 mg/g and 26.96%, implying negative repulsive forces of outer surface of HNT.

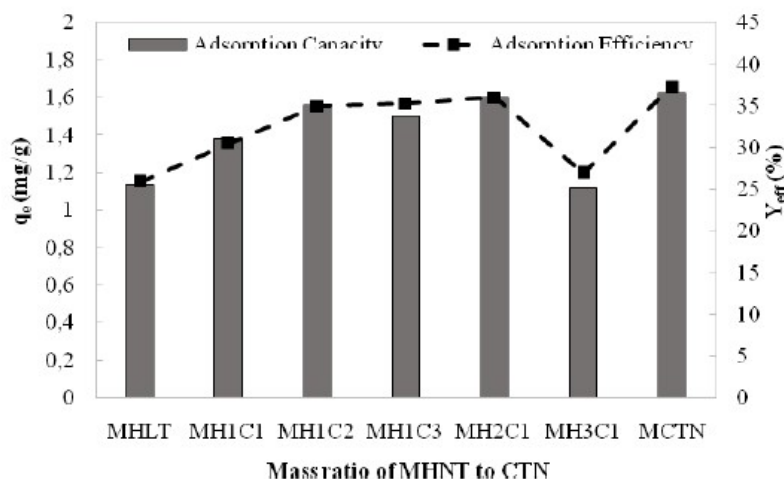


Figure 4. Effect of the mass ratio of MHNT to CTN on Cr(VI) adsorption capacity and adsorption efficiency [Experimental Parameters: V=25 mL; Concentration of MHNT-CTN= 6 g/L; Initial Cr(VI) concentration= 30 mg/L; Contact time = 24 h; Temperature = 25°C; pH= 5.0]

Effect of initial Cr(VI) ion concentration

The initial adsorption rates of Cr(VI) increased with increasing concentration of Cr(VI) ions up to 150 mg/L and the maximum initial adsorption rate was obtained as 0.61 mg/g-min (Fig. 5). The amount of Cr(VI) adsorbed per unit weight of MHNT-CTN reached a maximum value of 2.29 mg/g with increasing concentration of Cr(VI) up to 100-150 mg/L, then remains constant and a saturation kinetics was observed in this concentration range.

As MHNT-CTN nanocomposites have a finite number of surface binding sites, equilibrium uptake would be expected to show saturation kinetics at high Cr(VI) concentrations, and this was observed. On the other hand, the adsorption efficiency decreased continually with increasing concentrations of Cr(VI). The maximum Cr(VI) adsorption efficiency was obtained as 77.63% at 10 mg/L initial Cr(VI) ion concentration.

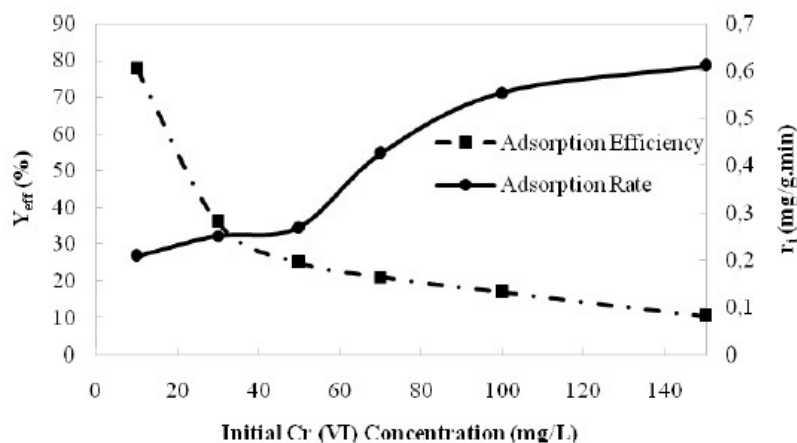


Figure 5. Effect of initial Cr(VI) concentration on adsorption efficiency (%) and initial adsorption rate
 [Experimental Parameters: V=25 mL; Concentration of MHNT-CTN= 6 g/L; mass ratio of MHNT-CTN=1:2; contact time= 24 h; temperature = 25°C; pH= 5.0]

IV. CONCLUSIONS

Magnetic HNT-CTN nanocomposites were used efficiently in the removal of Cr(VI) ions from aqueous solutions. The maximum initial adsorption rate, the amount of adsorbed Cr(VI) per unit weight of MHNT-CTN, and the adsorption efficiency were found as 0.55 mg/g-min, 2.29 mg/g, 16.94%, respectively, at pH 5.0, the mass ratio of MHNT-CTN of 1:2, concentration of MHNT-CTN of 6.0 g/L, and initial Cr(VI) concentration in the range of 100-150

mg/L. Using magnetic HNT-CTN nanocomposites, separation of the metal-sorbed nanocomposites from treated wastewater becomes easy, safe and environmentally friendly process by a permanent magnet without any downstream processing such as centrifugation or filtration. As the cost of magnetic HNT-CTN nanocomposites preparation and adsorption process itself are very low, this methodology can be suitable for the large scale removal of the pollutant metals from waste water.

V. ACKNOWLEDGEMENTS

The authors wish to thank H.U. BAP (Hacettepe University Scientific Research Projects Coordination Unit) for financial support of this study (project no: FED-2017-14059) and TUBITAK, the Scientific and Technical Research Council of Turkey with 2210-C programme.

REFERENCES

- [1] Choo, C.K., Kong, X.Y., Goh, T.L., Ngoh, G.C., Horri, B.A., Salamatinia, B., 2016. Chitosan/halloysite beads fabricated by ultrasonic-assisted extrusion-dripping and a case study application for copper ion removal. *Carbohydr Polym*, 138: 16-26.
- [2] Duranoglu, D., Buyruklardan, Kaya, I.G., Beker, U., Senkal, B.F., 2012. Synthesis and adsorption properties of polymeric and polymer-based hybrid adsorbent for hexavalent chromium removal. *Chemical Engineering Journal*, (181-182): 103-112.

- [3] Jinhua, W., Xiang, Z., Bing, Z., Yafei, Z., Rui, Z., Jindun, L., Rongfeng, C., 2010. Rapid adsorption of Cr (VI) on modified halloysite nanotubes. *Desalination*, 259(1-3): 22-28.
- [4] Krishna Kumar, A.S., Jiang, S.J., Tseng, W.L., 2015. Effective adsorption of chromium(vi)/Cr(iii) from aqueous solution using ionic liquid functionalized multiwalled carbon nanotubes as a super sorbent. *Journal of Materials Chemistry A*, 3(13): 7044-7057.
- [5] Owoseni, O., Nyankson, E., Zhang, Y., Adams, D.J., He, J., Spinu, L., McPherson, G.L., Bose, A., Gupta, R.B., John, V.T., 2016. Interfacial adsorption and surfactant release characteristics of magnetically functionalized halloysite nanotubes for responsive emulsions. *Journal of Colloid and Interface Science*, 463: 288-298.
- [6] Peng, Q., Liu, M., Zheng, J., Zhou, C., 2015. Adsorption of dyes in aqueous solutions by chitosan-halloysite nanotubes composite hydrogel beads. *Microporous and Mesoporous Materials*, 201(C): 190-201.
- [7] Yang, W.C., Tang, Q.Z., Dong, S.Y., Chai, L.Y., Wang, H.Y., 2016. Single-step synthesis of magnetic chitosan composites and application for chromate (Cr(VI)) removal. *Journal of Central South University*, 23(2): 317-323.
- [8] Yao, J., Wang, Q., Wang, Y., Zhang, Y., Zhang, B., Zhang, H., 2015. Immobilization of laccase on chitosan-halloysite hybrid porous microspheres for phenols removal. *Desalination and Water Treatment*, 55(5): 1293-1301.
- [9] Zhai, R., Zhang, B., Wan, Y., Li, C., Wang, J., Liu, J., 2013. Chitosan-halloysite hybrid-nanotubes: Horseradish peroxidase immobilization and applications in phenol removal. *Chemical Engineering Journal*, 214: 304-309.
- [10] Zhang, Y., Tang, A., Yang, H., Ouyang, J., 2016. Applications and interfaces of halloysite nanocomposites. *Applied Clay Science*, 119(1): 8-17.

Synthesis of Magnetic Halloysite Nanotube-Alginate Hybrid Beads: Use in the Removal of Methylene Blue from Aqueous Media

GORKEM POLAT, YESIM SAG ACIKEL*

Hacettepe University, Beytepe Campus, Department of Chemical Engineering,
Cankaya/Ankara, 06800

Abstract

The aim of this study is to investigate the potential of magnetic halloysite nanotube-alginate (MHNT-ALG) hybrid beads for the removal of methylene blue (MB) from aqueous solutions. Magnetic halloysite nanotubes (MHNTs) were obtained according to co-precipitation method based on combination of Fe₃O₄ nanoparticles and HNTs. MHNT-ALG hybrid beads were produced by extrusion dripping method. The batch adsorption experiments of MB were performed to evaluate adsorption performance of beads. The influences of pH, amount of MHNT-ALG hybrid beads, mass ratio of ALG to MHNT and initial MB concentration on their adsorption capacity were analyzed. The optimum pH, mass ratio of ALG to MHNT, amount of hybrid beads, and initial MB concentration were found as pH 5.0, 2:1, 0.50 mg/mL, and 500 mg/L, respectively. At this conditions the initial adsorption rate, the amount of adsorbed MB per unit weight of MHNT-ALG, and the adsorption efficiency were found as 44.39 mg/g-min, 659.92 mg/g and 67.33%, respectively.

Keywords: Wastewater, adsorption, methylene blue, magnetic halloysite nanotube-alginate hybrid bead

I. INTRODUCTION

IN recent years, the removal of dyes from wastewater becomes an important issue. Industries such as leather, textile, paper, plastics, etc., are some of the sources for synthetic dyes. Many dyes such as MB have toxic and mutagenic effects (Ken Gillman, 2011). Therefore, contamination of dyes causes serious environ-

mental problems, which affect aquatic life and human health. Some methods such as flocculation, precipitation, ozonation, membrane filtration and electrochemical techniques are not always effective and economical (Dabrowski, 2001). Adsorption against these methods is more effective and simple process. In addition, this method has lower energy consumption.

Many biopolymer adsorbents have been

*Corresponding author e-mail: yesims@hacettepe.edu.tr

widely used in removal of dyes, as they are biodegradable, environmentally friendly, efficient and inexpensive (Crini, 2006). Among the wide variety of adsorbents, alginate which is mainly extracted from brown seaweed, is a linear polysaccharide with homopolymeric and heteropolymeric blocks of (1,4)-linked β -D-mannuronate and α -L-guluronate. Alginate may be formed to hydrogel through the ionic interaction with divalent cations such as Ca^{2+} and Zn^{2+} . This increases its mechanical strength and make it practical to use (Pawar and Edgar, 2012). Besides, this hydrogel form makes it easy to compose with materials such as carbon nanotubes, graphene, chitosan, halloysite nanotubes (HNTs), etc.

HNT is a kind of aluminosilicate clay mineral with layered hollow structure and has the molecular formula of $\text{Al}_2\text{Si}_2\text{O}_5(\text{OH})_4 \cdot n \text{H}_2\text{O}$. While the inner surface of tubular structure consists of Al-O groups, the outer surface consists of Si-O groups (Joussein, Petit, Churchman, Theng, Righi and Delvaux, 2005). Due to their structure and large specific surface area, HNTs have been proven to be attractive adsorbents for various metal ions and organic pollutants (Yuan, Tan and Annabi-Bergaya, 2015).

As magnetic separation technology is more selective, efficient and generally much faster than centrifugation or filtration processes, it has attracted great interest in recent years. Moreover, the use of an external magnetic field provided by a permanent magnet for separation is enough and power consumption is not necessary (Gomez-Pastora, Bringas and Ortiz, 2014). The combination of Fe_3O_4 nanoparticles has magnetic properties and HNTs makes it an ideal sorbent for magnetic separation (Duan, Liu, Chen, Zhang and Liu, 2012).

To the best of our knowledge, to date, there are only few published studies using HNT-ALG biocomposite beads as adsorbent to remove the dyes or heavy metals. However, magnetic HNT-ALG biocomposite gels for removal of heavy metals and dyes have not been used, yet. In this study, magnetic HNTs will be synthesized and magnetic halloysite nanotube-alginate (MHNT-ALG) hybrid beads will be

composed with synthesized MHNTs. In this way, while adsorption capacity of composite is increasing, HNTs are used as the supporting matrix for ALG and its mechanical properties and chemical stability also improves (Liu, Wan, Xie, Zhai, Zhang and Liu, 2012). The adsorption of MB by MHNT-ALG will be investigated as a function of medium pH, mass ratio of ALG to MHNT, amount of hybrid beads and initial dye concentration.

II. MATERIALS AND METHODS

Materials

HNTs were purchased from Sigma-Aldrich. The characteristic dimensions of the HNTs range from about 1-1.3 μm in length, 30-70 nm in diameter. All solutions were prepared using deionized (DI) water obtained from Thermo Scientific Smart2Pure water purification system, with resistivity of 18.2 $\text{M}\Omega \text{ cm}$. Iron(II) chloride tetrahydrate ($\text{FeCl}_2 \cdot 4\text{H}_2\text{O}$), iron(III) chloride hexahydrate ($\text{FeCl}_3 \cdot 6\text{H}_2\text{O}$), calcium chloride (CaCl_2) and sodium alginate were also supplied from Sigma-Aldrich. Ammonium hydroxide solution (NH_4OH) (32% NH_3 extra pure) was provided from MERCK.

Synthesis of halloysite-supported (MHNT)

In a typical synthesis, a weighed amount of HNTs (0.5 g) was dispersed in 200 mL of deionized water in a 500 mL five-neck glass reactor by stirring. To remove dissolved oxygen, the HNTs suspension was treated with N_2 under vacuum conditions for 20 min. Weighed amounts of $\text{FeCl}_2 \cdot 4\text{H}_2\text{O}$ and $\text{FeCl}_3 \cdot 6\text{H}_2\text{O}$ were then added to the reactor to obtain a molar ratio of Fe^{2+} to Fe^{3+} of 1:2. The N_2 purging to the reaction mixture was further continued under vacuum conditions for 20 min. The temperature of the mixture was then increased to 80 $^\circ\text{C}$. The NH_4OH (0.5 M) was poured slowly to the reaction mixture using a syringe pump. The reaction mixture was further stirred vigorously at this temperature under N_2 bubbling for 1 h. The MHNTs were allocated by magnetic decantation and then washed 4 times

with deionized water. The final washing step was followed by drying of the particles in a vacuum oven at 80 °C for 12 h (Owoseni et al, 2016).

Synthesis of MHNT-ALG hybrid beads

The preparation process of MHNT-ALG hybrid beads was given as follows. Sodium alginate (2 g) and MHNT (2 g) were mixed into deionized water (100 mL), and the mixture was kept at room temperature for 24 h with stirring. Then the mixture was slowly dropped into 20g/L calcium chloride solution by syringe under continuous stirring. The hybrid beads formed and then were kept waiting for 24 h. To remove the un-reacted materials which remained on the beads surface, the hybrid beads were washed several times with deionized water. Finally, the MHNT-ALG hybrid beads were freeze-dried for 24 h.

Adsorption experiments

The batch adsorption experiments were carried out in 50 mL tubes. Certain amount of MHNT-ALG hybrid beads was added to the adsorption media containing various concentrations of MB solutions. The tubes were shaken at

25 °C by the circular-rotator equipment. Samples were taken from the adsorption media at certain time intervals, the MHNT-ALG beads remained in the sample liquid were separated using an external magnetic field. The effects of different control parameters, such as the solution pH, contact time, initial dye concentration, amount of hybrid beads and mass ratio of components of the hybrid beads to each other on the MB adsorption by MHNT-ALG hybrid beads were investigated. The unadsorbed MB concentrations in the sample supernatant were measured at 668 nm using UV-visible spectrophotometer.

III. RESULTS AND DISCUSSION

The SEM images of the MHNT-ALG hybrid beads showed that MHNTs were encapsulated in alginate gels (Fig. 1). A porous structure on the MHNT-ALG hybrid bead surface was observed while surface of the pure ALG bead showed a smooth and dense structure. The MHNTs appeared to be overlap loosely together in the interior of the MHNT-ALG hybrid beads.

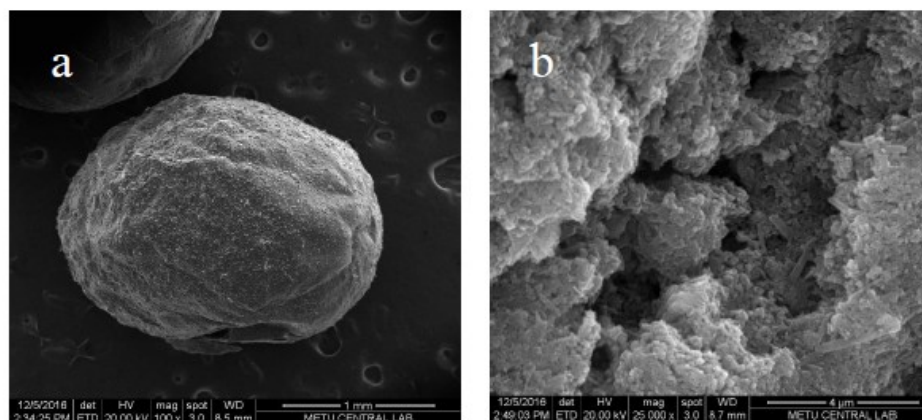


Figure 1. SEM images of the external surface (a) and the internal structure

(b) of MHNT-ALG hybrid beads

Effect of pH

HNTs includes gibbsite octahedral sheet (Al-OH) groups on the internal surface and siloxane groups (Si-O-Si) on the external surface.

For that reason, the surface charge of HNTs is negative at pH 2.0-8.0 and similar to the surface potential of SiO₂. The inner surface of HNTs is positive representing the surface

charge of positive Al_2O_3 . On the other hand, the negative carboxylic groups are the most wide acidic functional groups in the alginate polymer, and the sorption capacity of ALG is associated with the presence of these binding sites. MHNT-ALG biogels have negatively charged surface for electronic interaction with cationic pollutants. The initial adsorption rates

of MB and the amount of adsorbed MB per unit weight of MHNT-ALG increased with increasing pH at the range from 2.0 to 4.0. At the pH range from 4.0 to 6.0, the initial adsorption rates, equilibrium removal capacity and efficiency remained approximately constant (Fig. 2).

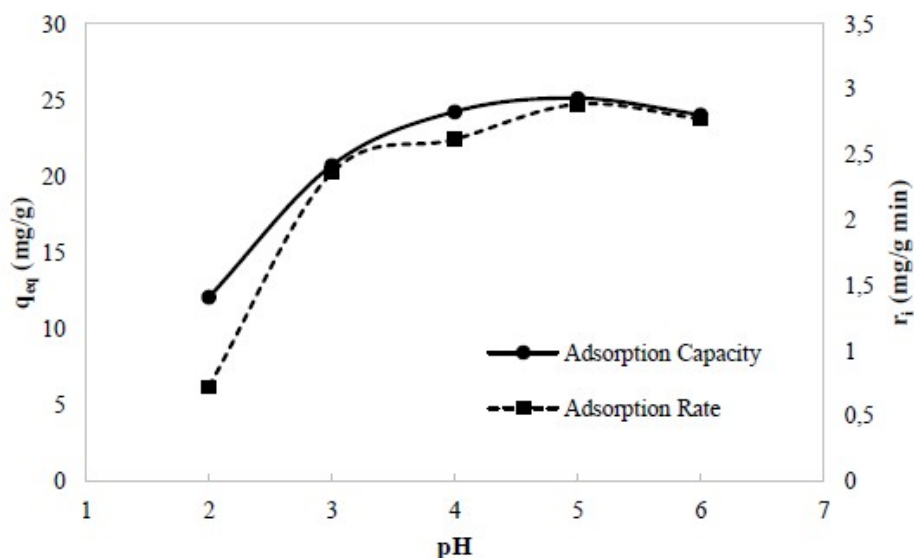


Figure 2. Effect of pH change for batch adsorption of MB on MHNT-ALG hybrid beads. Conditions: amount of adsorbent: 0.025 g; ALG-MHNT ratio: 2:2; solution volume: 25 mL; temperature: 25°C; initial MB concentration: 30 mg/L; contact time: 3h

At pH values lower than 4.0, excess amount of H^+ ions compete with the cationic MB for free adsorption sites on MHLT-ALG. When the ratio of ALG to MHNT was chosen as 2:2, the maximum initial adsorption rate, amount of adsorbed MB per unit weight of MHLT-ALG, and equilibrium efficiency at 30 mg/L initial MB concentration were obtained at pH 5.0, and determined as 2.88 mg/g min, 25.11 mg/g and 90.7%, respectively.

Effect of contact time

The adsorbed amount of MB per unit weight of

MHNT-ALG increased rapidly within a contact time of about 15-30 min depending on initial MB concentration, and then gradually to reach adsorption equilibrium. When the initial dye concentration was increased, the time required to establish adsorption equilibrium extended. A contact time of 60-180 min was sufficient for reaching adsorption equilibrium. The adsorption capacities reached 148.91 mg/g (75.78% removal) for 30 min and achieved 176.43 mg/g (91.29% removal) for 120 min at initial MB concentration of 100 mg/L (Fig. 3).

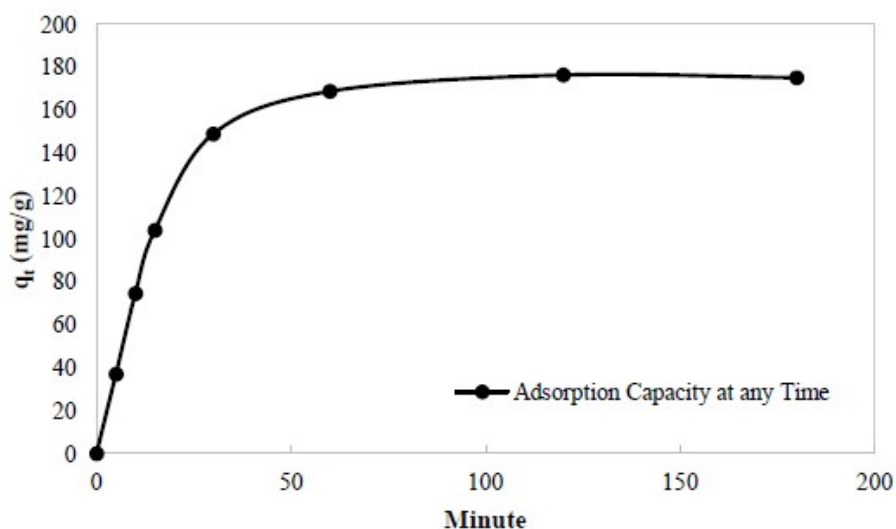


Figure 3. Effect of changing the adsorption capacity at any time for batch adsorption of MB on MHLT-ALG hybrid beads. Conditions: amount of adsorbent: 0.0125 g; pH: 5; ALG-HLT ratio: 2:1; solution volume: 25 mL; temperature: 25°C; initial MB concentration: 100 mg/L; contact time: 3h

Effect of amount of MHNT-ALG

The amount of MHNT-ALG beads at 2:2 ratio of ALG to MHNT in solution was increased in the range of 0.1-3.0 mg/mL, the adsorbed concentration of MB increased up to 1.0 mg/mL because of an increasing adsorption surface area, then remained approximately constant. On the other hand, the amount of adsorbed MB per unit weight of MHNT-ALG beads decreased with increasing amount of beads.

Amount of MHNT-ALG of 0.5 mg/mL appears to be an optimum adsorbent concentration with respect to the adsorbed MB concentration, efficiency and process economy (Fig. 4). Although the decrease in q_{eq} with increase in amount of beads is due to complex interactions of several factors, there are two main reasons. Firstly, the initial adsorption rate of MB decreased from 8.22 mg/g-min to 3.23 mg/g-min with increasing amount of MHNT-ALG between 0.1 mg/mL and 3 mg/mL, and hence more time is required to reach equilibrium. Secondly, the extent of desorption of MB can increase with enhancing amount of MHNT-ALG beads, as a result of collision of beads, and the potential of multilayer sorption can be

reduced. The adsorbed concentration of MB, the amount of adsorbed MB per unit weight of MHNT-ALG beads and the equilibrium efficiency obtained at 0.5 mg/mL MHNT-ALG, at 80 mg/L MB concentration and at pH 5.0 were determined as 74.54 mg/L, 128.21 mg/g, and 93.02%, respectively.

Effect of the mass ratio of ALG to MHNT on MB adsorption

The effect of the mass ratio of ALG to MHNT on MB adsorption was investigated at 2:0; 2:1; 2:2; 2:3. When the mass ratio of ALG to MHNT was chosen as 2:0; 2:1, the initial adsorption rate, equilibrium removal and efficiency increased slightly. When the mass ratio of ALG to MHNT was determined as 2:3, the equilibrium removal and efficiency of MB decreased at negligible level (Fig. 5). It can be explained that the dye binding sites on ALG cannot be covered by HNTs and HNTs are also effective MB adsorbent. At the mass ratio of ALG to MHNT changed from 2:1 to 2:3, only initial adsorption rate of MB decreased from 9.95 mg/g-min to 5.92 mg/g-min, it was indicated that pores of ALG were filled by HNT and diffusion

limitations for MB increased. The maximum initial adsorption rate, the amount of adsorbed MB per unit weight of MHNT-ALG and the adsorption efficiency at 80 mg/L initial MB

concentration and at pH 5.0 were obtained in the mass ratio of ALG to MHNT of 2:1, and were found as 9.95 mg/g-min, 124.84 mg/g, 92.85%, respectively.

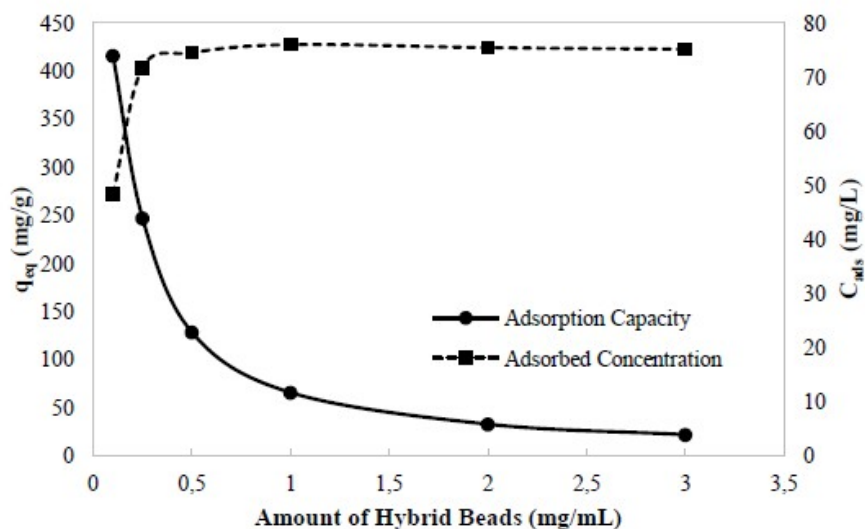


Figure 4. Effect of changing the amount of adsorbent for batch adsorption of MB on MHLT-ALG hybrid beads. Conditions: pH: 5; ALG-HLT ratio: 2:2; solution volume: 25 mL; temperature: 25°C; initial MB concentration: 80 mg/L; contact time: 3h

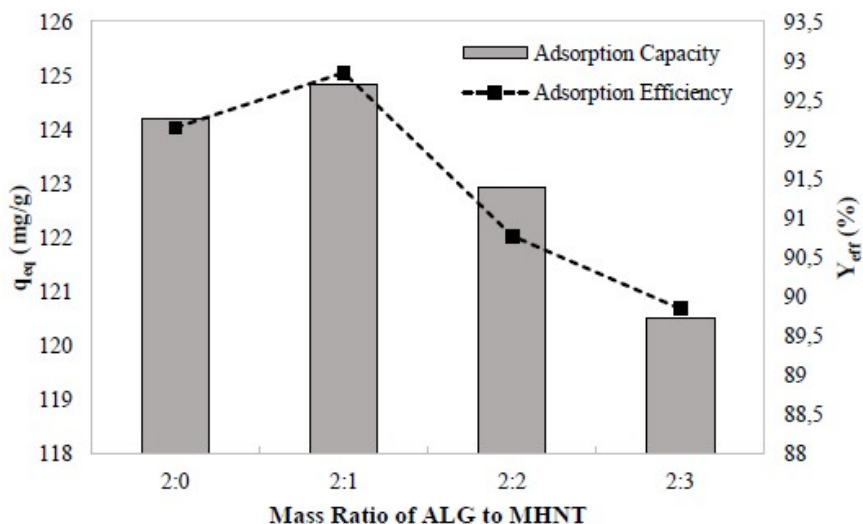


Figure 5. Effect of the mass ratio of ALG to MHNT for batch adsorption of MB on MHLT-ALG hybrid beads. Conditions: amount of adsorbent: 0.0125 g; pH: 5.0; solution volume: 25 mL; temperature: 25°C; initial MB concentration: 80 mg/L; contact time: 3h

Effect of initial MB concentration

Effect of initial MB concentration was investigated at pH 5.0, at 0.5 mg/mL MHNT-ALG, and at the mass ratio of ALG to MHNT of 2:1. The adsorbed MB concentrations and specific adsorbed MB quantities per unit weight of MHNT-ALG beads increased continually with increasing MB concentrations up to 500 mg/L, and were obtained as 337.52 mg/L, 659.92 mg/g, respectively at this initial MB concentration (Fig. 6). This can be attributed to the fact that increases in the initial dye concentra-

tion result in a large difference in concentration between composite surface and dye solution or a strong driving force and further uptake of the MB in the solution. The maximum initial adsorption rates of MB followed the same trend, and the maximum adsorption rate was found as 44.39 mg/g-min at 500 mg/L initial MB concentration. The adsorption efficiency remained approximately constant at 91% at initial MB concentrations between 30 mg/L and 200 mg/L, then began to decrease.

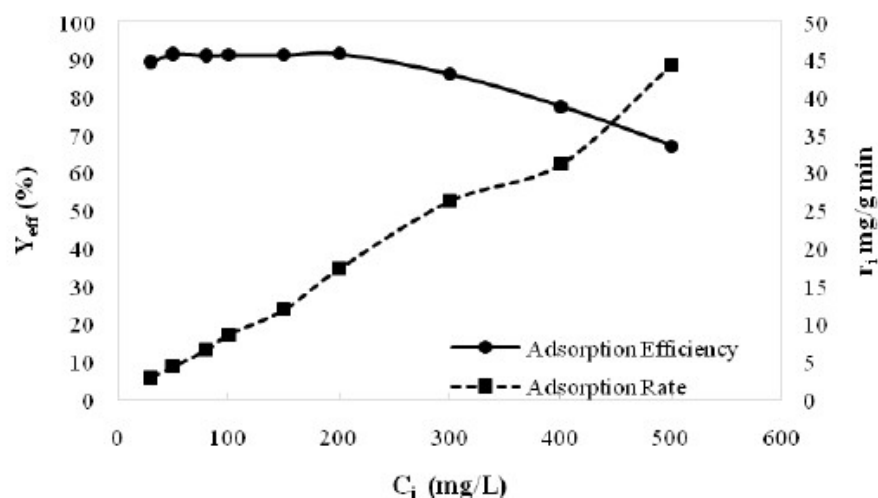


Figure 6. Effect of initial MB concentration for batch adsorption of MB on MHLT-ALG hybrid beads. Conditions: amount of adsorbent: 0.0125 g; ALG-MHLT ratio: 2:1; pH: 5.0; solution volume: 25 mL; temperature: 25°C; contact time: 3h

IV. CONCLUSIONS

In this study, novel magnetic HNT-ALG hybrid beads were shown to remove MB dye quickly and efficiently under acidic conditions (pH 5.0) via mainly electrostatic interactions between cationic MB and negative charged MHNT-ALG. The maximum initial adsorption rate, the amount of adsorbed MB per unit weight of MHNT-ALG, and the adsorption ef-

iciency were found as 44.39 mg/g-min, 659.92 mg/g and 67.33%, respectively, at pH 5.0, the mass ratio of ALG to MHNT of 2:1, the amount of hybrid beads of 0.50 mg/mL, and initial MB concentration of 500 mg/L. Magnetism property of MHNT-ALG hybrid beads makes them particularly suitable for dye removal because no centrifugation or filtration (versus non-magnetic HNT-ALG hybrid beads) of the treated wastewater are then required.

V. ACKNOWLEDGEMENTS

The authors wish to thank TUBITAK, the Scientific and Technical Research Council of Turkey with 2210-C programme.

REFERENCES

- [1] Crini, G., 2006. Non-conventional low-cost adsorbents for dye removal: A review. *Bioresource Technology*, 97(9): 1061-1085.
- [2] Dabrowski, A., 2001. Adsorption-From theory to practice. *Advances in Colloid and Interface Science*, 93(1-3): 135-224.
- [3] Duan, J., Liu, R., Chen, T., Zhang, B., Liu, J., 2012. Halloysite nanotube-Fe₃O₄ composite for removal of methyl violet from aqueous solutions. *Desalination*, 293: 46-52.
- [4] Gomez-Pastora, J., Bringas, E., Ortiz, I., 2014. Recent progress and future challenges on the use of high performance magnetic nano-adsorbents in environmental applications. *Chemical Engineering Journal*, 256: 187-204.
- [5] Joussein, E., Petit, S., Churchman, J., Theng, B., Righi, D., Delvaux, B., 2005. Halloysite clay minerals-A review. *Clay Minerals*, 40(4): 383-426.
- [6] Ken Gillman, P., 2011. Review: CNS toxicity involving methylene blue: The exemplar for understanding and predicting drug interactions that precipitate serotonin toxicity. *Journal of Psychopharmacology*, 25(3): 429-436.
- [7] Liu, L., Wan, Y., Xie, Y., Zhai, R., Zhang, B., Liu, J., 2012. The removal of dye from aqueous solution using alginate-halloysite nanotube beads. *Chemical Engineering Journal*, 187: 210-216.
- [8] Owoseni, O., Nyankson, E., Zhang, Y., Adams, D. J., He, J., Spinu, L., McPherson, G.L., Bose, A., Gupta, R.B., John, V.T., 2016. Interfacial adsorption and surfactant release characteristics of magnetically functionalized halloysite nanotubes for responsive emulsions. *Journal of Colloid and Interface Science*, 463: 288-298.
- [9] Pawar, S.N., Edgar, K.J., 2012. Alginate derivatization: A review of chemistry, properties and applications. *Biomaterials*, 33(11): 3279-3305.
- [10] Yuan, P., Tan, D., Annabi-Bergaya, F., 2015. Properties and applications of halloysite nanotubes: Recent research advances and future prospects. *Applied Clay Science*, 112-113: 75-93.

An Experimental Study of the Swelling Behavior of Starch Granules Under Heat Treatment

A., PLANA-FATTORI *, G., ALMEIDA, G., MOULIN, CH., DOURSAT, D., FLICK

UMR Ingenierie Procedes Aliments, AgroParisTech, INRA,
Universite Paris-Saclay, 91300 Massy, France

Abstract

Current models for predicting the transformation state of starch suspensions define the swelling degree in terms of the mean diameter of granules, with no information regarding the observed diversity of size and swelling onset. This article analyzes the thermal history of 143 granules as obtained from images captured during hot-stage normal light microscopy of droplets of a modified waxy maize starch suspension. The evolution of 0.5 mL samples was studied under heat treatment from 50 to 90 °C at rate of 5 °C/min. No relationship was found between initial granule diameter and swelling onset temperature. Changes in the starch swelling state were relatively weak below 60 °C and above 80 °C. Simultaneous occurrence of uncooked starch and swollen granules was observed at intermediate temperatures.

Keywords: Starch, swelling, size distribution, heat treatment, thermal history, hot-stage microscopy

I. INTRODUCTION

THE mechanisms driving the transformation of ingredients along the processing pathway need to be understood as a necessary step for manufacturing food products in a reproducible manner. To predict the product transformation and the associated rheological evolution represents a challenging task, even for a simple liquid product like an aqueous suspension of starch granules submitted to heat treatment.

Efforts have been devoted, since the early 1800s, in understanding the structural changes of starch granules heated in water (Ratnayake

and Jackson, 2008). Modifications experienced by starch under heating have been summarized as: disruption of crystalline and molecular order of starch granules, swelling and rupture of the granules, and reorganization of the disordered molecules (Matignon and Tecante, 2016). Swelling of granules plays a major role in driving the flow behavior of dilute starch suspensions (Lagarrigue and Alvarez, 2001). Current models for predicting the transformation state of starch suspensions define the swelling degree in terms of the mean diameter of granules, with no information regarding the diversity of size and swelling onset. Starch phase transition processes have been studied through a

*Corresponding author e-mail:artemio.planafattori@agroparistech.fr

number of techniques, including: normal and polarized light microscopy, scanning electron microscopy, differential scanning calorimetry, X-ray diffraction, high-performance size exclusion chromatography, and confocal laser scanning microscopy (e.g. Ratnayake and Jackson, 2007; Chen et al., 2011; Schirmer et al., 2013). Some techniques allow the real-time monitoring of the starch suspension while it is submitted to heat treatment; they enable the assessment of swelling kinetics with no additional starch transformation between the end of the heat treatment and laboratory analysis. This is the case of hot-stage microscopy, a standard technique employed since the 1960s (Carlson, 2011). The study of the granule size distribution along its thermal history constitutes the first step towards the prediction of transformation state and flow behavior of starch suspensions. This article analyzes the thermal history of individual granules as obtained from images captured during hot-stage normal light microscopy of droplets of a starch suspension.

II. EXPERIMENTAL METHODS AND DATA PROCESSING

The liquid product is a 0.5 g/kg starch suspension in water. Chemically-stabilized and cross-linked waxy maize starch (acetylated adipate distarch, C* Tex 06205) was kindly provided by Cargill (Baupte, France). It consisted of at least 99% of amylopectin (less than 1% of amylose). For this type of starch neither disruption of swollen granules nor release of amylose is expected (Matignon et al., 2014). The product was prepared by adding the starch powder to a 0.1 M NaCl aqueous solution. Before heat treatment, the resulting liquid remained at 50 °C for 30 min under continuous gentle stirring.

Samples of 0.5 mL were placed on a Linkam LTS120 stage (Linkam Scientific Instruments, Surrey, UK) and observed under 50 X magnification using an optical Olympus BX-51 mi-

croscope (Olympus Optical Co. Ltd., Tokyo, Japan). Adhesive spacers (total thickness of 250 μm) were fixed on the microscope slides in order to ensure free swelling of starch granules. The Linksys32 temperature control software was used for programming the hot-stage operation. The evolution of samples of the starch suspension was studied under the following heat treatment: firstly one minute at 50 °C, then heating from 50 to 90 °C at rate of 5 °C/min, and finally one minute at 90 °C. Images were captured every second with a Basler A102fc digital camera (Basler AG, Ahrensburg, Germany). Images at selected temperatures were retained for this study, namely: a) after one minute at 50 °C, b) at 60, 68, 70, 75, 80 and 90 °C during heating, and c) after one minute at 90 °C. Image processing was applied only to the starch granules which were recognized at all these temperatures. The characterization of each granule was performed through the public domain Java image processing program Image-J (version 1.42q, National Institutes Health, Bethesda, Maryland, USA), including the plug-in component that implements the active contour method AB-Snake (Andrey and Boudier, 2006). After manual recognition of granules, the software automatically contoured and measured them. The geometric mean of major and minor diameters of the ellipse with the same area than the surface occupied by the granule is hereafter called granule diameter. In a final processing step, conducted through routines written in MATLAB code (Mathworks, Natick, Massachusetts, USA), each granule was associated with the same numbering order over the set of images at different temperatures. In this article we discuss the results obtained for 143 starch granules, satisfactorily monitored after submitting 17 samples to the prescribed heat treatment. Figure 1 illustrates one of the samples at 50, 70, and 90 °C, as captured by the camera coupled to the microscope and after image processing through Image-J and MATLAB routines.

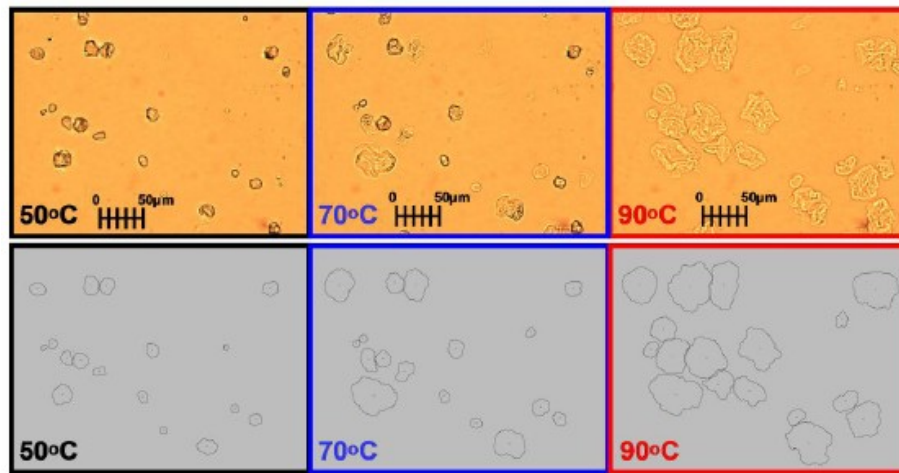


Figure 1: One sample at three selected temperatures, as captured by the digital camera (top), and after processing through Image-J and MATLAB routines (bottom).

III. RESULTS

All the observations considered in this study are shown in Figure 2A. Thin lines connect observations associated with a same thermal / swelling history. Selected histories are presented in Figure 2B. Firstly, starch granules associated with quite similar diameter at 50 °C

(as granules 50, 80 and 110) can evolve differently under a same heat treatment. Secondly, the final swelling state (say, the diameter observed after one minute at 90 °C) can be reached quite early during the heat treatment (between 60 and 68 °C in the case of granule 20). Lastly, in many cases, swelling is relatively weak above 75 – 80 °C.

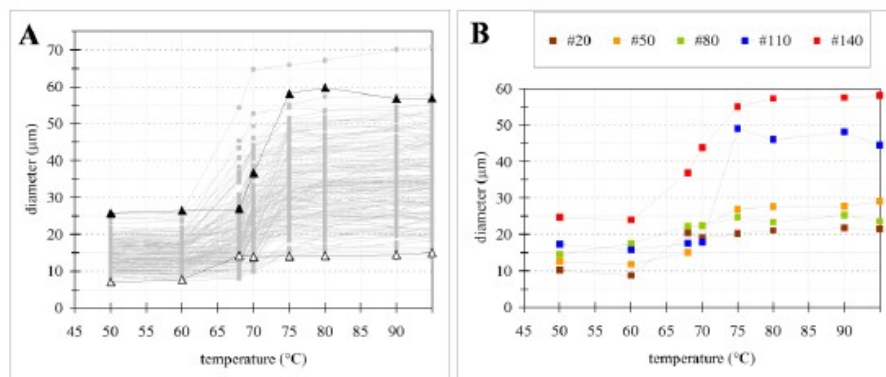


Figure 2: A) All the observations under consideration; white and black triangles indicate the thermal histories associated with the smallest (rank #1) and the largest (rank #143) granule diameter at 50 °C, respectively. B) Selected thermal histories, labeled by their rank. The right-most points correspond to the observation performed after one minute at 90 °C.

Figure 3A presents all the observations corresponding to the temperatures at the start (50 °C), at the middle (70 °C) and at the end

(90 °C) of the 8-min heating period (i.e. from 50 to 90 °C at rate of 5 °C/min). Observations are ordered increasingly with the granule di-

iameter at 50 °C. Observations are less scattered at 90 °C (near the end of the heat treatment) than at 70 °C. Figure 3B put in evidence that there are cases where there is no starch

swelling at 70 °C (103 and 110), cases where swelling is weak at 70 °C (102, 107, 108), and cases where the granule diameter has almost already reached its final value at 70 °C.

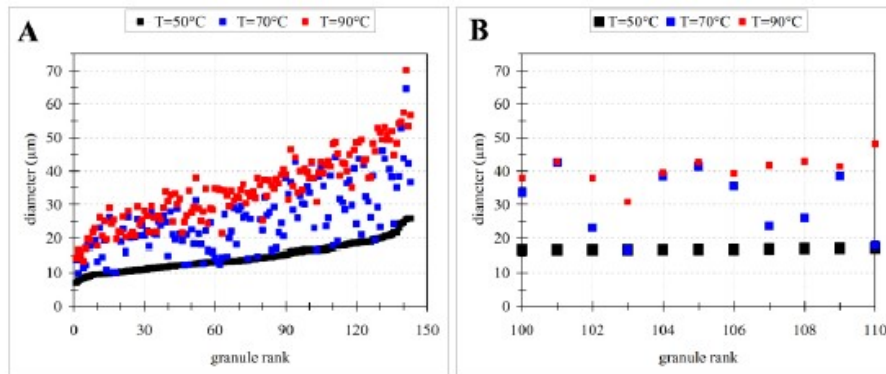


Figure 3: A) All the observations at three temperatures, showing granule diameters ordered increasingly with their value at 50 °C. B) The same, but for a selection of thermal histories.

The granule diameter at a given temperatures can be presented as a function of its value at the beginning of the heat treatment, as shown in Figures 4A and 4B. There are a lot of starch granules that exhibit similar diameters at 50 and 70 °C; such situation corresponds to

the points situated near the line $d_{70} = d_{50}$ on Figure 4A. Looking for the mean relative increase of granule diameter (with respect to its value at 50 °C), we obtained a regression line intercepting zero for each scatter diagram.

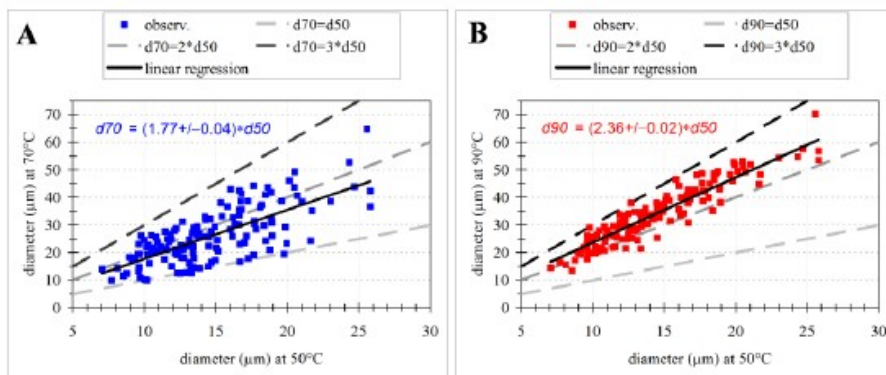


Figure 4: Granule diameter d_{70} at 70 °C (A) and d_{90} at 90 °C (B) as a function of its value d_{50} at 50 °C. Dashed lines correspond to three hypothetical values for the increase. Bold continuous lines indicate linear regressions intercepting zero.

The regression lines shown in Figure 4 constitute zero-order models for predicting the granule diameter at a selected temperature, provided that the diameter is known at 50 °C.

A higher-order predictive model might consider the relative increase dT/d_{50} in function of the diameter at 50 °C. Figure 5A presents the diameter increase values up to 70 and 90 °C, or

dered increasingly with the diameter at 50 °C. The increase d_{90}/d_{50} exhibits higher average (2.34) and smaller standard deviation (0.28) than the increase d_{70}/d_{50} (1.77 and 0.45, respectively). Figure 5B displays the observations as function of the diameter at 50 °C, as well as the regression lines $dT/d_{50} = \alpha d_{50} + \beta$. In the case of d_{70}/d_{50} , the standard error of α ($0.01 \mu\text{m}^{-1}$) is many times larger than the α value itself ($0.0006 \mu\text{m}^{-1}$); the probability of null value for α is high (about 95%). The dependence of the increase d_{70}/d_{50} with the diameter at 50 °C is overwhelmed by its own variability (Figure 5A), which is associated in

a large extent with the variability of diameters at 70 °C (Figures 3A and 4A). Contrarily, in the case of the increase d_{90}/d_{50} , the standard error of α ($0.006 \mu\text{m}^{-1}$) is smaller than the α value ($0.011 \mu\text{m}^{-1}$) and the probability of null value for α is relatively low (about 6 %). The dependence of the increase d_{90}/d_{50} with the diameter at 50 °C is significant: on average, larger is the granule before the heat treatment, higher is the increase between 50 and 90 °C; nevertheless, this dependence remains weak. The variability of d_{90}/d_{50} can be explained for a small part by the initial diameter ($r^2 = 0.03$).

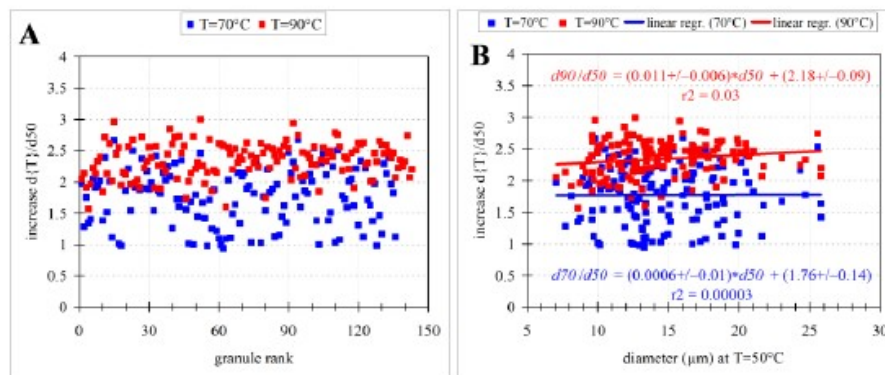


Figure 5: Diameter increase from 50 °C up to two selected temperatures, as a function of the granule rank (A), and of the granule diameter at 50 °C (B). Bold lines indicate linear regressions; equation parameters are presented plus/minus one standard error.

Figures 6A and 6B show the cumulative distribution of granule diameters. In increasing the temperature, the distribution of diameters becomes progressively wider and associated with larger median values. Early steps of the heat treatment are summarized by the distributions at 50 and 60 °C; their relative proximity indicates that, on average, starch swelling is weak below 60 °C. Final steps of the heat treatment are summarized by the three last distributions: they span over the last 3 minutes of the treatment and suggest that maximum swelling is essentially concluded at about 80 °C. Between these two groups of results, the distributions at 68 and 70 °C are clearly distinct despite

their proximity in time; following a 5 °C/min heating rate, images at 70 °C were captured 24 seconds after than those at 68 °C. Starch swelling can, for a great number of granules, be pictured as a somewhat 'explosive' transformation phenomenon. Figure 6B employs a logarithmic scale for granule diameters: they can be supposed to follow log-normal distributions. Observations at 50 °C correspond to a mean of 14.6 μm and a standard-deviation of 4.0 μm ; observations at 90 °C correspond to a mean of 34.5 μm and a standard-deviation of 11.2 μm . Relative standard deviations are a little different: about 27% at 5 °C and 33% at 90 °C.

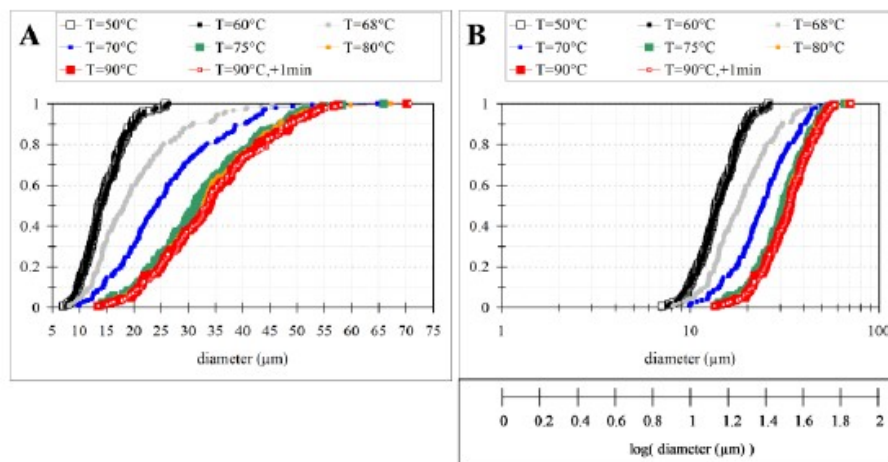


Figure 6: Cumulative distribution of the granule diameter (A) and of its logarithm (B) at each temperature considered.

Figure 7A presents the cumulative distribution of the diameter increase from 50 °C up to each temperature considered. The distributions corresponding to 60, 68 and 70 °C start below the unity. One may ask the influence of experimental errors on such a finding. The estimation of granule diameters can be affected by random errors due to the automatic acquisition of images and to the human-made recognition of the granule of interest in each image. The occurrence of bias between samples is expected to be negligible, firstly because the prescribed heat treatment was repeated to droplets of starch suspensions which were prepared following the same protocol, and secondly because the same image processing method was applied to all the available observations.

Figure 7B focus the attention on values near to the unity. A range of diameter increase values is indicated, centered at the unity; its half-width equals 0.14, which corresponds to the difference between the unity and the smallest value observed at 60 °C (about 0.86). Changes in the granule size distribution of cross-linked waxy maize starch under heating rate close to 5 °C/min are not expected to be important for temperatures below 60 °C (Ziegler et al., 1993). Therefore, the shape of the cumulative distribution corresponding to 60 °C cannot be attributed to changes in starch swelling state.

A plausible explanation for these patterns near the unity is that starch granules do not remain immobile during the heat treatment. Once in diluted aqueous suspension, they are free to change their orientation with respect to the observing device. Starch granules are not spherical; if one granule is assimilated to an axisymmetrical ellipsoid, its projection becomes an ellipse: one axis length is the equatorial diameter, while the other varies between the later and the pole-to-pole distance depending on the orientation. Hence, from an image to its following, even if no starch swelling occurs, the visible area of a given granule can either increase or decrease. Such an explanation turns easier to understand why the diameter value may (apparently) decrease not only between 50 and 60 °C but also elsewhere in the granule history (for instance, granules 80 and 100 in Figure 2A).

We argue that observations associated with increase values smaller than the 1.14 correspond to conditions where granule orientation, and not starch swelling, dominates the diameter increase value. The distribution corresponding to 60 °C falls almost entirely into the range indicated in Figure 7B; actually, only 3 observations (over 143) are associated with values higher than 1.14 for the diameter increase from 50 up to 60 °C. At higher temperatures, the

fraction of diameter increase values higher than 1.14, which can only be explained by starch swelling, becomes significant: 78/143 \sim 55% at 68°C and 123/143 \sim 86% at 70°C. The in-

fluence of granule orientation is secondary for all the observations at 50°C75 and higher temperatures.

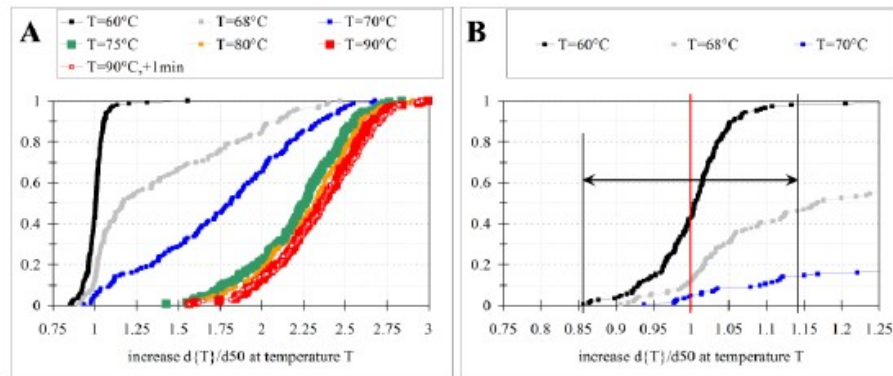


Figure 7: A) Cumulative distribution of the diameter increase from 50 °C up to each temperature considered. B) The same, but focusing on diameter increase near to the unity.

IV. CONCLUSIONS AND FUTURE WORK

The study of the thermal history experienced by 143 granules of a modified waxy maize starch suspension, exposed to the same heat treatment, confirmed the diversity of granule size and temperature associated with swelling onset. No simple relationship emerges between initial size and swelling onset. Secondly, changes in the starch swelling state were relatively weak under temperatures below 60°C, as well as above 80°C. At the intermediate temperatures, distinct populations of granules co-existed: starch swelling can be negligible at 70°C for some granules but significant for others.

Thirdly (and consequently), the diameter increase from 68°C50 up to 70°C exhibited more important variability than up to 90°C; under such conditions it appears more difficult to

predict the diameter increase from 50°C up to 70°C than up to 90°C.

Lastly, the analysis of diameter increase values near the unity revealed that a great number of observations below 70°C corresponded, actually, to a diameter decrease. This was interpreted as being due to changes of granules orientation with respect to the observing device, the granules being not spherical. Combined effects of starch swelling and granule orientation are intrinsically included in all the observations resulting from our experimental approach.

Looking for the development of predictive models for the starch granule size distribution, ongoing efforts are devoted to the influence of the heat treatment (both intensity and duration) as well as to the role played by granule orientation on observations.

V. ACKNOWLEDGEMENTS

Authors acknowledge Professor Camille Michon for helpful discussions and Camila Pinheiro Silva Cazado (trainee in May-June 2016) for her dedication in conducting experimental work and image processing.

REFERENCES

- [1] Andrey, P., Boudier, T., 2006. Adaptive active contours (snakes) for the segmentation of complex structures in biological images. Proceedings of the 1st Image-J User & Developer Conference, 18-19 May, Luxembourg.
- [2] Carlton, R.A., 2011. Pharmaceutical Microscopy. Springer.
- [3] Chen, P., Yu, L., Simon, G.P., Liu, X., Dean, K., Chen, L., 2011. Internal structures and phase-transitions of starch granules during gelatinization. *Carbohydrate Polymers* 83: 1975-1983.
- [4] Lagarrigue, S., Alvarez, G., 2001. The rheology of starch dispersions at high temperatures and high shear rates: A review. *Journal of Food Engineering*, 50: 189-202.
- [5] Matignon, A., Moulin, G., Barey, P., Desprairies, M., Mauduit, S., Sieffermann, J. M., Michon, C., 2014. Starch / carrageenan / milk proteins interactions studied using multiple staining and Confocal Laser Scanning Microscopy. *Carbohydrate Polymers*, 99: 345-355.
- [6] Matignon, A., Tecante, A., 2016. Starch retrogradation: from starch components to cereal products. *Food Hydrocolloids*, in press.
- [7] Ratnayake, W.S., Jackson, D.S., 2007. A new insight into the gelatinization process of native starches. *Carbohydrate Polymers*, 67: 511-529.
- [8] Ratnayake, W.S., Jackson, D.S., 2008. Starch Gelatinization. *Advances in Food Science and Nutrition Research*, 55: 221-268.
- [9] Schirmer, M., Hochstotter, A., Jeckle, M., Arendt, E., Becker, T., 2013. Physicochemical and morphological characterization of different starches with variable amylose / amylopectin ratio. *Food Hydrocolloids*, 32: 52-63.
- [10] Ziegler, G.R., Thompson, D.B., Casanovas, J., 1993. Dynamic measurement of starch granule swelling during gelatinization. *Cereal Chemistry*, 70(3): 247-251.

Application of Ultrasound to Extraction of Biologically Active Substances of Some *Serratula* Species

Larisa Zibareva^{1*}, Anan Athipornchai², Orawan Wonganan²,
Apichart Suksamrarn²

¹Tomsk State University, pr. Lenina, 36, Tomsk, 634050 Russia

²Ramkhamhaeng University, Bangkok, 10240, Thailand

Abstract

The ecdysteroid constituents of three Serratula species introduced in culture into the Siberian Botanical Garden were studied. The ecdysteroids discovered in S. cupuliformis for the first time include 20-hydroxyecdysone, polypodine B, 2-deoxy-20-hydroxyecdysone, ecdysone and makisterone A. HPLC analysis showed that both S. manshurica and S. gmelinii contained 20-hydroxyecdysone, polypodine B, 2-deoxy-20-hydroxyecdysone and ecdysone. The unusual accumulation of ecdysteroids in the studied species was investigated. The structures of isolated three compounds were identified by spectroscopic methods (NMR, MS) and the presence of other ecdysteroids was defined by HPLC method. Comparison of the composition of the ecdysteroids three species of Serratula, imposed into culture to Western Siberia, has shown that they have high content and similar composition of main of ecdysteroids. High intensity ultrasound can speed the extraction flow, increase yield of ecdysteroids, and to carry out extraction at room temperature. The application of the method of ultrasonic extraction of biologically active compounds from plant material reduce the time and volume of solvents. Extraction time of biologically active substances from the aerial parts of Serratula cupuliformis reduced to 12 times. High-intensity ultrasound has accelerated process and increased the yield of flavonoids. Devastating effect of ultrasound on secondary metabolites no observed, as confirmed by the UV spectra, high performance liquid chromatography and high contents of these substances.

Keywords: Species Serratula, ecdysteroids, flavonoids, ultrasonic extraction

*Corresponding author e-mail: zibareva.lara@yandex.ru

I. INTRODUCTION

Phytoecdysteroids contribute to the protection of plants against invertebrate predators. All insects need ecdysteroids, but they are not able to synthesize ecdysteroids from simple compounds. The steroid precursors (for example, cholesterol, schottenol and sitosterol) are therefore needed. Plants synthesize steroid skeleton from simple compounds. Phytoecdysteroids are hormonally inactive and they are not toxic to mammals. It has been established that they have anabolic (Syrov and Kurmukov, 1976), restorative, adaptogenic, immunostimulative, antiradiation (Zibareva, 2012) and haemorrhological (Plotnikov et al., 2000) properties. Their ability to significantly reduce the content of cholesterol in blood serum was observed (Akhrem and Kovganko, 1989).

The inhibition of sarcoma cell growth and other cancers by ecdysone has been reported (Akhrem and Kovganko, 1989). The ecdysteroid constituents of *S. coronata*, which is used as pharmacological raw material for making the agents of anabolic, adaptogenic, tonic, hepatoprotective actions, such as Ekdifit (Adykenov, 2010) and Serpisten (Volodin et al., 2006), have intensively been studied. Flavonoids are not the common constituents of *Serratula* plants. However, they have been found in the following species: *S. coronata*, *S. gmelinii*, *S. lycopifolia* (*S. heterophylla*), *S. tinctoria* (*S. inermis*) (Bathori et al., 1999), *S. strangulata* (Wang et al., 2002). The richest ecdysteroid-producing plant families are Asteraceae and Caryophyllaceae. So far it is known that ecdysteroids have been synthesized in the following *Serratula* (Asteraceae) species: *S. algida*, *S. centauroides*, *S. quinquefolia*, *S. procumbens* (Novoselskaya et al., 1981), *S. coronata* (Revina et al., 1986; Kholodova, 1979; Abubakirov, 1982), *S. chinensis* (Chen and Wei, 1989), *S. erucifolia* (L.) Boriss. (*S. xeranthemoides* Bieb.) (Abubakirov, 1984; Kholodova et al., 1979), *S. sogdiana* (Zatsny et al., 1971; Novoselskaya et al.,

1975), *S. cardunculus*, *S. coriaceae*, *S. gmelinii*, *S. lycopifolia*; *S. radiata* (Aleksieva et al., 2003), *S. lyratyfolia* (Ganiev, 1980), *S. komarovii*, *S. manshurica* (Zarembo, 2001; Vorobyeva et al., 2006), *S. marginata* (Munkhzhargal and Zibareva, 2008), *S. strangulata* (Wang et al., 2002; Wang et al., 2002), *S. tinctoria* L. (*S. inermis* Gilib.) (Bathori et al., 1986; Bathoriet et al., 1999), *S. wolffii* (Akhmed et al., 1990).

Distinctive ecdysteroids for this species of plants are 20-hydroxyecdysone, inokosterone, makisterone A and ecdysone, which were regarded as chemotaxonomic markers of the genus (Zatsny et al., 1971).

The purpose of this research is the study of the effects of ultrasound on the extraction of secondary metabolites, and study of the composition of ecdysteroids in some species of *Serratula*, introduced to the culture in Siberian Botanical Garden of Tomsk State University.

II. MATERIALS AND METHODS

Plant materials

Serratula cupuliformis grows in northern China in grass areas on slopes and in open forests (Rastitelny, 1993). The seeds were obtained from the Botanical Garden of the city of Jena (Germany). *Serratula gmelinii* is wide spread in the European part of the USSR, Western Siberia and Southern Urals (Rastitelny, 1993).

The seeds were obtained from the Botanical Garden of the city of Cluj-Napoca (Romania). *Serratula manshurica* is wide spread in Primorye and Priamurye (Vorobyeva et al., 2006). The seeds were obtained from the Botanical Garden of the city of Chita (Russia).

Processing of plant materials

The seeds plants were cultivated for the first time in the Siberian Botanical Garden of the Tomsk State University.

The aerial parts of plants were collected in flowering, dried at 20 °C and crushed to particles 0.1 mm. *S. cupuliformis* is firstly introduced as a source of ecdysteroids.

Extract preparation

Crude extract from the raw plant material was produced by ultrasonic extraction using 70% aqueous solution of ethanol (Zibareva and Yeremina, 2011) at 60 °C. Influence ultrasonic of the aerial parts of *S. cupuliformis*, collected in the flowering stage, was carried out with an ultrasonic extractor Elmasonic S 60 H, at a frequency of 37 kHz. Since ecdysteroids are chemically labile substances and could be destroyed at high temperatures, temperature 55 °C was during ultrasonic extraction.

Analysis of ethanol extracts

Chromatographic analysis and quantification of ecdysteroids were performed using the liquid chromatograph Shimadzu LC 20 (Japan). Chromatographic column Perfect Sil Target ODS-3 4.6 x 250 mm, particle size 5 microns. Gradient elution was carried out with acetonitrile and isopropyl alcohol solvent system (3:2 v/v) -0.1% trifluoroacetic acid from 15 to 35% from 0 to 40 min elution rate -1.0 ml/min. Analytical wavelength λ max = 254 nm for detecting phytoecdysteroids. Identification of signals in the chromatogram was carried out by comparing the retention times of components of fractions and standard samples, and also absorption maxima in UV spectra.

Isolation of ecdysteroids from the aerial parts of *S.cupuliformis*

Air-dried raw material of *S. cupuliformis* (266 g) was purified by extraction from lipophilic substances with n-hexane and chloroform. The raw material, purified from pigments, was extracted with ethyl acetate. Biologically active substances (BAS) were extracted from the dried raw materials with 70% the aqueous ethanol solution (5300 ml). Then, in order to remove the extractant, the combined extract was concentrated at 50 °C using a vacuum rotary evaporator (IKA HB 10 digital, Germany). A yellow-brown precipitate appeared during concentration of the extract. The filtrate was diluted with water to the ratio 1:2 (v/v) and filtered again. The extraction of BAS complex, containing ecdysteroids and flavonoids,

from the purified filtrate was achieved by repeated extraction with n-butanol. The combined butanol extracts were concentrated and further fractionated by the following solvent systems: chloroform-ethanol 9:1, 1:1 (v/v) and 70% the aqueous ethanol solution. The analyses showed that the fractions 9:1 enriched in ecdysteroids, and the fractions obtained during dissolving the residue using the solvent system 1:1 and 70% the aqueous ethanol solution consisted mostly of polar flavonoids.

The fraction which comprised mostly of ecdysteroids (2.75 g, yield 1.03% calculated using dried raw material) was repeatedly separated on columns with silica gel (KSK, Russia). The particle size of the silica gel was 0.1-0.16 mm, the column height 700 mm, the diameter 13 mm. During the process of chromatography, the solvents systems chloroform-ethanol in the ratios 9:1, 7:1, 5:1, 3:1 were used as eluents and 55 fractions were obtained. The combined fractions 30-45 (0.24 g, 0.09% yield based on dried raw material, 8.7% using butanol fraction) were once again separated on the silica gel column (KSK) using chloroform-ethanol in the ratios of 7:1, 5:1, 3:1. Control of BAS content in the fractions was achieved by TLC and HPLC methods. Recrystallization of the isolated compounds was conducted in ethyl acetate-ethanol in the ratios 7:1 and 5:1. As the result, a number of ecdysteroids was isolated, identification of which was achieved by HPLC, NMR and MS.

III. RESULTS AND DISCUSSION

The study of plant extracts and the dynamics of the content of ecdysteroids in the organs of plants *Serratula*

It was shown that there is no destructive effect of ultrasound on the structure of BAS in selected conditions, since (after ultrasound processing) absorption maxima of ecdysteroids and complexes of flavonoids with aluminum chloride are the same as those of the standards. The flavonoid complexes with $\text{D}\ddot{\text{R}}\text{ICl}_3$ of the species *Serratula* have absorption maxima in

the interval 412-414 nm. The ability of plants of the studied species to accumulate ecdysteroids, including a new source of *S. cupuliformis*, is demonstrated by the presence of the UV absorption band at 242-245 nm, which is caused by the presence of α,β -unsaturated keto group characteristic for ecdysteroids. The optimal time of ultrasonic extraction, at which the levels of extracted ecdysteroids reaches of control, is 60 min. This is 12 times faster than using the previously developed method (Yakubova et al., 1978). Ultrasonic exposure during 120

min and with heating up to 60 °C enables an increase in the level of extracted flavonoids by 20% (Zibareva and Yeremina, 2011).

The study of BAS accumulation showed that the highest content of flavonoids in the aerial parts was found in the flowering stage. High levels of flavonoids are found in all the organs, the highest being in the leaves: *S. cupuliformis* (5.7%), *S. gmelinii* (5.0%), *S. manshurica* (3.1%) whereas in the flowers the amounts were 1.0, 1.8 and 1.5%, respectively.

Table 1. Distribution of 20-hydroecdysone in *Serratula* species (% by dried raw material)
ND*—not determined.

Plant organs	<i>S. cupuliformis</i>	<i>S. gmelinii</i>	<i>S. manshurica</i>	<i>S. coronata</i> (Revina et al., 1986)	<i>S. centauroides</i> (Zarembko, 2001)	<i>S. komarovii</i> (Zarembko, 2001)
	Budding					
Aerial parts	1.94±0.03	2.30±0.03	1.32±0.02	1.7	ND*	ND*
Flowering						
Flowers	1.23±0.01	1.81±0.02	1.13±0.01	1.9	ND*	ND*
Leaves	1.61±0.02	1.74±0.02	1.44±0.02	1.3	1.4	0.3
Stems	1.92±0.03	2.62±0.02	0.73±0.01	1.7	1.7	0.3
	0.24±0.01	0.44±0.01	0.24±0.01	0.4	0.7	0.2

The greatest accumulation of 20-hydroecdysone (20E) in aerial parts of all the studied species is noted during the budding period: *S. gmelinii* (2.3%), *S. cupuliformis* (1.94%), *S. manshurica* (1.32%). In the flowering period, the levels of ecdysteroids in the aerial parts remain high: in *S. gmelinii* (1.81%), *S. cupuliformis* (1.23%), *S. manshurica* (1.13%) (Table 1). The highest accumulation of ecdys-

teroids is observed in the leaves and flowers.

HPLC-analysis of isolated of ecdysteroids

Identification of signals on HPL chromatograms was carried out by comparing the retention times of components of extracts with retention time of standard samples, and by comparing their UV spectrum characteristics.

Table 2. The contents of ecdysteroids in the overground part of the species *Serratula*

Ecdysteroids	Concentration of ecdysteroids, % by dried raw material		
	<i>S. cupuliformis</i>	<i>S. gmelinii</i>	<i>S. manshurica</i>
Polypodine B	0.21±0.01	0.25±0.01	0.14±0.01
20-Hydroxyecdysone	1.23±0.01	1.81±0.02	1.13±0.01
Makisterone A	0.03±0.01	-	-
Ecdysone	0.19±0.01	0.69±0.01	0.02±0.01
2-Deoxy-20E	0.05±0.01	0.26±0.01	0.03±0.01

A chromatographic study of ecdysteroids of *Serratulacu puliformis*, *S. manshurica*, *S. gmelinii* using the HPLC method showed that all the studied plant species synthesized 20-hydroxyecdysone, polypodine B, 2-deoxy-20-hydroxyecdysone and ecdysone, and also, in the case of *S.cupuliformis*, makisterone A too. Good agreement was observed between times retention of ecdysteroids standards and compounds in the extracts of plants. UV-spectra confirm that compounds with these retention times are ecdysteroids. In UV-spectra discovered characteristic absorption maxima of ecdysteroids in the region 240-250 nm. The highest content of ecdysteroids is noted in *S. gmelinii*. It is shown that the major ecdysteroid in the studied species is 20-hydroxyecdysone (Table 2). The different ratio of ecdysteroids was observed in each species. The largest ratio between the 20 E and polypodine B, characterized by the presence of additional OH group in the 5 β position, were noted in *S. manshurica*. The composition of isolated major ecdysteroids from a new source *S. cupuliformis* is identical to those of other species of genus. Makisterone A besides *Serratula cupuliformis* only *S.coronata* synthesizes. 2 Deoxy -20-hydroxyecdysone was detected in other species-*S. centauroides*, *S. komarovii*, *S. gmelinii*, *S. manshurica*.

Identification of isolated compounds from *S. cupuliformis*

Isolated ecdysteroids from 70% ethanol extracts of *S. cupuliformis* were identified by ¹H-NMR, ESMS. Ecdysone and makisterone A were identified by HPLC method.

20-Hydroxyecdysone: UV-spectra: λ_{max} 247 nm. ¹H-NMR (CDCl₃ + CD₃OD, ppm): δ 0.75 (3H, s, Me-18), 0.87 (3H, s, Me-19), 1.09 (3H, s, Me-21), 1.11 (6H, s, Me-26 and Me-27), 2.21 (1H, t-like, J= 8.4 Hz, H-17), 2.29 (1H, dd, J = 3.7, 12.8 Hz, H-5), 2.94 (1H, t-like, J= 8.0 Hz, H-9), 3.26 (1H, m, H-22), 3.72 (1H, br d, J = 11.6 Hz, H-2), 3.86 (1H, br s, H-3), 5.72 (1H, s,

H-7). ESMS (+ve): m/z (% rel. intensity) 481.0 [M+H]⁺ (100).mp.233 – 234 °C.

Polypodine B: UV-spectra: λ_{max} 245 nm. ¹H-NMR (CDCl₃ + CD₃OD, ppm): δ 0.73 (3H, s, Me-18), 0.76 (3H, s, Me-19), 1.06 (3H, s, Me-21), 1.09 (6H, s, Me-26 and Me-27), 2.19 (1H, t-like, J= 8.4 Hz, H-17), 2.99 (1H, t-like, J= 8.1 Hz, H-9), 3.22 (1H, m, H-22), 3.76 (1H, m, H-2), 3.85 (1H, br s, H-3), 5.79 (1H, s, H-7). ESMS (+ve): m/z (% rel. intensity) 497.2 [M+H]⁺ (100).mp.215 – 217 °C.

2-Deoxy-20-hydroxyecdysone:UV-spectra: λ_{max} 243 nm. ¹H-NMR (CDCl₃ + CD₃OD, ppm): δ 0.79 (3H, s, Me-18), 0.91 (3H, s, Me-19), 1.13 (3H, s, Me-21), 1.16 (6H, s, Me-26 and Me-27), 2.27 (1H, t-like, J= 8.4 Hz, H-17), 2.37 (1H, dd, J = 3.9, 12.1 Hz, H-5), 3.05 (1H, m, H-9), 3.33 (1H, m, H-22), 3.97 (1H, br s, H-3), 5.78 (1H, s, H-7). ESMS (+ve): m/z (% rel. intensity) 465.2 [M+H]⁺ (100).mp.244 – 245 °C.

IV. CONCLUSION

All investigated species of the genus *Serratula* produce ecdysteroids. The most common ecdysteroids are 20-hydroxyecdysone, polypodine B, ecdysone, integristerone A, viticosterone E. Ecdysteroids were isolated from *Serratula cupuliformis* for the first time. This species is a promising source of ecdysteroids because the content of 20E in flowers and leaves of which is higher than those in *S. manshurica*, *S. coronata*, *S. centauroides* and *S. komarovii*. The studied *Serratula* species have synthesized 20-hydroxyecdysone, polypodine B, 2-deoxy-20-hydroxyecdysone and ecdysone, whereas *S. cupuliformis* also produced makisterone A as an additional ecdysteroid. Destructive effects of ultrasound on ecdysteroids were not observed, that is confirmed by UV-spectra, HPLC and high content of these substances. Time of ecdysteroids extraction is reduced by 12 times, while yield of flavonoids increased by 20%.

V. ACKNOWLEDGEMENTS

This research is supported by Tomsk State University Competitiveness Improvement Program for 2013-2020, by grant number 16-44-700634 r Ďř RFBR (Russia), and Ramkhamhaeng University and Center of Excellence for Innovation in Chemistry, Office of the Higher Education Commission (Thailand).

REFERENCES

- [1] Adykenov, S.M., Patent 23093. 15.11.2010. (Kazakhstan). Method for producing anabolic and adaptogenic drug 'ekdifit' from *Serratula coronata* L.
- [2] Akhmed, I., Voziyan, P.A., Klyashtornaya, G.V., Miladera, K., and Kholodova, Y.D., 1990. *Serratula tinctoria* L. and *S. wolfii* Andrae-promising sources of biologically active ecdysteroids: Ukrainian Biochemical Journal, 47(4): 81-83 (in Russian).
- [3] Akhrem, A.A., Kovganko, N.V., 1989. Ecdysteroids: chemistry and biological activity: Minsk: Nauka i tekhnika, 327 p. (in Russian).
- [4] Bathori, M., Kalasz, H., Csikkelne, S.A., Mathe, I., 1999. Components of *Serratula* species; screening for ecdysteroid and inorganic constituents of some *Serratula* plants: Acta Pharmaceutica Hungarica, 69(2): 72-76.
- [5] Abubakirov, N.K. 1982. Ecdysteroids of flowering plants (Angiospermae). Proceedings of the Indian: National Science Academy 48A (supplement 1): 122-138.
- [6] Abubakirov, N.K., 1984. Insect moulting hormones in plants from Central Asia: Uzbekistan Academy of Sciences Series: Chemistry (4): 49-53 (in Russian).
- [7] Alekseeva, L.I., Anufrieva, E.N., Volodin, V.V., 2003. Phytoecdysteroids. Spb. Science, 293p. (in Russian).
- [8] Bathori, M., Szendrei, K., and Herke, I., 1986. Application of combined chromatographic techniques in the screening and purification of ecdysteroids: Chromatographia, 21: 234-238.
- [9] Chen, J., and Wei, Y., 1989. Isolation and identification of ecdysterone in *Serratula chinensis* root: Zhongcaoyao, 20(7): 296 (in Chinese).
- [10] Dai, J.Q., Shi, Y.P., Li., Yang, L.Y., 2002. Two new components from *Serratula strangulate* Iljin: Pharmazie, 57(5): 340-2.
- [11] Ganiev, S.G., 1980. Amount of ecdysones in some plants of *Serratula* L. and *Rhaponticum Ludw*: Rastitelny Resursy, 16(2): 193-198 (in Russian).
- [12] Kholodova, Yu.D., 1979. Phytoecdysones-biologically active polyhydroxylic sterols: Ukrainian Biochemical Journal, 5(5): 560-575 (in Russian).
- [13] Kholodova, Yu.D., Baltaev, U., Volovenko, W.O., 1979.: Phytoecdysteroids of *Serratula xeranthemoides* L.: Khimiya Prirodnykh Soedineniy, 2: 171-174.
- [14] Munkhzhargal, N., Zibareva, L.N., 2008. Flora of Mongolia-a promising source of medicinal plants. Culture and peoples of Northern Asia and adjacent areas in the context of interdisciplinary study: The collection of the Museum of archaeology and ethnography of Siberia to them. V.M. Florinskii. Tomsk: TSU. 309-310 (in Russian)

- [15] Novoselskaya, N.L., Gorovits, M.B., and Abubakirov, N.K., 1975. Phytoecdysones of *Serratula*. IV. Sogdisterone: Khimiya Prirodnikh Soedineniy, 429-430 (in Russian).
- [16] Novoselskaya, I.L., Gorovits, M.B., and Abubakirov, N.K., 1981. Phytoecdysteroids from *Serratula coronata*: Khimiya Prirodnikh Soedinenii, 668-669 (in Russian).
- [17] Plotnikov, M.B., Aliyev, O.I., Vasiliev, A.S., Maslov, M.Yu., Zibareva, L.N., Dmitruk, S.Ye., Kalinkina, G.I., 2000. Gemoreological effects of extracts *Lychnis chalconica* L: Experimental and Clinic Pharmacology, 63(2): 54-56 (in Russian).
- [18] Rastitelny Resursy of USSR. Flowering plants, their chemical composition, using. Family Asteraceae. SPb: Science., 1993. 352 p.
- [19] Revina, T.A., Karnachuk, R.A., Tajlasheva, T.J., 1986. Dynamics of 20-hydroxyecdysone in over ground part of *Serratula coronata* L. and influence of different spectral composition on it: Rastitelny Resursy, 22: 70-72 (in Russian).
- [20] Syrov, V.N., Kurmukov, A.G., 1976. About anabolic activity of phytoecdysone-ecdysterone, isolated from *Rhaponticum carthamoides* (Willd.): Farmakologiya i Toksikologiya, 6: 690-693 (in Russian).
- [21] Volodin, V.V., Pchelenko, L.D., Volodina, S.O., Kudryasheva, A.G., Shevchenko, O.G., Zagorskaya, N.V., 2006. Pharmacological evaluation of new ecdysteroid containing substances 'Serpisten': Rastitelny Resursy, 42(3): 113-129 (in Russian).
- [22] Vorobyeva, A.N., Zarembo, Ye.V., Rybin, V.G., 2006. Far eastern species of genera *Stemmacantha* Cass. And *Serratula* L. promising sources of phytoecdysteroids: Bulletin of the Physiology and Pathology of the Respiratory System, 22: 90-93 (in Russian).
- [23] Wang, S., Dai, J., Chen, X., Hu, Z., 2002. Identification and Determination of Ecdysones and Flavonoids in *Serratula strangulata* by Micellar Electrokinetic Capillary Chromatography: Planta Medica, 68(11): 1029-1033.
- [24] Yakubova, M.R., Genkina, G.L., Shakirov, T.T., Abubakirov, N.K., 1978. Chromatospectrophotometric method for determination of ecdysterone in vegetative raw materials: Khimiya Prirodnikh Soedinenii 737-740 (in Russian).
- [25] Zatsny, I.L., Gorovits, M.B., Abubakirov, N.K., 1971. Phytoecdysteroids from *Serratula Sogdiana*: Khimiya Prirodnikh Soyedineniy, 6: 840-841
- [26] Zarembo, Ye.V., 2001. Content of 20-hydroxyecdysone in the genera *Rhaponticum* Ludw. and *Serratula* L. of the Far East flora: Rastitelny Resursy, 3: 59-64 (in Russian).
- [27] Zibareva, L.N., 2012. Phytoecdysteroids of plants Caryophyllaceae family. Saarbrücken, Germany-LAP Lambert Academic Publishing GmbH&Co. 195 p.
- [28] Zibareva, L.N., Yeremina, V.I. Patent 2472519 (Russia). Priority 03.08.2011. Way to increase the extraction of ecdysteroids from plant.

Effect of the Drying Conditions in a Pulsed Fluidized Bed Dryer on the Sulforaphane Content of Broccoli

Andrea Mahn^{1*}, Carmen Perez², Alejandro Reyes¹

¹Departamento de Ingenieria Quimica, Universidad de Santiago de Chile, Avenida Libertador Bernardo O'Higgins 3363, Estacion Central, Santiago, Chile

²Departamento de Ingenieria Agroindustrial, Universidad Pontificia Bolivariana, Cra. 6 No. 97A-99, Monteria, Colombia

Abstract

Sulforaphane is considered as the most powerful anticancer compound found naturally in food. Sulforaphane is thermo labile and therefore its preservation in dehydrated food still remains a challenge. Fluidized bed drying is one of the most efficient drying methods, with shorter drying time thus reducing the loss of bioactive compounds found in the raw material. The performance of this type of dryer is improved by incorporating a pulsed air inlet system. Currently there is a lack of information about the effect of the drying conditions in pulsed fluidized bed dryers on sulforaphane content of broccoli. The aim of this work was identifying the operation conditions in a pulsed fluidized bed dryer that maximize the content of sulforaphane in the dehydrated product. A central composite design was used, whose factors were drying air temperature and plate rotational speed. The drying time diminished with higher drying air temperature and higher plate rotational speed. The regression model predicted that 29 °C and 108 rpm were the optimal drying conditions, resulting in a sulforaphane content equal to 1.5 μmol/g in dry basis, corresponding to 1.36-fold the sulforaphane content in fresh broccoli.

Keywords: Pulsed fluidized bed dryer, broccoli, sulforaphane, drying kinetics

I. INTRODUCTION

Sulforaphane is an isothiocyanate found in Brassicaceae that is recognized as the most powerful anti-cancer compound naturally occurring in food (Matusheski et al.,

2004). Its precursor glucosinolate is glucoraphanin, which is found mainly in broccoli, and therefore this vegetable is the main source of sulforaphane. Since broccoli is mostly consumed as a processed food, the sulforaphane

*Corresponding author e-mail:andrea.mahn@usach.cl

content is affected. The effect of processing on sulforaphane content of broccoli florets has been studied. Perez et al., (2014) proposed the optimal blanching conditions that maximize sulforaphane content in broccoli. Mahn and Perez (2016) suggested to add an optimized incubation step after blanching, achieving 94% of glucoraphanin conversion into sulforaphane. Once the sulforaphane content in broccoli is maximized, it is necessary to further process the vegetable aiming to preserve it or to facilitate sulforaphane extraction from the food matrix. Drying is one of the most attractive and useful food preservation method, which presents a relatively low operation cost, and it also results in an easy-to-handle product due to the physical properties of the dehydrated product. The drawback of drying sulforaphane-rich broccoli relies on the high thermolability of sulforaphane, which hinders the use of hot air drying (Tanongkankit et al., 2011; Lekcharoenkul et al., 2014; Mahn et al., 2016). Thermal degradation of sulforaphane begins when the temperature exceeds 40 °C.

Fluidized-bed drying is one of the most efficient methods because of the excellent air-particle contact, with high mass and heat transfer coefficients (Reyes et al., 2007). The extension of the drying period is considerably lower than in tunnel driers, thus reducing the losses of bioactive compounds of the substrate. The performance of a fluidized-bed dryer can be improved by incorporating a pulsed air inlet, by locating a rotational perforated disc below the drying chamber. This modification conforms a pulsed fluidized-bed drier (PFBD), producing the intermittent fluidization of the particles inside the chamber (Reyes et al., 2008). The PFBD is adequate for irregularly shaped particles, fragile particles, or for particles of heterogeneous size distribution, since it improves fluidization uniformity and reducing the formation of channels. In addition, the PFBD reduces the air requirement by up to 50% in comparison with a traditional pulsed bed dryer (Reyes et al., 2012). This opens the possibility of using lower drying air temperatures. Since the sulforaphane enrichment process described by

Perez et al. (2014) and Mahn and Perez (2016) results in particles of irregular shape and heterogeneous size distribution, in this work we propose that drying sulforaphane-rich broccoli particles using a PFBD will minimize the loss of sulforaphane in the dehydrated product. The aim of this work was to identify the optimal drying air temperature and rotational plate speed that maximize the sulforaphane content in broccoli florets.

II. MATERIALS AND METHODS

Vegetal material

Broccoli (*Brassica oleraceavar Italica* cv. Avenger) heads (three days after harvesting) were purchased at the local market (Santiago, Chile) from a single supplier. Broccoli heads were washed and cut into single florets of 5 cm length and 0.7-0.9 cm width (stem) immediately after washing. Then, broccoli was subjected to blanching using the optimal conditions determined by Perez et al. (2014). Broccoli florets (300 g) were immersed in 1.5 L deionized water in a thermostatic bath (Stuart, United Kingdom, Great Britain) at 57 °C for 13 min. After blanching, broccoli florets were immediately put in an ice-water bath and then crushed in the presence of 0.22 mg ascorbic acid per gram of broccoli, to obtain 0.5-cm broccoli pieces. Then, broccoli particles were incubated in closed flasks in a water bath (Tri-lab, Ciudad de Mexico, Mexico) at 38 °C for 3 h.

Equipment

The pulsed fluidized-bed dryer used in this work corresponds to the equipment described by Reyes et al., (2012). A scheme is given in Figure 1. The PFBD was made of stainless steel, equipped with a controllable power up to 8000 W, a 10-HP centrifugal exhauster, and a system to collect the product (cyclone). The drying chamber consisted of a 1-m high cylindrical column connected to a truncated conical base section with a 0.25 m bottom diameter and a 0.4 m upper diameter. The drying air enters the chamber of the dryer through a perforated rotatory plate with 6% of free section area.

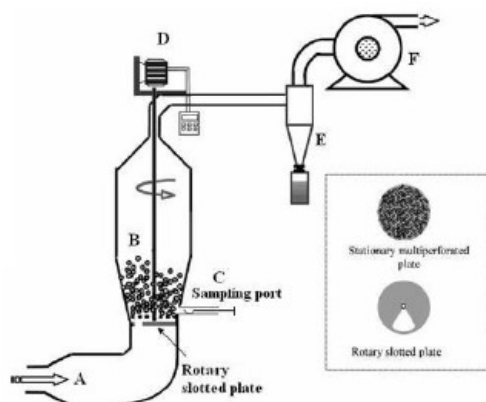


Figure 1. Pulsed fluidized bed dryer. (A) heater;
 (B) conical trunk drying chamber;
 (C) sampling system;
 (D) rotary slotted plate rate control;
 (E) cyclone;
 (F) centrifugal exhauster (adapted form Reyes et al., 2012).

Experimental design

The system was studied through a central composite design of uniform precision, whose factors (and levels) were drying air temperature (35 – 65 °C) and rotational plate speed (60-100

rpm), with four axial points and five central points. The air flow rate was fixed at 1.5 m/s. Table 1 shows the experimental matrix, in standard order.

Table 1. Experimental matrix in standard order. R3 is the central point.

Run	Temperature [°C]	Rotational speed [rpm]	Sulforaphane [$\mu\text{mol/g d.w.}$]
R1	65	100	0.9 ± 0.0
R2	35	100	1.4 ± 0.1
R3	50	80	0.9 ± 0.1
R4	65	60	0.7 ± 0.0
R5	35	60	0.7 ± 0.0
R6	50	108	1.1 ± 0.1
R7	71	80	0.5 ± 0.1
R8	29	80	0.9 ± 0.0
R9	50	52	0.8 ± 0.1
Sulforaphane content in fresh broccoli			1.1 ± 0.2
Sulforaphane content in broccoli before drying			8.1 ± 0.3

Sulforaphane content

Sulforaphane content was determined by reverse phase HPLC, using the method proposed by Liang et al., (2006). Broccoli samples were homogenized in a mortar, until obtaining a homogeneous meal. One gram of the sample was extracted two times with 10 mL methylene chloride (J.T. Baker, Center Valley, PA, USA), which was combined with 0.5 g anhydrous sodium sulfate (Sigma-Aldrich, Schnellendorf, Germany). The equipment was a HPLC-DAD (Shimadzu, Kyoto, Japan), and a C₁₈ column (5 μm particle size, 250 x 4.6 mm) (Agilent Technologies, Santa Clara, CA, USA) was used. Quantification was carried out by comparison with a sulforaphane standard curve (0.056-6.75 μg). Organic solvents (HPLC grade) were purchased from Merck (Darmstadt, Germany). Sulforaphane content was expressed in μmol g⁻¹ (dry weight). All determinations were made in triplicate.

Statistical analyses

The optimization design was analyzed by response surface methodology (at a 95% confidence), using a second order polynomial model to describe the experimental behavior (Eq. 1). In Eq. 1, Y is the predicted response; β₀, β_i, β_{ii}, and β_{ij} are the regression coefficients for interception, linear, quadratic and interaction effects, respectively; k is the number of independent parameters (k = 2 in this study), and X_i, X_j are the coded levels of the experimental conditions.

$$\hat{Y} = \beta_0 + \sum_{i=1}^k \beta_i x_i + \sum_{i=1}^k \beta_{ii} x_i^2 + \sum_{i < j=1}^k \beta_{ij} x_i x_j \quad (1)$$

The model quality was assessed by the determination coefficient (R²). The optimum drying conditions predicted by the regression model were validated experimentally. Statistical analyses were performed with JMP 9.0.1 software (SAS Institute).

III. RESULTS AND DISCUSSION

Sulforaphane content in broccoli subjected to PFBD is given in Table 1. Drying produced important losses of the compound in all drying runs, in comparison with blanched, incubated broccoli florets, despite the drying air temperatures were relatively low (29 – 71 °C). The lowest sulforaphane loss resulted from drying at 35 °C with a rotational plate speed of 100 rpm (R²), yielding a 17% retention of the compound. This value, equivalent to 1.1 μmol/gd.w., is 1.4-fold higher than the sulforaphane content in fresh broccoli.

Our results agree with Tanongkankit et al., (2011), who studied the evolution of sulforaphane content in cabbage outer leaves during tunnel drying at 50, 60 and 70 °C. The authors reported a loss of 90% of the initial sulforaphane content, attributed to thermal degradation. Lekcharoenkul et al., (2014) investigated the effect of a gradual change in temperature during hot air drying on the evolution of sulforaphane content in cabbage outer leaves. The authors reported sulforaphane losses higher than 90% in comparison with the fresh vegetable. In both studies, the authors attributed the sulforaphane loss to the high air temperature and the prolonged drying period. Mahn et al., (2016) reported a sulforaphane loss of 46% during tray drying at 70 °C during 4 hours, resulting in a sulforaphane content in the dehydrated broccoli of 4-fold the content in fresh broccoli. These results differ from the previous studies because of the considerable structural differences between cabbage leaves and broccoli florets.

In this work, the sulforaphane loss during PFBD cannot be attributed to thermal degradation due to the relatively low drying air temperatures (below 40 °C) and relatively short drying periods (22-25 min) used in this study. A possible explanation to the great losses is the occurrence of a dithiocarbamylation between sulforaphane and thiol-containing compounds through a reversible redox reaction (Shibata et al., 2011). This should be tested experimentally. Another interpretation of the behavior

observed in PFBD is the drag of sulforaphane with the drying air flow, since the PFBD configuration maximizes the particle-air contact thus promoting the compound drag. This effect is much less marked in other types of configurations, such as tray dryers and freeze-dryers.

The experimental factors had statistically significant effect ($p < 0.05$) on sulforaphane content in broccoli subjected to PFBD. An increase in drying air temperature produces a significant ($p = 0.0060$) decrease in sulforaphane content, while an increase in the rotational plate speed results in a significant ($p = 0.0012$) increase. Then, low air temperature and high rotational speed would minimize the sulforaphane loss in PFBD.

Eqn. (2) shows the regression model as a function of the experimental factors in coded levels. Here, [S] is sulforaphane content, T is temperature and U is rotational plate speed. This model explains 89.4% of the variability in the response, thus representing adequately the

system behavior.

$$[S] = 0.944 - 0.238 \cdot T + 0.321 \cdot U - 0.163 \cdot T^2 - 0.274 \cdot T \cdot U \quad (2)$$

Fig. (2) presents the response surface for sulforaphane content, showing that low drying air temperature and high rotational plate speed favor sulforaphane content. The highest sulforaphane content coincides with a vertex of the experimental space, therefore it is not possible to affirm that it corresponds to a maximum. The conditions predicted by the model to obtain the highest sulforaphane content were air temperature of 29 °C and rotational speed of 108 rpm, with a predicted response of 1.5 μg sulforaphane per g of dry weight. These conditions were tested experimentally, resulting in a sulforaphane content in dehydrated broccoli florets equal to the predicted ($1.5 \pm 0.1 \mu\text{g/g d.w.}$). This value represents an increase of 25% with respect to fresh broccoli.

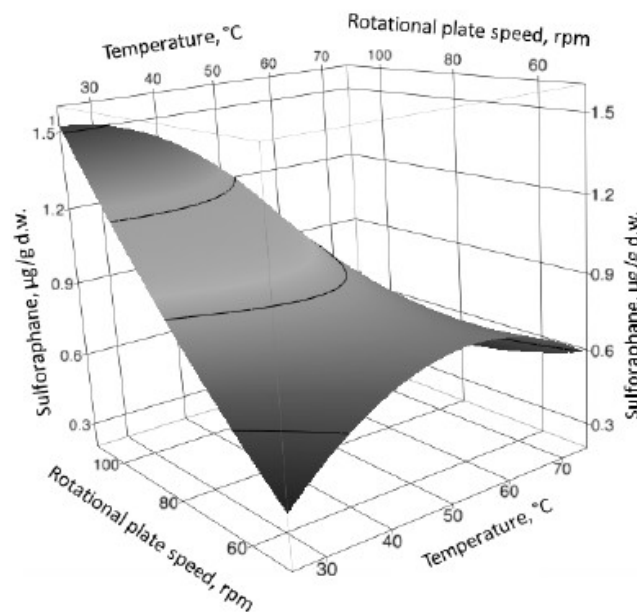


Figure 2. Response surface for sulforaphane content in dehydrated broccoli florets.

IV. CONCLUSION

Drying in a PFBD produces considerable decrease in the sulforaphane content in dehydrated broccoli. The sulforaphane losses are minimized by using low drying air temperature and high rotational plate speed. The

regression model described adequately the system, and allowed determining the best operating conditions: air temperature of 29 °C and rotational speed of 108 rpm. The highest sulforaphane content achieved after drying in a PFBD were $1.5 \pm 0.1 \mu\text{g/g d.w.}$, equivalent to 1.25-fold the content in fresh broccoli.

V. ACKNOWLEDGEMENTS

This work was supported by Proyecto Basal USA 1555, and Vridei 021711MO PUBLIC, Universidad de Santiago de Chile.

REFERENCES

- [1] Lekcharoenkul, P., Tanongkankit, Y., Chiewchan, N., Devahastin, S., 2014. Enhancement of sulforaphane content in cabbage outer leaves using hybrid drying technique and stepwise change of drying temperature. *Journal of Food Engineering*, 122: 56-61.
- [2] Liang, H., Yuan, Q.P., Dong, H.R., Liu, Y.M., 2006. Determination of sulforaphane in broccoli and cabbage by high-performance liquid chromatography. *Journal of Food Composition and Analysis*, 19(5): 473-476.
- [3] Mahn, A., Martin, C., Reyes, A., Saavedra, A., 2016. Evolution of sulforaphane content in sulforaphane-enriched broccoli during tray drying. *Journal of Food Engineering*, 186: 27-33.
- [4] Mahn, A., Perez, C., 2016. Optimization of an incubation step to maximize sulforaphane content in pre-processed broccoli. *Journal of Food Science and Technology*, 53(11): 4110-4115.
- [5] Matusheski, N.V., Juvik, J.A., Jeffery, E.H., 2004. Heating decreases epithiospecifier protein activity and increases sulforaphane formation in broccoli. *Phytochemistry*, 65(9): 1273-1281.
- [6] Perez, C., Barrientos, H., Roman, J., Mahn, A., 2014. Optimization of a blanching step to maximize sulforaphane synthesis in broccoli florets. *Food Chemistry*, 145: 264-271.
- [7] Reyes, A., Mahn, A., Guzman, C., Antoniz, D., 2012. Analysis of the drying of broccoli florets in a fluidized pulsed bed. *Drying Technology*, 30: 11-12.
- [8] Reyes, A., Moyano, P., Paz, J., 2007. Drying of Potato Slices in a Pulsed Fluidized Bed. *Drying Technology*, 25: 581-590.
- [9] Reyes, A., Vega, R., Bustos, R., Araneda, C., 2008. Effect of Processing Conditions on Drying Kinetics and Particle Microstructure of Carrot. *Drying Technology*, 26(10): 1272-1285.
- [10] Shibata, T., Kimura, Y., Mukai, A., Mori, H., Ito, S., Asaka, Y., Oe, S., Tanaka, H., Takahashi, T., Uchida, K., 2011. Transthiocarbamylation of Proteins by Thiolated Isothiocyanates. *Journal of Biological Chemistry*, 286(49): 42150-42161.
- [11] Tanongkankit, Y., Chiewchan, N., Devahastin, S., 2011. Evolution of anticarcinogenic substance in dietary fiber powder from cabbage outer leaves during drying. *Food Chemistry*, 127(1): 67-73.

Development of Agriculture Support System Using Plant Bioelectric Potential Responses and Gas Sensor

Yuki Hasegawa^{1,2,*}, Donatella Puglisi², Anita Lloyd Spetz²

¹Graduate School of Science and Engineering, Saitama University,
255 Shimo-okubo, Sakura-ku, 338-8570 Saitama, Japan

²Department of Physics, Chemistry and Biology, Applied Sensor Science,
Linköping University, 58183 Linköping, Sweden

Abstract

In this study, we focus on the plant bioelectric potential response as a low-cost and a high sensitivity evaluation technique of plant physiological activities for an agriculture support system. We developed a cultivation light intensity control system using bioelectric potential response. This system contributes to improvement of the cultivation environment and provides energy saving effect. In addition, we introduced a field effect transistor based on silicon carbide (SiC-FET) gas sensor and evaluated the characteristics of the sensor by changing several parameters. The results showed that iridium gated SiC-FET sensor has high sensitivity to ethylene, and the highest response is achieved at 200 °C. We aim at the development of an agriculture support system, which combines the plant bioelectrical potential and the SiC-FET gas sensor response.

Keywords: Field effect transistor, gas sensor, plant bioelectric potential, plant factory, agriculture support system, cultivation environment control, physiological activities of plant, ethylene

I. INTRODUCTION

The population in urban areas is currently increasing, 54% of the world's population lives in city regions and that proportion is expected to increase to 66% by 2050, according to United Nations report (United Nations, 2015). The production, distribution, and consumption of food in and near cities have received growing attention due to the urbaniza-

tion, and this has increased the attention to urban agriculture (Goldstein et al., 2016; Polling et al., 2016) and precision agriculture (Stafford, 2000; Baerdemaeker, 2013).

Especially, the artificial plant cultivation facilities such as plant factories have been in practical use during several decades for ensuring a stable amount of clean (no pesticides), safe (less bacteria) and high quality (high in nutrition and tasty) agricultural production of vegeta-

*Corresponding author e-mail:yuki@ees.saitama-u.ac.jp

bles, herbs, flowers, and fruits (Takatsuji, 1989; Hu et al., 2014). However, these facilities have problems with high cost and operating expenditures, because they need to maintain a stable and complete environment control system that includes air conditioner, a feed nutrient solution line, and sensing devices for control. Especially, the cost for electricity takes around 40% of the operating expenditure. Therefore, various studies have been carried out to investigate how to control the optimal environment for growing plants, reducing costs and improving the productivity of cultivation (Morimoto et al., 1995; Ioslovich and Gutman, 2000; Raviv et al., 2010; Srbinska et al., 2015; Shaw et al., 2016).

In our previous work, we focused on the plant bioelectric potential response, which is generated by ions inside the plant cells and related to physiological activities such as photosynthesis, respiration and transpiration, as a low-cost and a highly sensitive evaluation technique for an agriculture support system. Some papers clarified that the bioelectric potential follows the start and stop of the illumination and that the amplitude of this variation is correlated with the rate of photosynthesis. It was also stated that the characteristics of the bioelectric potential depend on the illumination period, wavelength, intensity, and temperature (Ando et al., 2013; Ando et al. 2014; Hasegawa et al., 2014). A non dispersive infrared (NDIR) carbon dioxide gas sensor was used to evaluate the photosynthetic rate, however, this is an expensive equipment and not convenient for practical use at the agricultural field or the plant cultivation facility. It is also necessary to observe the influence of other gas components such as ethylene, which is the smallest and color less gaseous plant growth hormone, and considered as a trigger of the ripening process of fruits (Burg and Burg, 1962; Kader, 2003; Garcia-Salinas et al., 2016). A number of different approaches has been used to address ethylene detection for fruit storage and post harvest ripening (Fonollosa et al., 2009; Steffens et al., 2010; Esser et al., 2012; Zaidi et al., 2016). For fruit storage, detection at low concentra-

tion level (low parts per million, ppm or even parts per billion, ppb) is required. On the other hand, for post harvest ripening, it is required to detect high concentrations: several hundred or thousand ppm. Therefore, it is necessary to develop a wide range sensor device.

In this study, we constructed the cultivation light intensity control system using bioelectric potential response. Generally, the condition of an optimal light intensity varies from kind of plants and growing stage. Especially, a photo inhibition effect was found to be caused by too strong light illumination, which suppressed the photosynthetic activity (Taiz and Zeiger, 2010). The light intensity control system contributes to improvement of the cultivation environment and has an energy saving effect.

In addition, we employed a field effect transistor based on a silicon carbide (SiC-FET) device as an ethylene gas sensor to evaluate fruit ripening. The SiC-FET gas sensors have been widely studied and proven as reliable, high performance and cost-efficient chemical sensors for high-temperature applications in harsh environments (Andersson et al., 2013) as well as for room temperature applications for highly sensitive and selective detection of trace amount of different target gases (Bur et al., 2015). The selectivity and sensitivity of SiC-FET sensors can be tailored toward one or a few target gases by changing the operating temperature, gate material and material structure (Bastuck et al., 2016; Darmastuti et al., 2013; Bur et al., 2015; Puglisi et al., 2015). We report the sensing characteristics of an iridium (Ir) gated SiC-FET sensor with different ethylene (C_2H_4) concentrations in 20% O_2 mixed with N_2 as the carrier gas at different operating temperatures and discuss the possible use for fruit storage and post harvest ripening.

II. EXPERIMENTAL

Light intensity control system using the bioelectric potential response of plant

We constructed a system for detecting the bioelectric potential and controlling the light intensity (Figure 1 (a)). The required condi-

tions for this system are potential measurement, feedback functions and convenient practical use. Therefore, we prepared a microcomputer (H8/3664), LED light source panel capable of light quantity adjustment, electroencephalogram (EEG) needle type electrodes (NE-224S, Nihon Kohden Corp.), hydroponic equipment and sample plant: cabbage seedlings (*Brassica oleracea* var. *capitata*). The sample plants have seven to nine leaves, and a leaf not being in shadow of other leaves was used for the measurement. To detect the potential response induced by photosynthetic reactions, an electrode was inserted to the base of the leaf as a reference electrode and another electrode was inserted to the vein in the center

of it, where photosynthesis takes place. The microcomputer amplified and analyzed the bioelectric potential, and transmitted a control signal to the light source. Figure 1 (b) shows the pattern of LED light source panel, which consisted of blue (450nm), red (660nm) and white (based on a blue LED and a yellow phosphor coating) LEDs, because the chlorophyll of plants has light absorption peaks in the wavelength of blue and red. The photosynthetic photon flux density (PPFD, $\mu\text{molm}^{-2}\text{s}^{-1}$) which is an index of the illumination intensity, was measured at the measured leaf surface. The PPFDs of blue, red and white LEDs during 100% light irradiation were 60, 310 and 30 $\mu\text{molm}^{-2}\text{s}^{-1}$ respectively, and totally 400 $\mu\text{molm}^{-2}\text{s}^{-1}$.

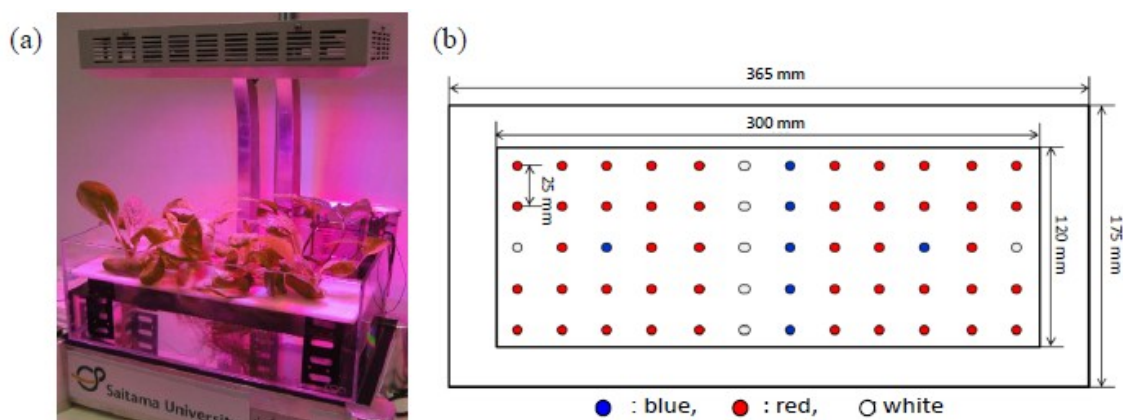


Figure 1. (a) Photograph of our developed system and (b) Pattern arrangement of LED light source panel of the system.

Gas sensor fabrication and measurement system

Ann-channel depletion type metal insulator semiconductor field effect transistor (MISFET) device was fabricated from 4H-SiC. A porous iridium thin film was deposited by DC magnetron sputtering to a total thickness of 30 nm on top of the device as gas sensitive gate contact. The SiC-FET gas sensor chip was mounted on a 16-pin TO8 header and glued on a ceramic heater with a Pt100 temperature sensor (Figure 2 (a)). The measurement set up is shown in Figure 2 (b). The gas testing equipment consisted

of several mass flow controllers operated by a gas mixing system program. Different concentrations of ethylene were injected to the sensor chamber by adjusting the flow of the ethylene and the carrier gas: 20% O₂ and 80% N₂. The ethylene concentration ranged from 0.5 to 2.5 ppm in steps of 0.5 ppm. The operating temperature was changed between 150 °C and 350 °C in steps of 50 °C. The exposure to the target gas was performed during 300 s and recovery in carrier gas was allowed for 300 s. Gas response characterizations have been obtained using a source meter (2601, Keithley Instru-

ments Inc.) keeping a constant drain-to-source voltage ($V_{DS} = 4\text{ V}$) and measuring the drain current (ID). Puglisi et al., 2016 reported that the Ir gated SiC-FET sensor's current-voltage

curve saturated at $V_{DS} = 4\text{ V}$ and the sensor response in saturation region was higher and more stable than that in linear region.

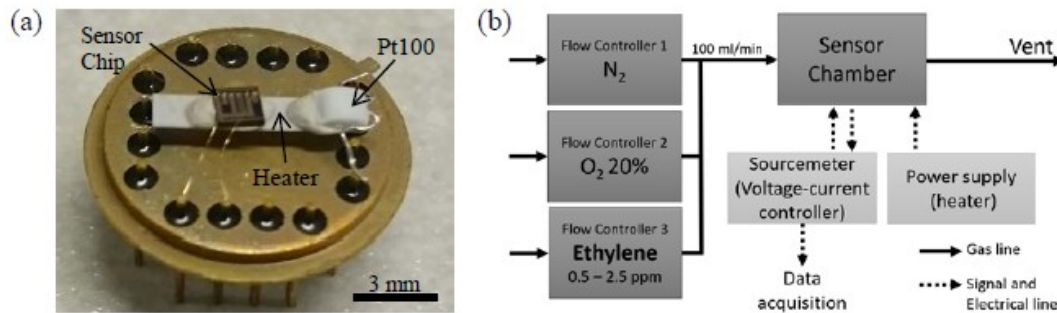


Figure 2. (a) Mounted Ir gated SiC-FET sensor and (b) schematic diagram of the gas sensor measurement set up.

III. RESULTS AND DISCUSSION

Light intensity control using plant bioelectric potential response

Figure 3 (a) shows an observed plant potential response by our system and the definition of the parameters for the feedback signal. The light intensity was controlled from 20 to 100% in 10% intervals depending on the feedback signal. In this figure, the potential responses changed immediately when switching between light (ON) and dark (OFF) period. Some papers reported that the amplitude of the potential variation when starting the illumination has a strong correlation with the photosynthetic rate (Ando et al., 2013). Therefore, it is considered that the amplitude can be used to evaluate the plant physiological activity as a control parameter.

In this system, when the system changes the light intensity at time 0 on the x-axis in Figure 3 (a), we defined the potential difference of the last light illumination as V_{on} , and the potential difference of the previous illumination

as pre V_{on} . Specifically, we used the difference between V_{on} and pre V_{on} as the parameter to be studied (Hasegawa, et al., 2015).

Figure 3 (b) shows an example of the execution of the automatic light intensity control system using the cabbage plant bioelectric potential. This figure includes the bioelectric potential, the value of V_{on} , and auto controlled light intensity. The light intensity was increased from time A to time B depending on the previous operating conditions and the difference between V_{on} and pre V_{on} . We observed, though, that the variation of V_{on} at B did not increase and at C the light intensity decreased again. These results showed that our developed system can operate correctly depending on the feedback signal from the plant bioelectric potential, therefore offering the possibility of improving the cultivation environment control system. A more detailed investigation of the usefulness of this system concerning, e.g., the energy saving performance and plant growing rate, will be carried out in future work.

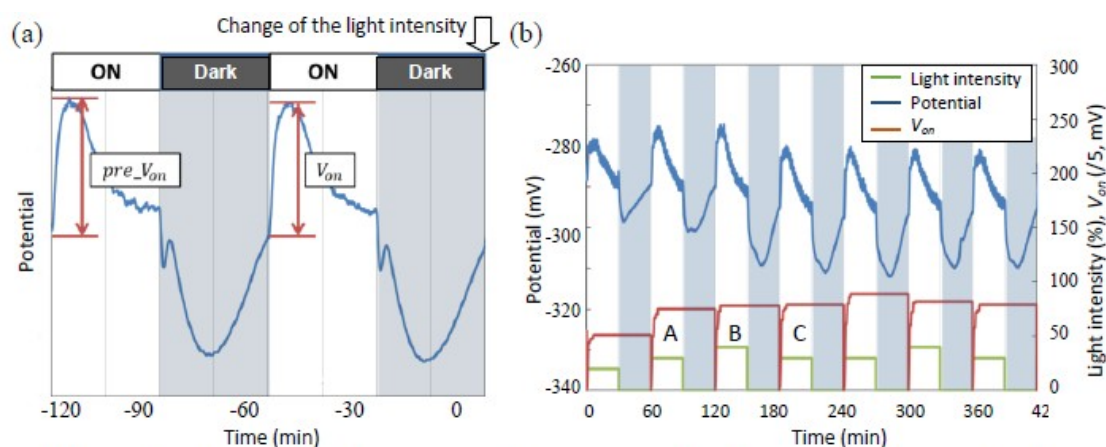


Figure 3. (a) Typical bioelectric potential response and definition of parameters for the feedback signal and (b) example of automatic light intensity control.

Gas sensor response to ethylene

We studied the sensing characteristics with different ethylene concentrations in 20% O₂ and 80% N₂ as carrier gas at different operating temperatures (150 – 350 °C). The sensor response, ΔI_D , is defined as the change in drain current, I_D , in presence of ethylene gas as compared to I_D in only carrier gas at a constant drain-to-source voltage, $V_{DS}(= 4 \text{ V})$. Figure 4 (a) shows the sensor signals at different ethylene concentrations (0.5, 1.0, 1.5, 2.0, 2.5 ppm) at 200 and 300 °C. This figure indicates that the sensor responds to all concentrations of ethylene at both temperatures but the sensor response is significantly higher at 200 °C whereas at 300 °C it shows sharp peaks for both gas exposure and recovery. The sensing mechanism of the SiC-FET sensor to ethylene was not studied, however, the ethylene is a small molecule and probably quite easily decomposes on the catalytic sensor surface at high temperature, possibly followed by oxidation reactions with absorbed oxygen, which may consume the gas more quickly at higher temperature. Figure 4 (b) shows the change in sensor response vs. ethylene concentration at different operating temperatures. As shown in this figure, the maximum response was achieved at 200 °C and the response increased almost linearly with increasing ethylene concentrations. Thus, it indicates

the possibility to detect both lower and higher concentrations. The response at 150, 250 and 300 °C had similar characteristics while that at 350 °C was significantly lower. This result is important for the optimization of the sensor's operation in dynamic mode employing temperature cycles.

The obtained results show that the Ir gated SiC-FET sensor has high sensitivity to ethylene and can potentially be used to control fruit storage and post harvest ripening. In our future work, the response to ethylene at the higher concentration range up to 200 ppm and measurement of ethylene emissions produced by climacteric fruits will be carried out. In the latter case, it will also be needed to investigate what other gas molecules that may be produced when fruit get damaged. This may be performed e.g. by combined gas chromatography-mass spectrometry, GC-MS. With knowledge about this, it is possible to use a combination of temperature cycled and gate bias cycled operation of the SiC-FET sensor together with advanced data evaluation (Bur et al., 2014; Bur et al., 2015) to enhance the selectivity to ethylene in presence of other gases produced from fruits. When using the temperature and gate bias cycled operation mode of the sensor on line measurement are possible at a sampling rate of 1 min.

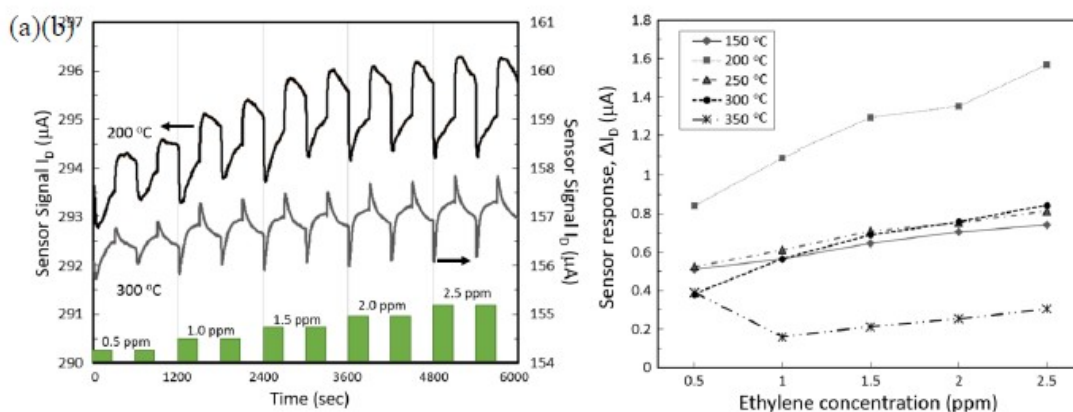


Figure 4. (a) Sensor signal of the Ir gated SiC-FET sensor during ethylene (C_2H_4) exposure at 200 and 300 °C and (b) sensor response, ΔI_D , towards 0.5-2.5 ppm C_2H_4 for different operating temperatures.

IV. CONCLUSIONS

In this paper, we studied and evaluated the plant bioelectric potential and the performance of a SiC-FET gas sensor for use in an agriculture support system. We constructed and evaluated a cultivation light intensity control system using the bioelectric potential response and we used a SiC-FET gas sensor to detect ethylene in the low ppm concentration level. We showed that the plant bioelectric potential through a microcomputer could give a feedback signal to the light intensity controlled light source. We suggest that the bioelectric potential contributes to the improvement of the cultivation environment control system and that it has an energy saving effect, since photo

inhibition from too high intensity light can be avoided. Moreover, a gas sensor based on silicon carbide field effect transistor was used to study the sensitivity to ethylene. Our results showed that the Ir gated SiC-FET sensor operated from 150 to 350 °C detect small concentrations (0.5 to 2.5 ppm) with a linear dependence, indicating a much larger dynamic range. The maximum sensor response was achieved at 200 °C. These results suggest that the Ir gated SiC-FET sensor can potentially be used to control fruit storage and post harvest ripening. In the future, we aim to develop an agriculture support system e.g. for optimized plant growth or fruit ripening control by combining the information from the SiC-FET sensor and the plant bioelectrical potential.

V. ACKNOWLEDGEMENTS

This work was supported by a JSPS KAKENHI Grant Number JP15KK0228. The authors would like to thank SenSiC AB, Sweden, for supplying the SiC-FET sensor and M. Rodner for his contribution with the gas mixing system setup.

REFERENCES

- [1] Andersson, M., Pearce, R., Lloyd-Spez, A., 2013. New generation SiC based field effect transistor gas sensors. *Sensors and Actuators B*, 179: 95-106.

- [2] Ando, K., Hasegawa, Y., Yaji, T., Uchida, H., 2013. Study of Plant Bioelectric Potential Response Due to Photochemical Reaction and Carbon-Fixation Reaction in Photosynthetic Process. *Electronics and Communications in Japan*, 96: 85-92.
- [3] Ando, K., Hasegawa, Y., Uchida, H., Kanasugi, A., 2014. Analysis of Plant Bioelectric Potential Responseto Illumination by Curve Fitting. *Sensors and Materials*, 26: 471-482.
- [4] Baerdemaeker, J., 2013. Precision Agriculture Technology and Robotics for Good Agricultural Practices. *IFAC Proceedings Volumes*, 46: 1-4.
- [5] Burg, S.P., Burg, E.A., 1962. Role of ethylene in fruits ripening. *Plant Physiology*, 37: 179-189.
- [6] Bastuck, M., Puglisi, D., Houtari, J., Sauerwald, T., Lappalainen, J., Lloyd-Spetz, A., Andersson, M., Schutze, A., 2016. Exploring the selectivity of WO₃ with iridium catalyst in an ethanol/naphthalene mixture using multivariate statistics. *Thin Solid Films*, 618: 263-270.
- [7] Bur, C., Bastuck, M., Lloyd-Spetz, A., Andersson, M., Schutze, A., 2014. Selectivity enhancement of SiC-FET gas sensors by combining temperature and gate bias cycled operation using multivariate statistics. *Sensors & Actuators B*, 193: 931-940.
- [8] Bur, C., Bastuck, M., Puglisi, D., Schutze, A., Lloyd-Spetz, A., Andersson, M., 2015. Discrimination and Quantification of Volatile Organic Compounds in the ppb-Range with Gas Sensitive SiC-FETs Using Multivariate Statistics. *Sensors and Actuators B*, Vol. 214: 225-233.
- [9] Darmastuti, Z., Bhattacharyya, P., Andersson, M., Kanungo, J., Basu, S., Kall. P.O., Ojamae, L., Lloyd-Spetz, A., 2013. SiC-FET methanol sensors for process control and leakage detection. *Sensors and Actuators B*, 187: 553-562.
- [10] Esser, B., Schnorr, J.M., Swager, T.M., 2012. Selective Detection of Ethylene Gas Using Carbon Nanotube-based Devices: Utility in Determination of Fruit Ripeness. *Angewandte Chemie International Edition*, 51: 5752-5756.
- [11] Fonollosa, J., Halford, B., Fonseca, L., Santander, J., Udina, S., Moreno, M., Hildenbrand, J., Wollenstein, J., Marco, S., 2009. Ethylene optical spectrometer for apple ripening monitoring in controlled atmosphere store-houses. *Sensors and Actuators B*, 136: 546-554.
- [12] Garcia-Salinas, C., Ramos-Parra, P.A., Diaz de la Garza, R.I., 2016. Ethylene treatment induces changes in folate profiles in climacteric fruit during postharvest ripening. *Postharvest Biology and Technology*, 118: 43-50.
- [13] Goldstein, B., Hauschild, M., Fernandez, J., Birkved, M., 2016. Testing the environmental performance of urban agriculture as a food supply in northern climates. *Journal of Cleaner Production*, 135: 984-994.
- [14] Hasegawa, Y., Hoshino, R., Uchida, H., 2015. Development of Cultivation Environment Control System Using Plant Bioelectric Potential. *Proceedings of NOLTA 2015*, 860-863.
- [15] Hasegawa, Y., Yamanaka, G., Ando, K., Uchida, H., 2014. Ambient Temperature Effectson Evaluation of Plant Physiological Activity Using Plant Bioelectric Potential. *Sensors and Materials*, 26: 461-470.
- [16] Hu, M., Chen, Y., Huang, L., 2014. A sustainable vegetable supply chain using plant factories in Taiwanese markets: A Nash-Cournot model. *International Journal of Production Economics*, 152: 49-56.

- [17] Ioslovich, I., Gutman, P., 2000. Optimal control of crop spacing in a plant factory. *Automatica*, 36: 1665-1668.
- [18] Kader, A.A., 2003. A perspective on post harvest horticulture (1978-2003). *HortScience*, 38: 1004-1008.
- [19] Morimoto, T., Torii, T., Hashimoto, Y., 1995. Optimal control of physiological processes of plants in a green palnt factory. *Control Engineering Practice*, 3: 505-511.
- [20] Puglisi, D., Eriksson, J., Andersson, M., Huotari, J., Bastuck, M., Bur, C., Lappalaine, J., Andreas, S., Lloyd-Spetz, A., 2016. Exploring the Gas Sensing Performance of Catalytic Metal/Metal Oxide 4H-SiC Field Effect Transistors. *Materials Science Forum*, 858: 997-1000.
- [21] Puglisi, D., Eriksson, J., Bur, C., Schuetze, A., Lloyd-Spetz, A., Andersson, M., 2015. Catalytic metal-gate field effect transistors based on SiC for indoor air quality control. *Journal of Sensors and Sensor Systems*, 4: 1-8.
- [22] Polling, B., Mergenthaler, M., Lorleberg, W., 2016. Professional urban agriculture and its characteristic business models in Metropolis Ruhr, Germany. *Land Use Policy*, 58: 366-379.
- [23] Raviv, M., Medina, S., Wendin, C., Lieth, J.H., 2010. Development of alternate cut-flower rose greenhouse temperature set-points based on calorimetric plant tissue evaluation. *Scientia Horticulturae*, 126: 454-461.
- [24] Shaw, R., Lark, R.M., Williams, A.P., Chadwick, D.R., Jones, D.L., 2016. Characterising the within-field scale spatial variation of nitrogen in a grassland soil to inform the efficient design of *in-situ* nitrogen sensor networks for precision agriculture. *Agriculture, Ecosystems and Environment*, 230: 294-306.
- [25] Srbínovska, M., Gavrovski, C., Dimcev, V., Krkoleva, A., Borozan, V., 2015. Environmental parameters monitoring in precision agriculture using wireless sensor networks. *Journal of Cleaner Production*, 88: 297-307.
- [26] Stafford, J.V., 2000. Implementing precision agriculture in the 21th century. *Journal of Agricultural Engineering Research*, 76: 267-275.
- [27] Steffens, C., Franceschi, E., Corazza, F.C., Herrmann, Jr. P.S.P., Oliveir, J.V., 2010. Gas sensors development using supercritical fluid technology to detect the ripeness of bananas. *Journal of Food Engineering*, 101: 365-369.
- [28] Taiz, L., Zeiger, E., 2010. *Plant physiology*, 5th ed., Sinauer Associates, Inc., Sunderland.
- [29] Takatsuji, M., 1989. Fundamental study of plant factories. *Plant Factory*, 1: 31-47.
- [30] United Nations, 2015. *World Urbanization Prospects: The 2014 Revision*.
- [31] Zaidi, N.A., Tahir, M.W., Vinayaka, P.P., Lucklum, F., Vellekoop, M., Lang, W., 2016. Detection of ethylene using gas chromatographic system. *Procedia Engineering*, 168: 380-383.

Recovery and Analysis of the Biological Activity of Lycopene Produced by *Rhodotorula glutinis* P4M422

Ayerim Hernandez-Almanza¹, Jae Kweon Park², Nallely E. Carlos-Interior¹,
Jose G. Fuentes-Aviles¹, Cristobal N. Aguilar^{1*}

¹School of Chemistry. Autonomous University of Coahuila. Saltillo, 26280,
Coahuila, Mexico

²Department of Life Sciences, Gachon University. Seongnam-si, 461-701,
Gyeonggi-do, South Korea

Abstract

*Lycopene is a carotenoid intermediate of the β -carotene biosynthetic pathway. It is obtained from vegetable source and chemical synthesis. It has roused considerable interest due to its beneficial effect on human health, e.g. cancer and tumor prevention, cardiovascular protection and antioxidant activities. Due the increasing interest of this bioactive molecule, it is necessary to develop alternative methodologies to produce it in higher amounts, for example, the microbial production. In the present study, the lycopene production by the yeast *Rhodotorula glutinis* P4M422 was evaluated. *R. glutinis* was inoculated in YM broth at 30 °C and 130 rpm. Incubation time optimization and imidazole effect in the specific accumulation of lycopene were evaluated. On the other hand, the antioxidant and thermal stability of lycopene capsules (GNC Mexico) were evaluated. The effect of imidazole at different concentrations (0, 1.5, 3, 6 and 12 mM) was studied, however, the results show that the highest biomass production and the major carotenoids concentration was obtained in absence of imidazole. Also, different organic solvents were evaluated in carotenoids extraction; we found that the use of methanol allowed the highest lycopene extraction (0.01 g/L). Carotenoids are a pigments with antioxidant activity, in the present study, ABTS, FRAP and DPPH(78.9, 71.19 and 44.77 mg/L Trolox equivalent, respectively) assays showed this property.*

Keywords: Lycopene, imidazole, cell disruption, antioxidant activity, TGA assay

*Corresponding author e-mail:cristobal.aguilaar@uadec.edu.mx

I. INTRODUCTION

Carotenoids are an important group of natural pigments found in plants and microorganisms, contain a series of conjugated double bonds, which are sensitive to oxidation modifications. Carotenoids are a class of lipophilic compounds with a polyisoprenoid structure (Bone et al., 2001; Ceron-Garcia et al., 2010).

Lycopene is a carotenoid intermediate of the β -carotene biosynthetic pathway (Choudhari et al., 2009; Frengova and Beshkova, 2009) obtained from vegetable source and chemical synthesis. It is an unsaturated lipophilic isoprenoid pigment, of 40 carbon atoms, with a molecular weight of 536.8 g/mol, containing 11 conjugated and 2 non-conjugated double bonds in an all-trans form (Agarwal et al., 2014; Honda et al., 2015; Kim et al., 2011; Omoni and Aluko, 2005).

Lycopene is the primary carotenoid found in human serum. It has roused considerable interest due to its beneficial effect on human health, e.g. cancer and tumor prevention, cardiovascular protection, antiproliferative and antioxidant activities (Heber and Lu, 2002; Hsiao et al., 2004; Marova et al., 2012). Due the increasing interest of this molecule, alternative methodologies to produce higher amounts have been developed. However, oxidation and isomerization from all-trans to cis-isomer are the main forms of degradation of lycopene (Colle, 2013; Che et al., 2009). Lycopene stability is affected by different factors such as heat, light, certain chemical reaction, pro-oxidant conditions and other environmental conditions.

Despite of its instability, lycopene is widely used as a supplement in functional foods, feeds, nutraceuticals and pharmaceuticals, and as an additive in cosmetics (Chen et al., 2013), then the total loss of lycopene may vary depending on temperature of heating and the method of heating matrix. The aim of this study is to evaluate the production conditions, extraction and stability of lycopene.

II. MATERIAL AND METHODS

Microorganism

The yeast *Rhodotorula glutinis* P4M422 was inoculated in YM broth and incubated during 48 h at 30 °C, 130 rpm.

Imidazole optimization

Imidazole effect in lycopene production was evaluated a different concentration (0, 1.5, 3, 6 and 12 mM). Briefly, 200 μ L of pre-culture were inoculated into 20 mL YM broth and biomass production and lycopene extraction were evaluated after 120 h of fermentation at 30 °C and 130 rpm. The biomass production was evaluated by optical density at 600 nm.

Incubation time optimization

Once the effect of imidazole was evaluated, the incubation time optimization was performed. *R. glutinis* P4M422 was inoculated in YM medium at 30 °C, 130 rpm during 144 h. Kinetic growth was evaluated by sampling each 24 h.

Cell disruption and carotenoids extraction

For the extraction of pigments produced by *R. glutinis* P4M422, different solvents were employed. Tubes containing biomass in 1 mL of acetone, hexane, ethanol, methanol or ethyl acetate were agitated using vortex agitator and freeze during 2 h. concentration of total carotenoids was measured spectrophotometrically at 470 nm.

For the TLC analysis, 6 μ L of the sample was loaded in plate of silica gel, the mobile phase was a mixture of acetone and ethyl acetate 5:4. The plate was dried and irradiated at 254 and 365 nm. Subsequently, the sample was analyzed in FT-IR spectra (FT-IR 7000, Lambda Scientific, Australia).

Antioxidant activity of carotenoids

The antioxidant activity of carotenoids produced by *R. glutinis* was determinate by FRAP, ABTS and DPPH assay.

Thermogravimetric assay (TGA)

In the present study the stability of lycopene capsules (GNC Mexico) under high temperatures was evaluated. The samples were analyzed at temperatures 0 to 800 °C in presence of oxygen and in an inert atmosphere employing a Thermogravimetric analyzer (TGA Q5000 TA Instruments).

Statistical Analysis

The experimental data were compared with the control by calibration curve. All experiments were performed in triplicate. Statistical significance was determined with $p < 0.05$.

III. RESULTS AND DISCUSSION

Imidazole optimization

The lycopene is a precursor of cyclic carotenoids into biosynthetic pathway (Mantzouridou and Tsimidou, 2008). The imidazole

can be used to inhibit the lycopene cyclase enzyme; this enzyme is responsible of cyclization of terminal group on lycopene molecule. In this study the effect of imidazole at different concentrations were evaluated, however, the results (Figure 1) show that the highest biomass production and the major carotenoids concentration was obtained in absence of imidazole. Wang et al., (2012) studied the lycopene accumulation by *Blakeslea trispora* NRLL 2895 and 2896 with addition of piperidine and creatinine like cyclase inhibitors and the highest lycopene production (98.1 mg/L) was obtained with creatinine at 6 g/L. On the other hand, Lopez-Nieto et al., (2004) reported that the imidazole addition at 0.6 g/L allowed 100% of lycopene production by *B. trispora* F-816 and F-744. In this study imidazole addition reduced the lycopene accumulation, it may be due imidazole acts like antifungals agent and can to inhibit the microorganism growth.

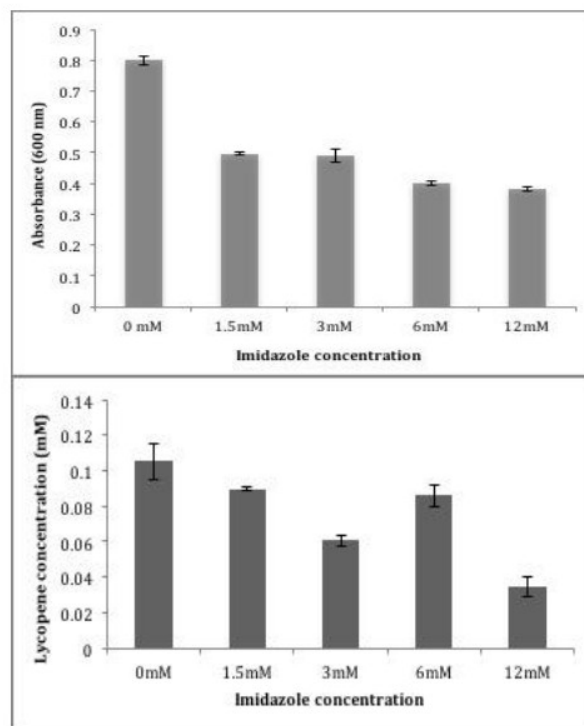


Figure 1. Biomass production (a) and lycopene production (b) by the yeast *Rhodotorula glutinis* P4M422 in YM broth with imidazole addition at different concentration

Incubation time optimization

The Figure 2 indicate that the highest biomass accumulation is at 96 h of fermentation, after this time the yeast growth is in stationary phase. The next steps were performed at this fermentation time. Different organic solvents were evaluated in carotenoids extraction, in the Figure 3 appears the results obtained. The use

of methanol allowed the highest lycopene extraction (0.01 g/L). Yoo et al., (2015) evaluated the production and characterization of antibacterial carotenoids produced by *R. mucilaginosa* AY-01 and reported that the use of methanol only for carotenoids production was the best technique compared with other.

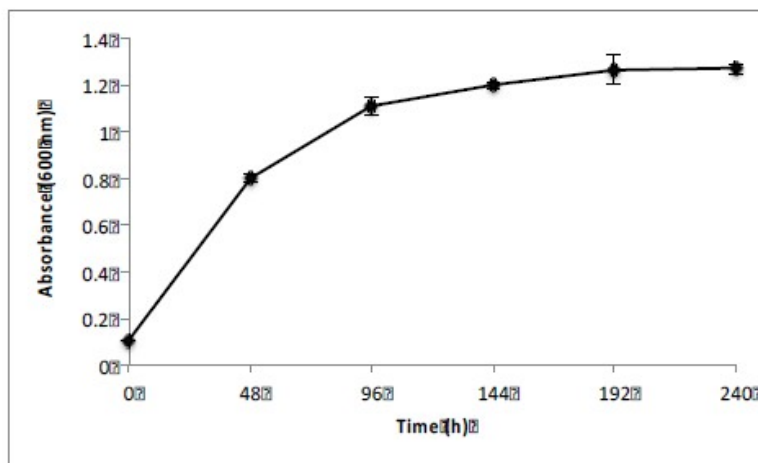


Figure 2. Time course growth of the yeast *R. glutinis* P4M422 in YM broth. Relative growth (5) was estimated under 600 nm.

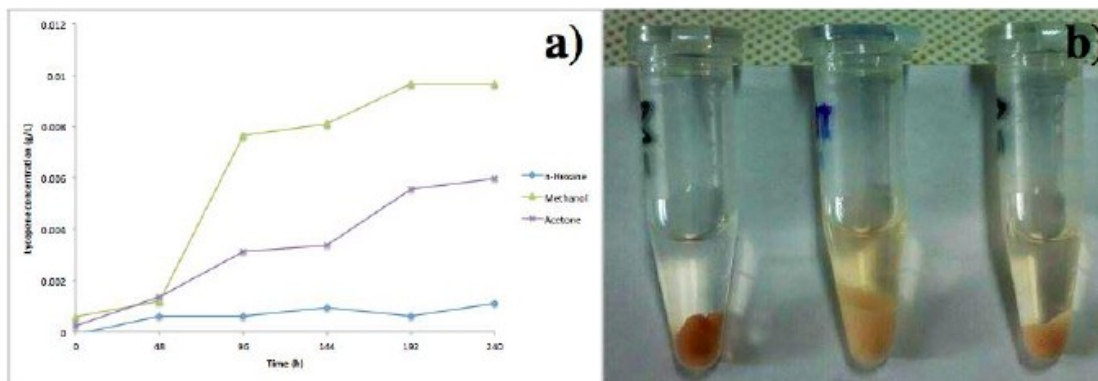


Figure 3. Lycopene concentration (a) obtained by extraction with hexane, methanol and acetone, respectively (b).

Antioxidant activity

Carotenoids are a pigments with antioxidant activity, however, in this study the extracts obtained showed low antioxidant activity (Table 1). This results could be due the instability of compounds or the presence of other molecules.

Table 1. Antioxidant activity of carotenoids extractd from *Rhodotorula glutinis* P4M422.

%RA	Lycopene standard	Sample
DPPH	60.34	17.89
ABTS	51.99	22.29

Thermogravimetric assay (TGA)

On the other hand, some studies indicate that the degradation reactions of lycopene are influenced by various factors, such as exposure to oxygen, water, light, heat, metals, as well as environmental conditions such as temperature and humidity, physical state, among others (dos Santos et al., 2016; Mahfoudhi and Hamdi, 2015). The Figure 4 shows the behavior of lycopene capsules under high temperatures and under oxygen absence and presence. The weight of lycopene starts to degradation about 180 °C in both cases. However, the derivative weight of lycopene shown that major degradation of lycopene weight was about 400 °C, under inert atmosphere (Figure 5).

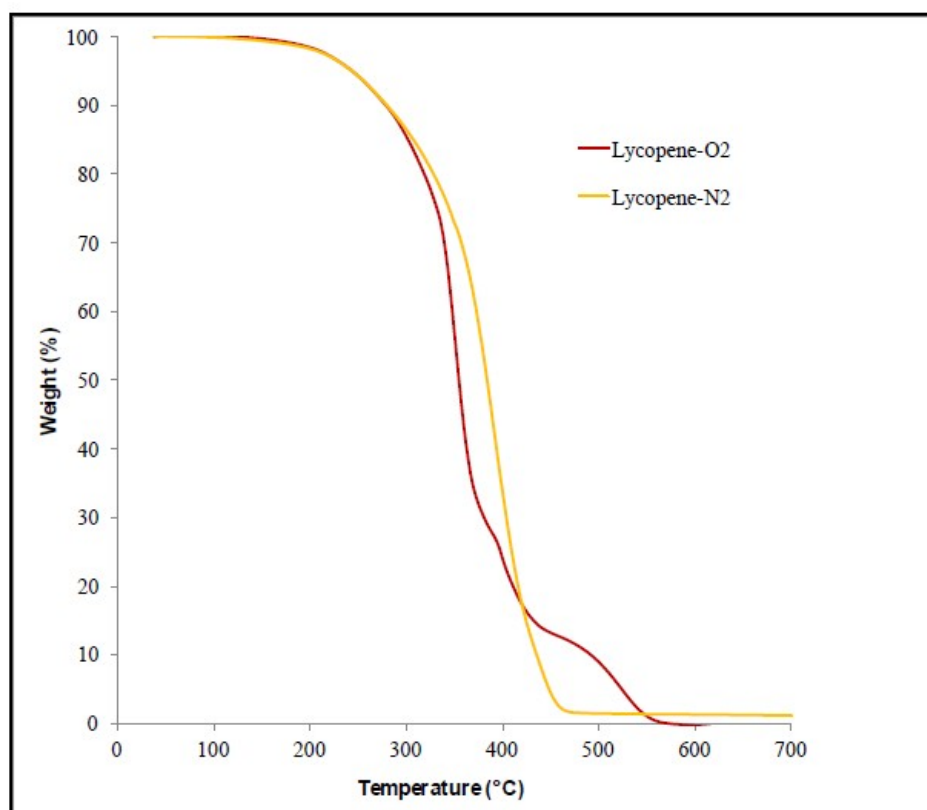


Figure 4. Evaluation of weight loss (%) of lycopene capsules in presence of oxygen and under inert atmosphere at different temperatures.

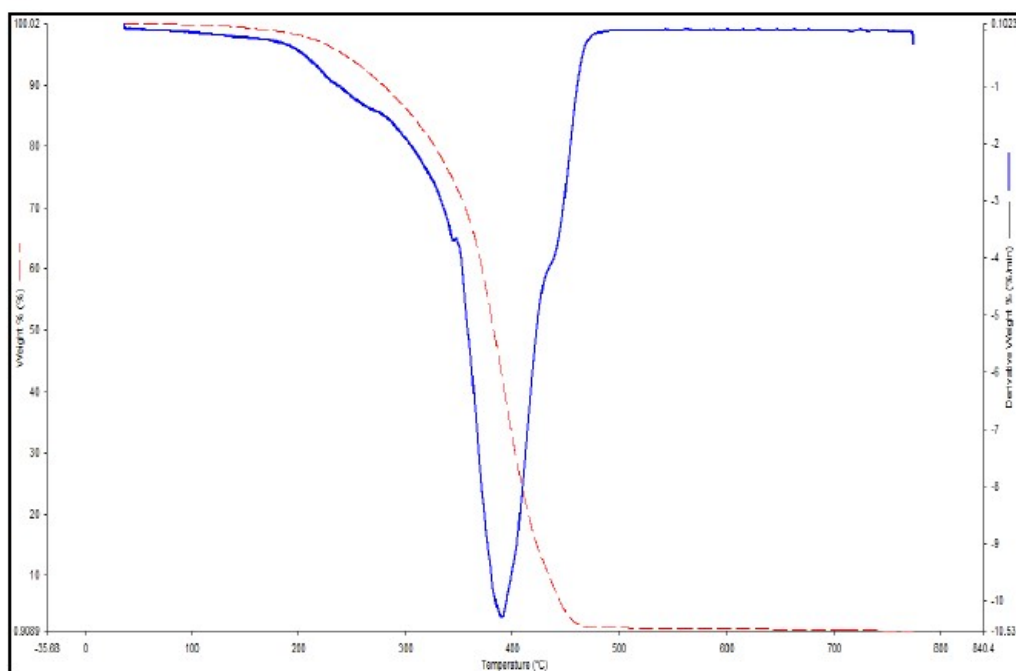


Figure 5. Derivative weight of lycopene capsules under inert atmosphere.

There are some reports about degradation and storage of lycopene and other carotenoids, however, these studies were based in carotenoids into matrix, for example, tomato sauce, tomato puree, carotenoids encapsulated or biomass of carotenoid-producer microorganisms.

Ceron-Garcia et al., (2010) evaluated the stability of carotenoids in *Scenedesmus almeriensis* biomass and extracts under various temperatures (ambient temperature, at 4 and -18°C) and solvents (acetone and olive oil). They found the olive oil extracts was stable for 5 months at temperatures of 4 and -18°C , showing no significant change. On the other hand, Mayeaux et al., (2006) studied thermal stability using pure lycopene standard at 100, 125 and 150°C during 10, 20, 30 and 60 min. The authors indicated that after 10 min of heating, the pure lycopene was degraded with approximately 90%, 70% and 30% of the original pure lycopene content remaining at temperatures of 100, 125 and 150°C , respectively. The proposed pathway of lycopene degradation consists of 2 stages: isomerization and auto-oxidation due

to the unsaturated double bonds. The isomerization of lycopene increased at a temperature above 75°C (Mayeaux et al., 2006; Srivastava and Srivastava, 2015). However, the studies about lycopene stability shows that the degradation is influence by factors such as time of exposition, temperature, additives, specially by the matrix in which lycopene is dissolved or stored.

IV. CONCLUSION

Rhodotorula glutinis has been employed to carotenoids production, but the production is intracellular type and cell disruption is necessary. In this study we found that methanol is the best agent to carotenoids extraction, however, the 100% of disruption was not possible. On the other hand, the low antioxidant activity compared with lycopene standard could be because the pigments produced by *R. glutinis* P4M422 are unstable and the study of special techniques to recovery these compounds is important.

V. ACKNOWLEDGEMENTS

Author Hernandez-Almanza thank the National Council of Science and Technology (CONACYT), Mexico for financial support to her postgraduate studies at DIA-FCQ/UAdC.

REFERENCES

- [1] Agarwal, S., Sharma, V., Kaul, T., Abdin, M., Singh, S., 2014. Cytotoxic effect of carotenoid phytonutrient lycopene on *P. falciparum* infected erythrocytes. *Molecular and Biochemical Parasitology*, 197(1-2): 15-20. doi: <http://dx.doi.org/10.1016/j.molbiopara.2014.09.005>
- [2] Ceron-Garcia, M.d.C., Campos-Perez, I., Macias-Sanchez, M.D., Bermejo-Roman, R., Fernandez-Sevilla, J M., and Molina-Grima, E., 2010. Stability of Carotenoids in *Scenedesmus almeriensis* Biomass and Extracts under Various Storage Conditions. *Journal of Agricultural and Food Chemistry*, 58(11): 6944-6950. doi: 10.1021/jf100020s
- [3] Colle, I.J.P., Lemmens, Lien, Van Buggenhout, Sandy, Van Loey, Ann M, Hendrickx, Marc, E., 2013. Modeling Lycopene Degradation and Isomerization in the Presence of Lipids. *Food and Bioprocess Technology*, 6(4): 909-918. doi: 10.1007/s11947-011-0714-4
- [4] Chen, J., Shi, J., Xue, S., and Ma, Y., 2009. Comparison of lycopene stability in water- and oil-based food model systems under thermal-and light-irradiation treatments. *LWT-Food Science and Technology*, 42(3): 740-747. doi: <http://dx.doi.org/10.1016/j.lwt.2008.10.002>
- [5] Chen, Y., Shen, H., Cui, Y., Chen, S., Weng, Z., Zhao, M., and Liu, J., 2013. Chromosomal evolution of *Escherichia coli* for the efficient production of lycopene. *BMC Biotechnology*, 13(1): 6.
- [6] Choudhari, S., Ananthanarayan, L.a., and Singhal, R., 2009. Purification of Lycopene by Reverse Phase Chromatography. *Food and Bioprocess Technology*, 2(4): 391-399. doi: 10.1007/s11947-008-0054-1
- [7] Frengova, G., and Beshkova, D., 2009. Carotenoids from *Rhodotorula* and *Phaffia*: yeasts of biotechnological importance. *Journal of Industrial Microbiology & Biotechnology*, 36(2): 163-180. doi: 10.1007/s10295-008-0492-9
- [8] Honda, M., Takahashi, N., Kuwa, T., Takehara, M., Inoue, Y., and Kumagai, T., 2015. Spectral characterisation of Z-isomers of lycopene formed during heat treatment and solvent effects on the E/Z isomerisation process. *Food Chemistry*, 171(0): 323-329. doi: <http://dx.doi.org/10.1016/j.foodchem.2014.09.004>
- [9] Kim, Y., Lee, J., Kim, N., Yeom, S., Kim, S., and Oh, D., 2011. Increase of lycopene production by supplementing auxiliary carbon sources in metabolically engineered *Escherichia coli*. *Applied Microbiology and Biotechnology*, 90(2): 489-497. doi: 10.1007/s00253-011-3091-z
- [10] Bone, R. a., Landrum, J.T., Mayne, S.T., Gomez, C.M., Tibor, S.E., Twaroska, E.E., 2001. Macular pigment in donor eyes with and without AMD: A case-control study. *Investig. Ophthalmol. Vis. Sci.* 42: 235-240.
- [11] dos Santos, P.P., Paese, K., Guterres, S.S., Pohlmann, A.R., Jablonski, A., Flores, S.H., Rios, A. de O., 2016. Stability study of lycopene-loaded lipid-core nanocapsules under temperature and photosensitization. *LWT-Food Sci. Technol.* 71: 190-195.

- [12] Heber, D., Lu, Q., 2002. Overview of mechanisms of action of lycopene. *Exp. Biol. Med.* 227, 920-923.
- [13] Hsiao, G., Fong, T.H., Tzu, N.H., Lin, K.H., Chou, D.S., Sheu, J.R., 2004. A potent antioxidant, lycopene, affords neuroprotection against microglia activation and focal cerebral ischemia in rats. *In Vivo (Brooklyn)*. 18, 351-356.
- [14] Lopez-Nieto, M.J., Costa, J., Peiro, E., Mendez, E., Rodriguez-Seiz, M., De La Fuente, J.L., Cabri, W., Barredo, J.L., 2004. Biotechnological lycopene production by mated fermentation of *Blakeslea trispora*. *Appl. Microbiol. Biotechnol.*, 66: 153-159.
- [15] Mahfoudhi, N., Hamdi, S., 2015. Kinetic Degradation and Storage Stability of B-Carotene Encapsulated by Freeze-Drying Using Almond Gum and Gum Arabic as Wall Materials. *J. Food Process. Preserv.*, 39: 896-906.
- [16] Mantzouridou, F., Tsimidou, M.Z., 2008. Lycopene formation in *Blakeslea trispora*. Chemical aspects of a bioprocess. *Trends Food Sci. Technol.*, 19: 363-371.
- [17] Marova, I., Carnecka, M., Halienova, A., Certik, M., Dvorakova, T., Haronikova, A., 2012. Use of several waste substrates for carotenoid-rich yeast biomass production. *J. Environ. Manage.*, 95: S338-S342.
- [18] Mayeaux, M., Xu, Z., King, J., Prinyawiwatkul, W., 2006. Effects of Cooking Conditions on the Lycopene Content in Tomatoes. *J. Food Sci. C Food Chem. Toxicol.* 71: 461-464.
- [19] Omoni, A.O., Aluko, R.E., 2005. The anti-carcinogenic and anti-atherogenic effects of lycopene: A review. *Trends Food Sci. Technol.*, 16: 344-350.
- [20] Srivastava, S., Srivastava, A.K., 2015. Lycopene; chemistry, biosynthesis, metabolism and degradation under various abiotic parameters. *J. Food Sci. Technol.*, 52: 41-53.
- [21] Wang, J., Liu, X.J., Liu, R., Li, H.M., Tang, Y.J., 2012. Optimization of the mated fermentation process for the production of lycopene by *Blakeslea trispora* NRRL 2895 (+) and NRRL 2896 (-). *Bioprocess Biosyst. Eng.*, 35: 553-564.
- [22] Yoo, A.Y., Alnaeeli, M., Park, J.K., 2015. Production control and characterization of antibacterial carotenoids from the yeast *Rhodotorula mucilaginosa* AY-01. *Process Biochem.*, 51: 463-473.

High Pressure Processing of Raw and Marinated Mackerel Fillets. Study on the Inactivation of Anisakidae Larvae and Some Quality Aspects

Anna G. Fiore^{1*}, Luigi Palmieri², Andrea Lo Voi², Ivana Orlando²,
Giovanni Normanno¹, Antonio Derossi¹, Carla Severini¹

¹Department of Science of Agricultural, Food and Environmental (SAFE),
University of Foggia, Via Napoli 25, 71122 Foggia, Italy

²Experimental Station for the Food Preserving Industry (SSICA), Via Nazionale 121-123,
Angri, Salerno, Italy

Abstract

*The nematode larvae of the Anisakidae family are one of the main health hazards for consumers of raw fish or marinated products. The effects of high-pressure were investigated to observe the efficacy of non-thermal process on Anisakidae larvae in ready-to-use and ready-to-eat mackerel fillets (*Scomber scombrus*). Live and vital larvae were collected from the viscera of heavily parasitized fish and inoculated in raw fillets with the aim to reproduce infection by larvae. Raw and marinated samples were submitted to different process conditions (100 and 200 MPa for 5 and 8 minutes respectively and 300 MPa for 5 min) to evaluate the viability of the larvae and some quality aspects of minimally processed mackerel fillets. Treatments at pressures higher than 200 MPa, were able to devitalize all the larvae present in the both raw and marinated fillets, even if a pressure above 300 MPa can also give to seafood an opacity similar to that obtained by a very light cooking. The muscles of mackerel become opaque and showed higher values of luminosity (L*), following HP-treatment. Results showed that the application of a pressure of 200 MPa for 8 min could be sufficient to devitalize living larvae only in marinated mackerel fillets. Both the pressure levels and pressure holding time affected the content of moisture, ash, and lipid in pressurized samples, improving their nutritional values in terms of total PUFAs content, especially in marinated samples.*

Keywords: High pressures, Anisakidae larvae, mackerel fillets, minimally processed fish, inactivation, quality

*Corresponding author e-mail:anna.fiore@unifg.it

I. INTRODUCTION

THE seafood products play an important role in human nutrition, since they are considered as a significant source of important nutrients. For many centuries, fish has been one of main foods and nowadays accounts for almost 17% of the global population's intake of animal-origin proteins; this proportion is much higher in developing countries, where fish may be the only source of animal protein (FAO, 2014). Nevertheless, the great importance from the nutritional point of view is attributed to the lipid composition of the fish, that constitutes an excellent source of n-3 polyunsaturated fatty acids (n-3 PUFAs), predominantly EPA and DHA known to their important role in immune system regulation, blood clots, neurotransmitters, cholesterol metabolism, and structure of membrane phospholipids in the brain and the retina (Abedi and Sahari, 2014). Nowadays, the increased consumer information towards healthier aspects of the foods, has led to a higher demand of fresh and natural products. However, due to its high value in proteins and lipids, fish is a very perishable food. Since degradation of certain nutritive constituents, in particular lipids, begins during handling and it may increase during industrial processing, the nutritional content of raw seafood products could significantly reduced. For these reasons, convenience foods, minimally processed with characteristics closer to that of the fresh products are gaining importance and have led to new interventions in the fish-processing for extending the shelf life with minimal use of preservatives or severe heating procedures.

Nevertheless, the development of new mild technologies, could increase the risk of exposure of the consumer to pathogens considered autochthonous in certain fish products, as the third larval stage of Anisakidae family. The majority of larvae in fish are found in the viscera and internal organs, with a lesser extent in the muscle. The genera of Anisakidae family implicated in case of human infection (i.e. *Anisakis*) represents a hazard to con-

sumer health, since it may cause pathogenic diseases like gastric or intestinal anisakiasis (Lopez-Serrano et al., 2003; Nawa et al., 2005), and gastro-allergic disorders (Audicana and Kennedy, 2008; Hochberg and Hamer, 2010). The effects of anisakids on the reduction of commercial value of fish (Vidacek et al., 2009) and its impact on human health has given these parasites a public health concern, which was recently recognized by the Panel on Biological Hazards of the European Food Safety Authority (EFSA, 2010).

Freezing, thermal processing, salting, and high hydrostatic pressure (HHP) treatments can be used to kill Anisakidae larvae. Among these methods, freezing and thermal processing are proved to be effective. According to the Food and Drug Administration (FDA, 2001), raw or undercooked fish products should be frozen at -35°C for 15 h. European Food Safety Authority supports the effectiveness in controlling parasites by freezing at -20°C (-4°F) at the centre of the product for 24 h and underlines to cook fish at 60°C for at least 1 min to kill *Anisakis* larvae (EFSA, 2010). The current European Union, ruling on food hygiene (Hygiene Package), permits the consumption of raw products only when they have been made safe through freezing (-20°C in all part of the product) or with other methods of proven efficacy, such as smoking at over 60°C or marinating treatments sufficient to devitalize any parasites present (EU, Reg. 853/2004, Section VIII, Chap. III, point D). Recently, effects on the inactivation of *Anisakis* larvae by high-pressure process (Molina Garcia and Sanz, 2002; Dong et al., 2003; Brutti et al., 2010) were investigated. Brutti et al., (2010) reported that HP-treatment at 300 MPa for 5 min was sufficient to completely inactivate *Anisakis* larvae located in whole mackerel (*Scomber scombrus*). Although high hydrostatic pressure was effective in killing *A. simplex* larvae in raw fish fillets, its significant and negative effect on color and overall appearance of the fillets may limit its application to the processing of fish for raw fish markets (Dong et al., 2003).

The aim of this work has been to evaluate

the efficiency of time and pressure applied on the inactivation of Anisakidae larvae in raw and marinated mackerel fillets and their effects on quality of processed fish.

II. MATERIAL AND METHODS

Preparation samples

Live Anisakidae larvae were collected from the viscera of heavily parasitized fish. Live larvae adhering to the viscera tissue were collected, immediately placed in saline (0.85% NaCl), and stored at 4 °C. To standardize the conditions of each pressurized treatment, 20 live larvae were inoculated in the cavity produced in the raw mackerel fillets and, before marinating, in marinated samples. Each sample was under-vacuum sealed in a high-density polyethylene (HDPE) bag. Following packaging, raw and marinated samples were stored at 4 °C for 2 h to let the larvae adapt to the changed conditions. Live larvae isolated from viscera of parasitized fish were kept in saline and stored at 4 °C for control. Mackerel (*Scomber scombrus*) were purchased within 24-48 h post-caught, from a local seafood market in Foggia, Italy, in January 2017. The average length and weight of the samples was of 31 ± 1.5 cm and 160 ± 5 g, respectively. Raw fishes were eviscerated, headed, washed, gutted, skinned and filleted into two sides (80 ± 7 g each one) in a cold room at 4 °C. Then each fillet was marinated by immersion in a pre-chilled (4 °C) solution patented in Italy (n. 0001394882, Severini and Fiore, 2012) having a pH of ~ 2.16 . The high pressure treatments were carried out through high pressure pilot autoclave (Quintus Food Press 35L-600, SSICA Parma, Italy), operating at 100, 200 for 5 and 8 minutes and 300 MPa for 5 min at 4 °C.

Measurement of viability

All experiments were carried out in triplicate. Live larvae recollected from each sample in saline were counted. In the absence of spontaneous movement, larvae in saline were gently touched with a sharp wooden stick approximately 5 times to observe movement.

If movement of the larvae was not observed shortly after touching, the experiment was repeated. All larvae that showed movement either spontaneously or by the stimulating tool were recorded as 'live'. If there was no movement after being stimulated 5 times, the larva was recorded as 'dead'. Following the observation, viability was calculated. Values of viability were shown as %.

Color

Color measurements were performed on fish fillets with a Minolta Chromameter 2 Reflectance (Minolta, Japan) equipped with the measurement head CR 300, according to the standard conditions of the Commission International d' Eclairage (CIE). Results were expressed as L* (brightness), a* (red index) and b* (yellow index).

Proximate composition analysis

Moisture content was determined using the dry oven method (AOAC, 1995) - method 954.01. Ash content was determined from the loss in weight that occurs during incineration of the sample at 525 ± 25 °C, according to AOAC, (1995)-method 942.05. Crude protein was determined by the Kjeldahl methods (AOAC, 1995)-method 954.01. Crude protein was determined by multiplying the nitrogen value by the conversion factor of 6.25. Crude fat was determined using AOAC (1995)-method 920.39. Fatty acids were analyzed by GC after from mackerel fillets by hydrolytic methods (AOAC, 1995)-method 996.06.

Statistical analysis

Results are presented as mean values and standard deviation. All experimental data were analyzed by using the one way ANOVA with a Fisher post hoc tests with a p-level of 0.05. Descriptive analysis of data were performed using the software package Statistica ver 10.0 (StatSoft, Tulsa, USA).

III. RESULTS AND DISCUSSION

The effects of pressure level and pressure holding time on the Anisakidae larvae viability in raw and marinated mackerel fillets are shown in figure 1.

No significant differences ($p > 0.05$) in the viability of larvae were found in raw and marinated fillet samples. According to the data reported in literature marinating is an inadequate treatment to kill the nematodes in seafood. The mortality rate of the nematodes is a function of time and dependent mainly by salt and acid concentrations in the aqueous phase of the fish tissue. It is reported that traditional marinating procedures (water phase 6% salt and 2.4% acetic acid) for marinating herring fillets require a storage time of at least 35 days, for all the larvae are killed (Karl et al., 1995). However,

the relatively high concentrations of salt and acetic acid make undesirable acidified products that may not be accepted by the consumers. In this study, mackerel fillets showed an average value of $\text{pH} \sim 4.25 \pm 0.03$ after marinating (data not shown), sufficiently low to prevent bacterial growth of some pathogens, but not sufficiently to devitalize Anisakidae larvae. It is known that parasite (i.e. *Anisakis*) are very resistant to the acidic conditions of the gastric juice of the host (Adams et al., 1999). When hyperbaric treatments were applied the viability of larvae in raw and marinated fillets showed a different behaviour as a function of both pressure and pressure holding time (fig. 1). A significant ($p < 0.05$) reduction of larvae viability in raw pressurized samples at 200 MPa in comparison to untreated samples was observed.

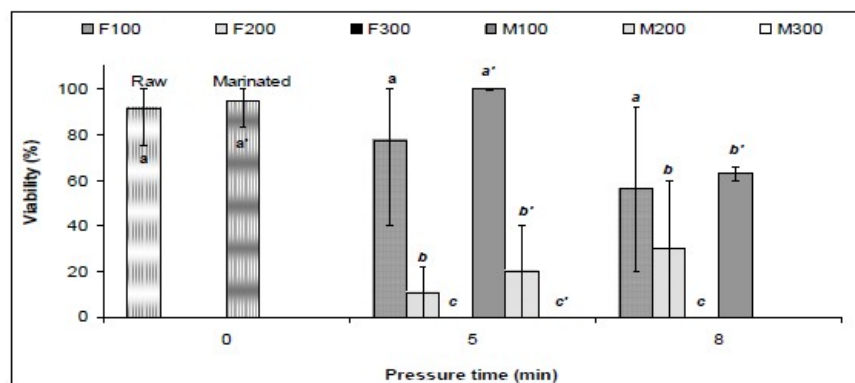


Figure 1: Viability of Anisakidae larvae in raw and marinated samples processed and non-processed at pressure of 100, 200, 300 Mpa for 5 and 8 minutes.

However, the great variability indicated that the applied pressure is still inadequate for the complete larvae devitalisation. On the contrary, the pressure of 300 MPa was significantly effective to kill all larvae present in raw mackerel fillets, in agreement with the data obtained by other authors (Brutti et al., 2010). At 200 MPa of pressure, time process significantly ($p < 0.05$) affected the larvae viability in marinated fillets, reducing the percentage from $94.33\% \pm 9.81$ of untreated sample to $20\% \pm 28.28$ after 5 min of process. Extending the time of process until

to 8 min, the larvae viability significantly ($p < 0.05$) decreased to 0%. This result was not obtained in raw processed fillets in the same conditions. The C.I.E. L^* a^* b^* color values before and after pressure treatments are presented in table 1. HP-treatment affected significantly ($p < 0.05$) the color of pressurized (raw and marinated) mackerel fillets. At 100 MPa the fillet luminosity decreased significantly ($p < 0.05$) as well as both a^* and b^* parameters. When pressure increase to 200 MPa, any difference in L^* values was not show between treated and

untreated fillets. Applying a pressure of 300 MPa for 5 min the significant ($p < 0.05$) increase of L^* in the raw pressurized fillets could be attributed to a reduction of red index (a^*). They particularly appeared as cooked. These changes were attributed to the denaturation of the myofibrillar and sarcoplasmic proteins (Ledward, 1998). Raw and marinated fillets not submitted to hyperbaric treatments, showed significant ($p < 0.05$) difference in L^* , a^* and b^* values. It is evident that marinating changed significantly the appearance of the fillets that can be visually observed.

The higher L^* index of marinated fillets could be attributable to a balance between the decrease of red (a^*) and increase of yellow (b^*) indexes, which made the marinated fillet similar to that cooked. High hydrostatic pressure affected significantly ($p < 0.05$) the color of marinated mackerel fillets only in terms of luminosity.

No significant ($p > 0.05$) changes in a^* values appeared for the pressurized marinated fillets, while a significant decrease of b^* values ($p < 0.05$) was noticed when marinated fillets were pressurized at 200 MPa for 8 min. Table 2 illustrates the effect of pressure level and pressure holding time on the proximate composition and PUFAs content of the untreated and pressurized mackerel fillets. Both the pressure level and pressure holding time significantly ($p < 0.05$) influenced the decrease in water content of pressurized raw fillets in comparison with untreated samples. Reasonably, this could be caused by the water loss of fish tissue as a consequence of the physical and chemical changes induced by the processing. High pressure can affect protein conformation leading to protein denaturation, aggregation or gelation, as a function of processing conditions (Gross and Jaenicke, 1994).

Table 1: Effects of pressure (MPa) and pressure holding time (min) on the L^* a^* b^* values of raw and marinated mackerel fillets.

Treatments	Raw			Marinated		
	L^*	a^*	b^*	L^*	a^*	b^*
Untreated	53.53 ±	7.5 ±	7.73 ±	69.22 ±	1.81 ±	14.34 ±
	2.14 ^{b,c}	2.15 ^a	0.69 ^a	0.99 ^a	0.52 ^a	0.59 ^a
100 MPa x 5 min	42.53 ±	1.23 ±	2.69 ±	78.58 ±	-0.30 ±	12.75 ±
	2.20 ^d	0.45 ^c	0.69 ^b	0.69 ^c	0.86 ^a	0.45 ^a
100 MPa x 8 min	47.63 ±	4.09 ±	4.67 ±	75.41 ±	0.05 ±	12.90 ±
	2.77 ^d	1.38 ^b	0.79 ^{b,c}	3.59 ^{b,c}	0.55 ^a	0.68 ^a
200 MPa x 5 min	52.19 ±	5.39 ±	6.34 ±	71.4 ±	0.91 ±	13.17 ±
	2.91 ^{c,d}	1.65 ^{a,b}	2.50 ^{a,c}	4.23 ^{a,b}	1.86 ^a	0.79 ^a
200 MPa x 8 min	57.74 ±	0.96 ±	2.55 ±	71.82 ±	1.30 ±	12.03 ±
	2.28 ^b	0.75 ^c	0.92 ^b	3.60 ^{b,c}	0.94 ^a	0.84 ^b
300 MPa x 5 min	68.74 ±	2.75 ±	6.50 ±	75.91 ±	1.00 ±	13.30 ±
	2.20 ^a	1.43 ^{b,c}	1.75 ^{a,c}	2.85 ^{b,c}	1.04 ^a	2.19 ^a

*all values are the means ± standard deviations of three replicates; **different letters in the same column indicate significant differences ($p < 0.05$).

For instance, Marcos et al., (2010) reported that the denaturation of sarcoplasmic proteins, induced by high pressure treatment, increased the water loss in pressurized meats. This was confirmed by ash values of pressurized samples that decrease significantly ($p < 0.05$) when pressure and time of process increase (table 2). The protein content didn't show any significant ($p > 0.05$) difference among treated and untreated samples. As for protein fraction, as well known, the pressurization produces both the denaturation of the con-

tractile proteins of meat (myosin and actin) and solubilization of the connective tissue (collagen) (Gomez-Guillen et al., 2005). It is possible to hypothesize that a balance between contractile proteins denaturation (myosin and actin) and the solubilization of collagen induced by high pressures would occur. Total percentage of lipid of raw fillets showed a significant ($p < 0.05$) increase with the increase of pressure level and pressure holding time, due to the significant water loss that occurred.

Table 2: Effects of pressurization and pressure holding time on the proximate composition and total PUFAs of raw and marinated mackerel fillets.

Raw					
Samples	Moisture g/100g	Ash g/100g	Protein g/100g	Lipid g/100g	PUFAs g/100g
Untreated	62.0 ± 0.71 ^a	1.5 ± 0.04 ^a	18.3 ± 0.6 ^a	17.6 ± 0.1 ^a	4.8 ± 0.01 ^a
100MPa x 5 min	63.6 ± 1.82 ^a	1.5 ± 0.02 ^a	17.0 ± 1.0 ^a	18.2 ± 0.8 ^a	3.5 ± 0.03 ^b
100MPa x 8 min	54.0 ± 2.93 ^b	1.4 ± 0.03 ^b	16.4 ± 0.9 ^a	25.0 ± 2.0 ^b	3.9 ± 0.03 ^c
200MPa x 5 min	58.0 ± 1.25 ^c	1.3 ± 0.05 ^b	16.7 ± 0.3 ^a	22.7 ± 0.9 ^c	4.7 ± 0.03 ^d
200MPa x 8 min	56.6 ± 2.75 ^{b,c}	1.4 ± 0.05 ^b	17.0 ± 2.0 ^a	21.6 ± 0.7 ^c	5.1 ± 0.09 ^e
Marinated					
Samples	Moisture g/100g	Ash g/100g	Protein g/100g	Lipid g/100g	PUFAs g/100g
Untreated	55.0 ± 1.23 ^a	1.5 ± 0.03 ^a	19.7 ± 0.2 ^a	27.0 ± 1.0 ^a	5.1 ± 0.02 ^a
100MPa x 5 min	58.0 ± 3.03 ^b	1.3 ± 0.03 ^b	19.0 ± 2.0 ^a	27.0 ± 1.0 ^a	4.3 ± 0.05 ^b
100MPa x 8 min	56.0 ± 0.63 ^{ab}	1.6 ± 0.01 ^c	19.1 ± 0.6 ^a	23.9 ± 0.0 ^b	3.0 ± 0.04 ^c
200MPa x 5 min	54.0 ± 0.91 ^a	1.5 ± 0.01 ^d	19.2 ± 0.8 ^a	28.7 ± 0.1 ^c	5.5 ± 0.07 ^d
200MPa x 8 min	58.0 ± 0.53 ^{b,c}	1.4 ± 0.03 ^e	18.4 ± 0.3 ^a	29.2 ± 0.2 ^c	4.9 ± 0.23 ^e

*all values are the means ± standard deviations of three replicates; **different letters in the same column indicate significant differences ($p < 0.05$).

Even if 100 MPa for 5 min didn't show any significant ($p > 0.05$) effect in the proximate composition, their content in total PU-

FAs decreased significantly ($p < 0.05$) as fast as in other pressurized samples. Regarding this important nutritional components our results

showed significant ($p < 0.05$) changes influence as a function of pressure and time conditions. The lowest value of total PUFAs (4.82 ± 0.01) was observed at 100 MPa of pressure for 8 min (3.5 ± 0.03), while the highest was shown by samples treated at 200 MPa for 5 min (5.1 ± 0.09). The extension of treatment time significantly increase the total PUFAs content in all pressurized raw fillets. Regarding the marinated samples, changes in the proximate composition are shown in table 2. Comparing raw and marinated untreated fillets, the loss in water content was the most effect that occurred after marinating. For this reason other nutritional compounds increased significantly ($p < 0.05$) than non-marinated fillets. The same effects of pressure levels and pressure holding time on untreated sample were observed for the marinated fillets submitted to high pressure, with exception for time of process that negatively affected total PUFAs content if prolonged from 5 to 8 min. Combined high-pressure and marinating treatments led to the highest value in total PUFAs.

IV. CONCLUSIONS

The application of high hydrostatic pressure was an effective technology to devitalize lar-

vae belonging to the Anisakidae family in raw and marinated fish. The results confirm those already known in literature regarding whole mackerel fillets. Marinating is not common for fish species as mackerel, but at low concentrations of salt and organic acids this practice exerts a synergistic effect if combined with high pressure to inactive Anisakidae larvae. Pressure of 200 MPa for 8 min were sufficient to devitalize 100% of larvae inoculated in mackerel fillets, while 300 MPa for 5 min were required for raw samples compromising its appearance similar to the cooked product. The changes in color, particularly in the raw pressurized fillets were gradual with both the pressure level and pressure holding time. From a nutritional point of view, raw and marinated pressurized samples didn't show significant variation in protein composition, while a significant influence was reported for PUFAs that were more sensible at lower pressure adopted in both raw and marinated samples. The combined effect of high pressure and marinating were able to reduce pressure level required to inactivate Anisakidae larvae from 300 MPa to 200 Mpa in minimally processing mackerel fillets, improving other qualitative aspects as appearance and nutritional value.

REFERENCES

- [1] Abedi, E., Sahari, M.A., 2014. Long-chain polyunsaturated fatty acid sources and evaluation of their nutritional and functional properties. Review. Food Science & Nutrition, 443-463.
- [2] Adams A.M., Miller, K.S., Wekell, M.M., Dong, F.M., 1999. Survival of *Anisakis simplex* in microwave-processed arrowtooth flounder (*Atheresthes stomias*). J. Food Prot., 62: 403-409.
- [3] AOAC, 1995. Official Methods of Analysis AOAC International. (16th ed) Arlington, VA:AOAC.
- [4] AOAC, 1995. Official Methods of Analysis AOAC International. Gaithersburg, MD: AOAC.
- [5] Audicana, M.T., Kennedy, M.W., 2008. *Anisakis simplex*: from obscure infectious worm to inducer of immune hypersensitivity. Clin. Microbiol. Rev., 21: 360-379.
- [6] Brutti, A., Rovere, P., Cavallero, S., D'Amelio, S., Danesi, P., Arcangeli, G., 2010. Inactivation of *Anisakis simplex* larvae in raw fish using high hydrostatic pressure treatments. Food Control, 21: 331-333.
- [7] Dong, F.M., Cook, A., Herwig, R.P., 2003. High hydrostatic pressure treatment of finfish to inactivate *Anisakis simplex*. J. of Food Prot., 66: 1924-1926.

- [8] EFSA European Food Safety Authority, 2010. Scientific Opinion on risk assessment of parasites in fishery products. EFSA Panel on Biological Hazards (BIOHAZ). EFSA J., 8(4) 1543: 1-91.
- [9] EU, 2004. Regulation (Ec) No 853/2004 of the European Parliament and of the Council of 29 April 2004 laying down specific hygiene rules for food of animal origin. Official Journal of the European Union L. 139 of 30 April 2004.
- [10] FAO, 2014. The state of world fisheries and aquaculture. Food And Agriculture Organization Of The United Nations, Rome, pp. 1-243.
- [11] FDA, 2001. Food code, Section 3-402.11 (A1 and A2). In 2001 Recommendations of the United States Public Health Service Food and Drug Administration, Washington, DC.
- [12] Gomez-Guillen, M.C., Gimenez, B., Montenero, P., 2005. Extraction of gelatin from fish skins by high pressure treatment. Food Hydrocolloids, 19: 923-928.
- [13] Gross, M., Jaenicke, R., 1994. Proteins under pressure. The influence of high hydrostatic pressure on structure, function and assembly of proteins and protein complexes. European Journal of Biochemistry, 221: 617-630.
- [14] Hochberg, N.S., Hamer, D.H., 2010. Anisakidosis: perils of the deep. Clin. Infect. Dis., 51(7): 806-812.
- [15] Karl, H., Roepstorff, A., Huss, H.H., Bloemsmas, B., 1995. Survival of Anisakis larvae in marinated herring fillets. Int. J. Food Sci. Technol., 29: 661-670.
- [16] Ledward, D.A., 1998. High pressure processing of meat and fish. In K. Autio, fresh and novel foods by high pressure (pp. 165-175). Espoo: VTT Biotechnology and Food Research.
- [17] Lopez-Serrano, M.C., Gomez, A.A., Daschner, A., 2003. Gastroallergic anisakiasis: findings in 22 patients. J. Gastroenterol. Hepatol., 15: 503-506.
- [18] Marcos, B., Kerry, J.P., Mullen, A.M., 2010. High pressure induced changes on sarcoplasmatic protein fraction and quality indicators. Meat Science, 85: 115-120.
- [19] Molina Garcia, A.D., Sanz, P.D., 2002. Anisakis simplex larva killed by high-hydrostatic-pressure processing. Journal of Food Prot., 65: 383-388.
- [20] Nawa, Y., Hatz, C., Blum, J., 2005. Sushi delights and parasites: the risk of fishborne and foodborne parasitic zoonoses in Asia. Clin. Infect. Dis., 41(9): 1297-1303.
- [21] Severini, C., Fiore, A., 2012. Metodo di produzione e stabilizzazione di filetti di pesce di V gamma. University of Foggia, Italy. Patent N. RM2009A000292, issued 20 July, 2012.
- [22] Vidacek, S., de las Heras, C., Tejada, M., 2009. Quality of fish muscle infested with Anisakis simplex. Food Sci. Technol. Int., 15(3): 283-290.

A Study on the Enrichment of Olive Oil with Natural Olive Fruit Polyphenols

Tsilfoglou Sotiria^{1,2*}, Petrotos Kostantinos¹, Leontopoulos Stefanos¹,
Hadjichristodoulou Christos², Tsakalof Andreas²

¹Technological Educational Institute of Thessaly,
Dept. of Biosystems Engineering, Ring Road of Larissa-Trikala, 41110 Larissa, Greece

²University of Thessaly, Dept. of Medicine,
Lab of Hygiene and Epidemiology, Papakyriazi 22, 41222 Larissa

Abstract

In the last years, has been a sudden and increased interest by scientists in producing creating plant origin food products. This is explained by their polyphenolic content, to which has been attributed a large scale bioactivity as described in many studies. Foods that have beneficial effects due to their high content in polyphenols are olive oil, wine, cocoa, coffee, fruits and vegetables with intense color, whole grain products, tea and other herbal beverages. The purpose of this study was the enrichment of olive oil with olive polyphenols and specifically with hydroxytyrosol, tyrosol, and oleuropein aglycones in order to produce a final product with increased bioactivity and official health claim. Initially, we developed a fast and accurate method of total polyphenols analysis by UV-VIS method, in order to evaluate the degree of enrichment of olive oils, by three specific chosen methods. Also, the UV-VIS method was used to examine and to measure the commercial olive polyphenols compared with cold pressed olive oil. The three alternative oil enrichment methods with olive polyphenols are: I) Addition of encapsulated polyphenol derivatives into liposomes, II) Extraction of polyphenols from olive oil using an organic solvent and then incorporating them with cryogenics sublimation with another olive oil, III) Extraction of polyphenols in the body olive oil from olive leaves using ultrasound at a controlled low temperature. Consequently, based on the results, the first two methods are effective. The final product combines nutritional and medical benefits in the prevention of diseases and can be used by the industry, for food and pharmaceutical products improvement.

Keywords: Olive oil, natural polyphenols, functional Foods

*Corresponding author e-mail:sotiria tsilfoglou@yahoo.gr

I. INTRODUCTION

Since ancient times, it is known that olive oil in our diet is important to our health. Olive oil was used for skin care and muscle luster, abrasion therapy, burn healing, and dehydration caused by the sun. It is a product with equally spectacular properties for both health and beauty. The body cells incorporate the valuable fatty acids of olive oil, making the arteries and the skin smoother. Today, modern medicine continues to recommend the widespread use of olive oil in the nutrition of adults and children, health, thanks to its valuable ingredients that provide health, well-being and longevity.

The Mediterranean diet derived from the olive oil producing countries of Greece, Spain and south Italy is famous all over the world for its beneficial properties. The beneficial effect of olive oil is due to its high content of substances with antioxidant action, combining effectively and effectively reducing the destructive action of free radicals, enhancing the defense of the body and shielding the heart and vessels (Dew et al., 2005; Visioli et al., 1998; Visioli and Galli, 2001; Visioli and Galli, 1998a; Visioli and Galli, 1998b; Visioli and Bernardini, 2011).

In the last years, has been an increased interest in producing natural food additives originated by plants. One of them are polyphenolic compounds, attributing a large scale bioactivity as described in many studies showing multiple benefits for human health captivating strong interest of the scientific community (Bulotta et al., 2014). The three polyphenols with the highest concentrations in olive oil are the glucoside elephrophin, hydroxytyrosol and tyrosol.

Studies have shown that the composition of polyphenols in olive oil depends on many factors such as the altitude of the area where the olive trees are grown, the maturity stage of the fruit, soil and climatic conditions (height of precipitation, temperature) (Cinquanta et al., 1997; Ryan and Robards, 1998). In the case of olive oil, the olive oil is also used for the production of olive oil. Concentration of polyphenols in olive oil varies from 50 to 1000 $\mu\text{g} / \text{g}$ (ppm) of

oil, depending on the olive variety and extraction system, and this amount of antioxidants in olive oil is only 1-2% (Rodis et al., 2002; Tsimidou et al, 1992).

The most important properties of the polyphenols are their antioxidant activity, their effect on the digestion of macronutrients and absorption of metal elements, their anticancer and antibacterial effect and their antiallergic properties. Furthermore, studies done by Leontopoulos et al., (2015); Leontopoulos et al., (2016) have demonstrated the antimicrobial activity since studies done by Kokkora et al., (2015); Kokkora et al., (2016) demonstrated the possible effect on maize production and soil properties.

Other ingredients of the olive oil are caffeic, vanilla, syringic and coumaric acids. Other antioxidant compounds present in olive oil are various flavonoids and anthocyanins (Visioli et al., 1998; Benavente-Garcia O et al, 2002; Scalbert et al., 2005). Several recent research works have been studied the extraction and absorption of polyphenolic compounds (Petrotos et al., 2015; Petrotos et al., 2016).

Foods that have beneficial effects due to their high content in polyphenols are olive oil, wine, cocoa, coffee, fruits and vegetables with intense color, whole grain products, tea and other herbal beverages.

The aim of this study was the enrichment of olive oil with olive polyphenols and specifically with hydroxytyrosol, tyrosol, and oleuropein aglycones in order to produce a final product with increased bioactivity for human health.

II. MATERIAL AND METHODS

In this work the measurement of total polyphenols in olive oils (derived from different sources) was studied. Studies of olive oil enrichment with olive polyphenols included addition of encapsulated derivative of polyphenols in lecithin liposomes, addition of polyphenols that extracted from olive oil incorporated with cryogenic sublimation with other olive oil. And extraction of polyphenols, in the 'body' olive oil, from olive leaves using ultrasound at

controlled low temperature.

Measurement of total Polyphenols in olive oil Pure polyphenols extracted from olive oil using a centrifuge followed by spectrophotometric determination of the extract using Folin-Ciocalteu reagent and measurement at 725nm (Tsimidou, 1998; Tsimidou, 2005).

Olive oil enrichment with encapsulated derivative of polyphenols in lecithin liposomes

Encapsulation of liquid polyphenol in lecithin using Freeze Dryer was used in this study. Then, Mix powder (lecithin with polyphenol) with olive oil at three different concentrations (200, 500 and 1000 ppm) to increase antioxidant activity was examined enriching olive oil by adding liquid polyphenol (200, 500, 1000 ppm). Finally, samples were measured with RANCIMAT method for their resistance to oxidation.



Figure1. Freeze drier

Extraction of olive oil polyphenols using organic solvent followed by a cryogenic sublimation technique to add polyphenols into other olive oil samples

Extraction of olive oil and collection of hydro alcoholic phase was the first step at this stud followed by adding hydro alcoholic phase

into a sample of olive oil. Then, evaporation of methanol in Freeze Dryer and determination of total polyphenols using UV-VIS method was used.

Extraction of polyphenols, in the 'body' olive oil, from olive leaves at controlled low temperature using ultrasound technique

Collection, washing and slicing of olive leaves was the first step of this study followed by incorporation of chopped olive leaves to the sample of olive oil at three different concentrations (1%, 5% and 10%). The placement of olive oil samples in an ultrasonic probe for 5 minutes and the determination of total polyphenols using UV-VIS method in the originals and the enriched samples of olive oil were the final steps.

III. RESULTS AND DISCUSSION

Observing the Figure 2, we conclude that both standardized and bulk olive oil producers have a lower total polyphenol concentration than cold pressed olive oils due to the heat treatment they present in the oil mills. It is therefore confirmed that the processing temperature of olive oil plays an important role in its quality as it also affects its polyphenol content.

Figure 3 shows the concentration of total polyphenols (ppm) in the original olive oil sample and after enrichment. It was observed that the concentration of total polyphenols after enrichment almost doubled. This method is therefore considered effective.

Figure 4 shows the results of the concentration of polyphenols (ppm) in the olive oil sample before and after enrichment with the olive leaves. It was observed that the olive leaf enrichment method did not give satisfactory results. There was not a large increase in the total polyphenols (6% increases).

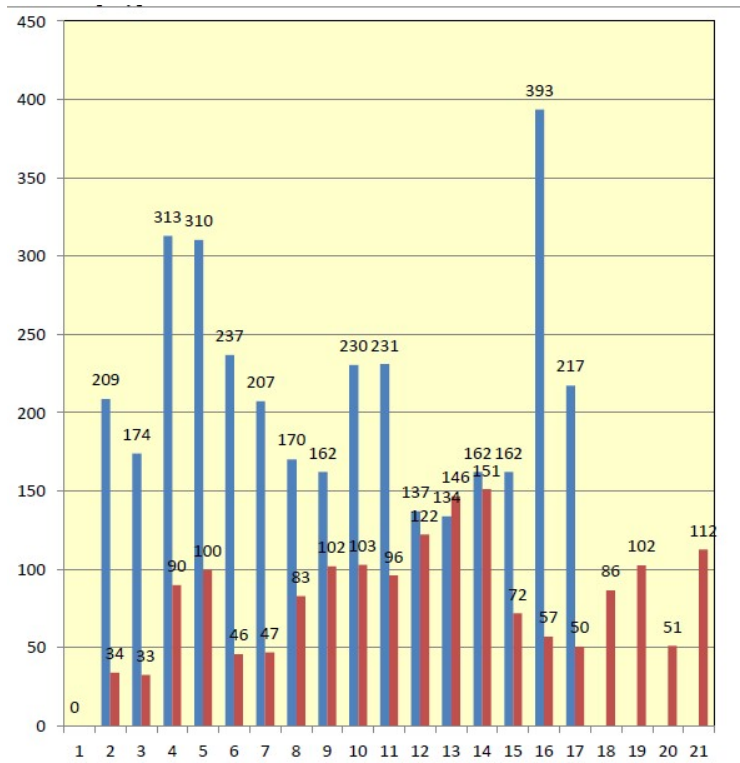


Figure 2. Concentration of polyphenols of olive oils 'cold pressed' (blue) and Commercial olive oils 'hot pressed' (red).

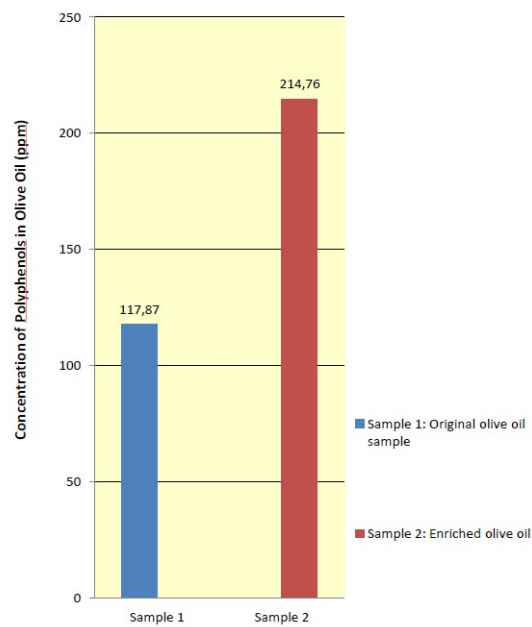


Figure 3. Concentration of polyphenols (ppm) in olive oil before and after enrichment.

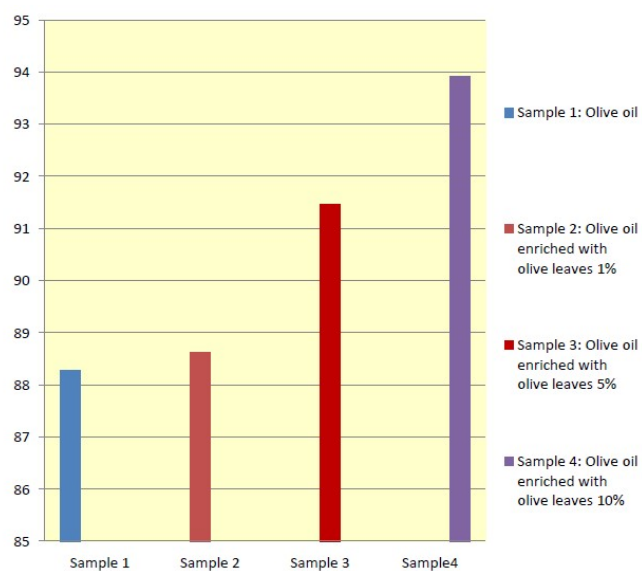


Figure 4. Effects of concentration of polyphenols (ppm) in olive oil before and after enrichment with olive leaves (in different concentrations).

In Figure 5 appeared that sample 4 enriched with encapsulated polyphenol in lecithin (1000 ppm) exhibits greater oxidative strength than that of the samples enriched with liquid polyphenol. Lecithin retains polyphenols in

the oil which in turn protects it from oxidation. Therefore, this particular enrichment process is effective as an increase in polyphenol concentration of 40% is achieved.

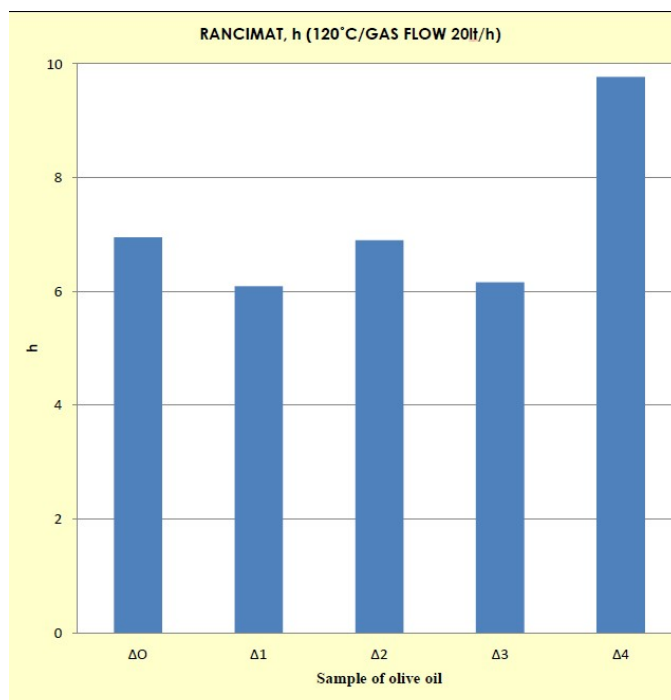


Figure 5. Oxidative resistance of enriched olive oils with liquid and encapsulated polyphenol in liposomes.

IV. CONCLUSIONS

The 'cold' pressed oil samples contained significantly higher amount of polyphenols. The use of ultrasound in olive oil with olive leaves dipped showed increased percentage of polyphenols in the treated oil samples. However, did not show remarkably high concentration (6%). Encapsulation in lecithin produces polyphenols soluble powder in the oil (1000 ppm) which enhances the antioxidant proper-

ties of the oil, increasing by a high proportion (40%) the resistance to oxidation as demonstrated by the RANCIMAT test. It can be also achieved that the increase of the content of the extracted olive oil polyphenols and their incorporation to the process of sublimation of the solvent under high vacuum is possible. This technique can be also used for olive oils with high levels of polyphenols showing beneficial properties for human health.

REFERENCES

- [1] Benavente-Garcia, O., Castillio, J., Lorente, J., Alcaraz, M., 2002. Radioprotective effects in vivo of phenolics extracted from *Olea europaea* L. leaves against X-ray-induced chromosomal damage: comparative study versus several flavonoids and sulfur-containing compounds. *Journal of Medicinal Food*, 5: 125-135.
- [2] Bulotta, S., Celano, M., Lepore, S., Montalcini, T., Pujia, A., Russo, D., 2014. Beneficial effects of the olive oil phenolic components oleuropein: focus on protection against cardiovascular and metabolic diseases. *Journal of Translational Medicine* 12: 219.
- [3] Dew, T., Day, A., Morgan, M., 2005. Xanthine Oxidase Activity *in vitro*: Effects of Food Extracts and Components. Department of Food Science, University of Leeds.
- [4] Kokkora, M.I., Petrotos, K.B., Papaioannou, Ch., Gkoutosidis, P.E., Leontopoulos, S.V., Vyrlas, P., 2016. Agronomic and economic implications of using treated olive mill wastewater in maize production. *Desalination and Water Treatment* 1-7.
- [5] Kokkora, M., Vyrlas, P., Papaioannou, Ch., Petrotos, K., Gkoutosidis, P., Leontopoulos, S., Makridis, Ch., 2015. Agricultural use of microfiltered olive mill wastewater: effects on maize production and soil properties. *Agriculture and Agricultural Science Procedia* 4: 416-424
- [6] Leontopoulos, S.V., Kokkora, M.I., Petrotos, K.B., 2016. *In vivo* evaluation of liquid polyphenols obtained from OMWW as natural bio-chemicals against several fungal pathogens on tomato plants. *Desalination and Water Treatment*, 1-15.
- [7] Leontopoulos, S.V., Giavasis, I., Petrotos, K., Kokkora, M., Makridis, Ch., 2015. Effect of Different Formulations of Polyphenolic Compounds Obtained from OMWW on the Growth of Several Fungal Plant and Food Borne Pathogens. *Studies in vitro and in vivo*. *Agriculture and Agricultural Science Procedia*, 4: 327-337.
- [8] Petrotos, K.B., Kokkora, M.I., Gkoutosidis, P.E., Leontopoulos, S., 2015. A comprehensive study on the kinetics of Olive Mill wastewater (OMWW) polyphenols absorption on macroporous resins. Part II. The case of Amperlite FPX66 commercial resin. *Desalination and Water Treatment*, 1-8.
- [9] Petrotos, K., Lampakis, D., Pilidis, G., Leontopoulos, S.V., 2016. Production and encapsulation of polyphenols derived from clarifies waste by using a combination of macroporous resins and spray drying. *International Journal of Food and Biosystems Engineering*. Accepted for publication.

- [10] Ryan, D., Robards, K., 1998. Phenolic compounds in olives. *Analyst*, 123: 31-44.
- [11] Rodis, P.S., Karathanos, V.T., Mantzavinou, A., 2002. Partitioning of olive oil antioxidants between oil and water phases. *Journal of Agriculture Food Chemistry*, 30(3): 596-601
- [12] Tsimidou, M., 1998. Polyphenols and quality of virgin olive oil in retrospect. *Italian Journal of Food Science*, 10: 99-116.
- [13] Tsimidou, M., Papadopoulou, G., Boskou, D., 1992. Phenolic compounds and stability of virgin olive oil. Part I. *Food Chemistry*, 45: 141-144.
- [14] Tsimidou, M.Z., Georgiou, A., Koidis, A., Boskou, D., 2005. Loss of stability of 'veiled' (cloudy) virgin olive oils in storage. *Food Chemistry*, 93: 377-383.
- [15] Tsimidou, M., Papadopoulou, G., Boskou, D., 1992. Determination of Phenolic Compounds in Virgin Olive Oil by RP-HPLC by Emphasis on UV Detection. *Food Chemistry*, 44: 53-60.
- [16] Visioli, F., Bellomo, G., Galli, C., 1998. Free radical-scavenging properties of olive oil polyphenols. *Biochem. Biophys. Res Comm*, 247: 60-64.
- [17] Visioli, F., Galli, C., 2001. Antitherogetic Components of Olive Oil. *Atheroscler Rep*, 3(1): 64-67.
- [18] Visioli, F., Galli, C., 1998. The Effect of Minor Constituents of Olive Oil on Cardiovascular Disease: New Findings. *Nutrition Reviews*, 56: 142-147.
- [19] Visioli, F., Galli, C., 1998. Olive Oil Phenols and their Potential Effects on Human Health. *Journal of Agricultural and Food Chemistry*, 46: 4292-96.
- [20] Visioli, F., Bernardini, E., 2011. Extra Virgin Olive Oil's Polyphenols: Biological Activities. *Curr Pharm Des.*, 17(8): 786-804.

Chemotactic Responses of *Pseudomonas oryzihabitans* and Second Stage Juveniles of *Meloidogyne javanica* on Tomato Root Tip Exudates

Stefanos Leontopoulos*, Kostantinos Petrotos, Vassiliki Anatolioti,
Prodromos Skenderidis, Sotiria Tsilfoglou, Ioannis Vagelas

Technological Educational Institute of Thessaly,
School of Agricultural Technology-Food Technology-Nutrition and Dietetics,
Dept. of Agricultural Engineering Technologists, 41110 Larissa, Greece

Abstract

The bacterium Pseudomonas oryzihabitans symbiotically associated with the entomopathogenic nematode Steinernema abbasi, is particularly effective against root-knot nematodes. The ability of P. oryzihabitans to colonise the root system was also investigated. Determination of chemotactic movement of the bacterium and second stage juveniles (J₂) of Meloidogyne javanica toward to a higher concentration of favourable chemicals secreted by tomato roots and away from an unfavorable source was investigated. The bacterium was found to have colligative stimulation in the simultaneous presence of tomato root tip exudates and J₂ of M. javanica. Positive chemotactic effects in the presence of root tip exudates near the J₂ were seen and neutral chemotactic response was seen when nematodes or root tip exudates was applied away from cells. Soil pre-inoculated with bacterial cells was found to affect the movement and behaviour of J₂, observations 4 months later

Keywords: Biological control, nematodes, bacteria, chemotaxis, tomato

I. INTRODUCTION

Despite all therapeutic measures that can be applied nowadays, plant diseases and pests still exist and become the limiting factor in tomato production in many parts of the world. In Greece, diseases caused by soil borne fungi and

bacterial-caused diseases such as bacterial wilt (*Ralstonia solanacearum*) and bacterial cancer *Clavibacter (Corynebacterium) michiganense* subsp. *michiganense* affect tomato plants and as a result can cause important economic losses (Rezzonico et al., 2017).

Among the pests that affect tomato plants, one of the most important are nematodes

*Corresponding author e-mail:sleontopoulos@yahoo.com

which are a part of the complex of root problems. *Fusarium oxysporum* and other *Fusarium* spp., *Verticillium* spp. and *Pythium* spp. are examples of fungi that interact with nematodes, mainly *Meloidogyne* spp., *Pratylenchus* spp. and *Rotylenchulus reniformis*, with synergistic effect on plant damage (Vagelas and Gowen, 2012; Vagelas and Leontopoulos, 2015; Rezzonico et al., 2017). Interactions are also known to occur between the disease causing bacteria *Clavibacter* spp., *Pseudomonas* spp. and *Agrobacterium* spp., and species of the nematode genera *Meloidogyne*, *Pratylenchus*, *Anguina* and *Ditylenchus* (Dash et al., 2017; Lamovsek et al., 2017). A well-known example of nematode-bacteria interaction is that of *Meloidogyne* spp. and *Ralstonia solanacearum* causing bacterial wilt of many crops including tomato (Bridge and Williams, 2001). Particularly *Meloidogyne incognita* (Kofoid and White) Chitwood, *M. javanica* (Treub) Chitwood, and *M. hapla* Chitwood, are the most widely distributed nematode pathogens of tomato (Jones et al., 1991).

Thus, according to Leontopoulos et al., (2015) Greek farmers are seeking for alternative crops such as energy crops in order to increase their income despite the development of resistant varieties (Stevens and Rick, 1986).

Control of plant parasitic nematodes

The term 'control' strictly refers to specific acts designed to reduce the numbers of pest or disease organisms and keep the disease level below the economic threshold of damage (Hooper and Evans, 1993). This term comes in contrast with that of the farmers, who refer to control as meaning the complete elimination of pest or disease on their farms.

When a crop is cultivated on a large scale conditions will favour the multiplication of pests and as a result the decrease of the productivity of the crop. These processes result in the establishment of an unstable equilibrium, which is called the natural balance. Hence the need for crop protection. Nowadays, several methods of effectively controlling nematodes are available (Agrios, 1988; Yawson et al., 2017).

Heald, (1987) divides them into the two broad categories of chemical and non-chemical, with a number of subdivisions within each. The alternatives for control are perhaps best considered as chemical control, use of resistant cultivars, cultural practices, physical methods and biological control (Hooper and Evans, 1993).

Biological control

Biological control *sensu stricto* refers to the use of one living organism to control another, the latter being a pest (Kerry and Hominick, 2001). Micro-organisms that can grow in the rhizosphere are ideal for use as biocontrol agents, since the rhizosphere provides the front-line defence for roots against attack by pathogens (Weller, 1988). Cobb, in 1920, seems to be the first to consider using parasites and predators of nematodes as biological control agents although his results were not so encouraging. Oorganic substances such as phenazines (Kavitha et al., 2005) and plant exudates are used to control plant parasitic nematodes and soil borne fungi (Gravanis et al., 2011; Leontopoulos et al., 2016; Skenderidis et al., 2017). Nowadays, fungi, bacteria, viruses, nematodes, insects, mites and miscellaneous invertebrates can act as biological agents for plant parasitic nematodes. However, biological control of soil-borne pathogens by introducing micro-organisms has been studied for over 85 years (Baker, 1987; Leontopoulos et al., 2004; Gravanis et al., 2011; Leontopoulos et al., 2011; 2015; 2016; Hu et al., 2017; Nile et al., 2017) and it has not yet been considered as commercially feasible (Weller, 1988) with a very few exceptions in which successful formulation of *Trichoderma* spp. used as biological control agents against soil borne disease. Also a formulation of the quite promising bacterium *Pasteuria penetrans* has been produced and it has been used to control plant parasitic nematodes in Japan. The most studied endoparasites of plant parasitic nematodes are *Drechmeria coniospora*, *Nematoctonus leiosporus* and *Verticillium balanoides*. They tend to be obligate parasites because of their small sized

spores, which have insufficient reserves to establish mycelium in soil (Stirling, 1991) and cannot so far be cultured on laboratory media (Kerry and Hominick, 2001).

Among fungi that are significant pathogens of root-knot and cyst nematodes, *Paecilomyces lilacinus* and *Pochonia chlamydosporia* are the most important and can be parasites of nematode eggs (Rodriguez-Kabana and Morgan-Jones, 1988). Another two well-studied nematode destroying fungi are *Phytophthora* and *Pythium* species (Li et al., 2005). The mode of parasitism of *Phytophthora palmivora* and *Pythium aphanidermatum* was found to be the same as that of *P. monospermum*. *P. monospermum* and it does parasitize apparently viable nematode eggs by unspecialised hyphae. The infected eggs are eventually consumed and destroyed (Tzean and Estey, 1981). However, the use of the fungi as biological agents has various limitations such their non-specific nature in predation, their slow growth and their requirement for high amounts of, and sometimes highly specific, nutrients. This can be a drawback to their success as candidates for commercial production (Jatala, 1986).

The second group of plant parasitic nematodes, are the bacteria. Despite the fact that they are present in most soils in prodigious numbers, there have been remarkably few attempts to investigate the relationships between them and plant parasitic nematodes (Sayre and Starr, 1988; Abd-Elgawad, 2015; Aballay et al., 2017; Lamovsek et al., 2017). Although a wide range of bacteria may be antagonistic to nematodes, only one genus (*Pasteuria*) contains species, which are obligate mycelial and endospore forming parasites that actually proliferate in the nematode (Kerry and Hominick, 2001). There are three species, *P. penetrans* on *Meloidogyne* spp., *P. thornei* on *Pratylenchus* spp., and *P. nishizawae* on cyst nematodes have been distinguished in this genus (Chen et al., 1996; 2000). However, Stirling (1991) considers the obligate nature of its parasitism may limit the biological control potential of *P. penetrans*.

So far, attempts to culture *Pasteuria in vitro* have failed and this prevents it from being used commercially (Tzortzakakis and Gowen, 1994; Tzortzakakis et al., 1997). Apart from *P. penetrans* which is the most researched and the most promising biological agent (Vagelas et al., 2007; 2011a; 2011b; 2012a; 2012b; Kamran et al., 2014; Kokalis-Burelle, 2015; Abd-Elgawad and Vagelas, 2015; Timper et al., 2016; Thakur et al., 2016), there are some other bacteria and rickettsia-like organisms (RLO) that have been observed in some plant parasitic nematodes.

Another potential bacterium for use in nematode control is *Pseudomonas oryzihabitans*. Currently, *Pseudomonas* spp. are receiving much attention as biocontrol agents (Samaliev et al., 2000; Leontopoulos et al., 2003; Vagelas et al., 2007; Leontopoulos et al., 2011; Dyson et al., 2015) inhibited the potato late blight disease caused by the fungus *Phytophthora infestans* (Thomson, 1999). It has also protected cucumber plants against bacterial wilt caused by the bacterium *Erwinia tracheiphila* (Luz, 2000) and being antagonistic to *Fusarium oxysporum* f.sp. *lycopersici*, it has suppressed the incidence of wilt caused by this fungus in tomato plants (Vagelas et al., 2000). However, more research needs to be done in the use of *P. oryzihabitans* as a biological control agent. *P. oryzihabitans* is a widely distributed bacterium having been isolated in the UK, USA, Germany Malaysia, Thailand, Japan and Switzerland. (Holmes et al., 1987). The natural habitat of *P. oryzihabitans* is thought to be water, soil or other damp environments (Gomez et al., 1986). Moreover, it has been found that it can remain viable in water at room temperature for several months (Elawad, 1998). On the basis of their biochemical characteristics, *Pseudomonas* spp. were initially classified as *Chromobacterium typhiflavum* by Pickett and Pedersen before being assigned to CDC (Centers for Disease Control, Georgia, USA) group Ve-1 and Ve-2 by Tatum et al., (1974). However, because they share features with *Pseudomonas*, *Xanthomonas*, and *Erwinia* spp., their taxonomic position remained uncertain (Freney et al., 1988).

Although the role of nematodes in vector-

ing plant viruses was established many years ago, the existence of viruses that cause disease in plant parasitic nematodes has not yet been conclusively demonstrated (Stirling, 1991). The major problem using viruses involved in sampling and examining large numbers of individuals from soil and roots. Also another problem is that the nematode's cuticle is likely to provide an effective barrier to the entry of virus particles (Hess and Poinar, 1988).

Finally, another group, which can act as a biological agent against plant parasitic nematodes, are nematodes themselves. Predatory nematodes are found in four main taxonomic groups. Each group has quite different feeding mechanisms and food preferences (Stirling, 1991; Abd-Elgawad, 2016).

Although the prolonged effects in the use of micro-organisms as biological agents, biological control techniques are very slow to develop and probably they are going to be an option giving poor results compared with chemical treatment. The control is never absolute, as some pest population must be present to support the biological agent population.

Nematodes and the role of root exudates

Nematodes have been described as being widely distributed organisms which attack a numerous of plants (Sasser and Freckman, 1987). To locate these food sources they are equipped with sensory organs which are localised mainly in their anterior (amphids, papillae) or in their posterior regions (phasmids).

Although, the stimuli may originate from plant roots, physical stimuli such temperature, chemical stimuli may also originate from other live organisms in the rhizosphere (Cohn and Spiegel, 1991).

However, the most important stimuli for plant parasitic nematodes are the plant root and its exudates, to which the nematode responds by a process known as chemotaxis (Prot, 1980; Baiocchi et al., 2017). Root exudates usually originate from the breakdown of sloughed root cap cells or others leak from points where soil microbial organisms try to penetrate it and enter into plant (Stirling, 1991).

Most of these substances secreted by roots, contain sugars and aminoacids and when present in sufficient quantities, can overcome fungistasis or cause stimulation of hatching nematodes by stimulating egg hatch (Bruehl, 1987; Griffin and Elgin, 1977; Perry, 1997).

However, it is well known that J₂ of root-knot nematodes are attracted to the roots by the root exudates and the newly formed epidermis, which is thin and is penetrated quite easily.

According to their diffusion rates, root exudates may be divided into three categories. In the first one, volatile or gaseous compounds such as carbon dioxide, ethylene etc. are responsible for nematode stimulation. Among those compounds carbon dioxide is the most important since it is detectable even 1 m away from a single long root and 2 m from a plant root mass (Dusenbery, 1987). In the second category, soluble and highly diffusable compounds were recorded as attractants to different nematode species. Finally, non-diffusable materials may cause attraction or repulsion to nematodes.

Bacterial chemotaxis and the role of root exudates

Flagellated bacterial cells occurring in a chemically uniform environment typically adopt a randomized movement due to their flagella. In that chemical environment the presence and the concentration of those chemical contents may play a critical role in movement of the cells overall and that will be towards the higher concentration of nutrients. Attractants and repellents affect special protein sensors located in the cell envelope that cause anticlockwise (less tumbling) or clockwise (more tumbling) flagellar rotation. This attraction or repellent bacterial movement to an enriched environment of nutrients or away from harmful substances is called chemotaxis (Singleton, 1991).

Therefore, bacterial chemotaxis is important because this may contribute to the ability of that organism used as a biological agent to colonize and adapt the root system effectively. Moreover, it may be especially important when

the biological agent (e.g. bacteria) is added to soil, and thus initially not in contact with the plant. One of the major constraints in the development of an effective biological agent is the poor colonisation of the rhizosphere by the introduced organism (Deacon, 1997; Walker et al., 2002; Baker, 1987). For that matter, the usage of pseudomonads as effective biocontrol agents may result in part because of their ability to colonise the rhizosphere and produce substances which are toxic and inhibit other potential rhizosphere colonists including root pathogens (Weller, 1985; Vagelas, 2002).

Sher et al., (1985) demonstrated chemotaxis of fluorescent pseudomonads to soybean exudates in water saturated soil, while Weller (1988) concluded, that chemotaxis toward seed or root exudates may contribute to the ability of bacteria to colonise roots.

Studies done by Scher et al., (1985) show the ability of *P. putida* RW1 to move 1 cm toward a soybean seed in 12 h. Likewise, *Azospirillum lipoferum*, *Pseudomonas fluorescens* and *Azospirillum brasilense* showed evidence of chemotaxis to wheat root exudates moving less when wheat roots were absent (Heinrich and Hess, 1985; Basham, 1986).

The endmost purpose of a biological agent such as the bacterium *P. oryzihabitans* should not only be the ability to affect and successfully suppress a plant parasite be it either a fungus or a nematode, but it should also provide good root colonization and stability to its sites of colonization. For these reasons a proper bacterial root colonizer is a bacterium that when introduced to a system of a natural soil becomes distributed along the root, multiplies and survives in the presence of competition by the indigenous rhizosphere microflora for several weeks. The ability of a bacterial strain to colonize, or establish a large population in the rhizosphere is a critical factor determining its importance as a root associate.

According to Howie et al., (1987) the process of colonization in all biocontrol systems, occurs in two phases. In phase I, the bacteria becomes attached to the root system by their exudates or by other stimuli and are then trans-

ported on the elongating root tip. In phase II the bacteria will spread locally and antagonize the indigenous rhizosphere microflora and survive.

However, root tips do not always become colonized. Generally losses of introduced bacteria by the root tip may occur from physical removal due to processes such as absorption to the soil particles, the displacement of the tip or due to competition from indigenous bacteria as result of bacterial inability to multiply rapidly enough and extend rapidly through the soil (Bahme and Schroth, 1987; Baker, 1987).

It is crucial if we are ambitious, to develop an effective microbial biological agent to understand how an externally introduced microorganism acts in a system and how abiotic factors such as physical factors or the indigenous microflora are likely to influence the introduced organism.

Aims and objectives of this study

The aim of this study was the determination of chemotactic movement of *P. oryzihabitans* and *M. javanica* toward to a higher concentration of favorable chemicals secreted by tomato roots (root exudates) and away from an unfavorable source.

II. MATERIAL AND METHODS

The bacterium *Pseudomonas oryzihabitans* was isolated from the entomopathogenic nematode *Steinernema abbasi* and cultures of the bacterium were incubated in an incubator (LMS) adjusted at $28 \pm 2^\circ\text{C}$. *Steinernema abbasi* isolates were taken from soil samples from fields of alfalfa in Oman (stored at the University of Reading cryogenic storage sample bank) using the larvae of *Galleria mellonella*.

The root-knot nematode *Meloidogyne javanica* originated from greenhouse soil cultivated previously with tomato plants in Larissa's region was used in these studies. The variety of tomato c.v. 'Majeo S1' was used in all the experimental work and to multiply the population of the nematode *M. javanica*. The experiments were replicated 3 times.

Mass production and extraction of *M. javanica*

A very reliable tomato variety (Majeo S1), which produces heavy crops of medium, sized tomatoes indoors or out was used. The nematode population was received as egg masses attached in the tomato root system. The tomato plants were used for the multiplication of the initial population for all further experiments. The plants were grown in 10 x 10 x 12cm pots filled with a mixture of high peat Potgrad P, suitable for propagation of horticultural seedling obtained from Company Klassman-Dolmann GmbH Germany as imported in Greek market from Agrochoum SA. Tomato roots infested with root-knot nematode *Meloidogyne javanica* were taken from the pots and gently washed free of soil.

The clean roots were placed in a jar with 1% sodium hypochlorite (NaOCl) and shaken for 4-5 minutes (Southey, 1986). To separate the organic debris from the eggs, the bleach suspension was poured through a series of sieves. Then the eggs were collected on a 38 μm -pore sieve, washed carefully with tap water in order to get rid of the remaining bleach and then finally poured into a beaker.

The washed egg suspension was poured onto a double tissue paper supported in a dish and then tap water added to the level of the tissue paper. The extraction dish was covered with another inverted dish to prevent water evaporation and kept in an incubator at 28°C for a maximum of 3-4 days until eggs hatched. Hatched J₂s were collected daily and only freshly hatched J₂ were used for the experiments. To determine the number of J₂/ml of water, the number of hatched nematodes were observed with a dissecting microscope at a magnification of 25x. Three samples of the nematode suspension were counted and their means and SDS calculated.

Four samples of the nematode suspension were counted and means calculated, in order to avoid highly significant error. All nematodes were sterilized according to method describing by Sawhney and Webster (1975) and the total number of nematodes applied in each

treatment was $200 \pm 18 J_2$ of *M. javanica* / ml of sterile distilled water (SDW).

Production and incorporation of freshly egg masses of *M. javanica*

Beside J₂ of *M. javanica*, five egg masses in each subplot were used to determine the chemotactic effect to cells of *P. oryzihabitans*. Using forceps, egg masses were hand-picked from a heavily infested root system of a tomato plant and surface sterilized in NaOCl and mixed into the soil to be tested.

Extraction of nematode's eggs

According to method described previously, roots of root-knot nematode infected tomato plant were washed gently to remove any of the remaining soil particles without any possible damage.

The roots were cut in to pieces of 2-3 cm in length and placed in a bottle containing 10% sodium hypochlorite.

After 3-4 minutes of vigorous shaking, sodium hypochlorite dissolves the gelatinous material covering the egg masses, and the eggs were dispersed into the suspension. A 150 μm sieve was used to collect the pieces of root while was placed below a 35 μm sieve which was used to collect the extracted eggs. When the entire quantity of the bottle was emptied, a quick rinse of the roots remaining on the upper sieve was applied with distilled water to remove any eggs from their surface. Afterwards, the eggs trapped on the lowered 35 μm sieve, were washed over the top of the sieve and placed in a clean bottle. To ensure that the final amounts of NaOCl were eliminated, froth created by earlier agitations must have completely disappeared from the surface of the sieve. Also the absence of the smell of chlorine is a good indicator that it has been removed.

Finally, samples of 1 ml of the suspension in the bottle was added in a 2.5 cm diameter Petri dish which was previously grid marked at the bottom to enable counting under a microscope at a x 35 magnification. A volume containing 200 ± 18 eggs were used for soil application in treatments to be examined.

Nematode sterilisation

Streptomycin sulphate (0.1%) was used to sterilise mature egg masses of *M. javanica*. The egg masses were picked off the roots and sterilised for 45 min. (Sawhney and Webster, 1975). Finally all the nematodes were rinsed in sterile distilled water before being used in the experiments.

Bacterial Techniques

In this study the bacterium *P. oryzihabitans* was used as biological agent against root-knot nematodes. An infected larva of *Galleria mellonella* was used to isolate from its oozing haemolymph the bacteria cells onto a Petri dish containing 30% of nutrient agar (NA).

To enable selective isolation of the bacterium from soil, a semi selective medium consisted of a basal medium of Nutrient agar to which antibiotics and a fungicide added was used. The basal medium was autoclaved first at 121 °C for 20 min. and then allowed to cool before adding antibiotics and fungicide in 10 ml of sterile water.

Fungicide and antibiotics were first filter-sterilised before adding. Basal medium in 1L of distilled water contained 37 g of Nutrient agar. Where antibiotics and fungicides applied 50 µm of Ampicillin or Spectinomycin or Benzimidazole was added.

Culture of *S. abbasi*

Instars larvae of *G. mellonella* were used to culture the entomopathogenic nematode *S. abbasi* using the technique described by Elawad (1998). Five to six last instars larvae of *G. mellonella* were placed on the bottom of a Petri dish that had been previously lined with two filter papers. Approximately 400 *S. abbasi*, infective juveniles were applied to the filter paper and surrounded the larvae in a suspension of 1 ml of distilled water. The Petri dish was then sealed with Parafilm and incubated for three days at 28 °C.

It was noticed that the bacterium symbiotically associated with *S. abbasi* turned the cadaver of *G. mellonella* larvae very dark brown

to black within 14 to 18 hours after infection. After that time of infection the dead larvae were transferred from the Petri dish to a modified White trap (White, 1927) which consisted of a 9 cm diameter plastic closed container. Inside the container a small Petri dish was placed upside down and a filter paper was placed on top of the Petri dish. To ensure that the filter paper was touching the bottom of the trap, 10 ml of distilled water were added.

After that the dead insect larvae were washed with distilled water and placed on the top of the filter paper. After 2-3 days stored at 28 °C the infective juveniles (IJs) started emerging and swimming at the bottom of the trap.

The emerged IJs were poured into a 100 ml beaker and left to settle down for about half an hour. Fresh distilled water was added into the beaker after the surplus water was decanted. To prevent contamination of the nematode cultures by fungal or other pathogens 2-3 drops of 0.1% formalin were added into the containers. The harvest was repeated every 2 days until the larval cadavers were depleted of their contents. The cultures were kept at 15 °C and they renewed the latest every six months to avoid loss of the primary stock. Moreover, stock of the bacterium *P. oryzihabitans* was stored at -80 °C in Animal and Microbial Science laboratory (Vagelas et al., 2000).

Isolation of *P. oryzihabitans*

Dead last instars larvae of *G. mellonella* killed by the entomopathogenic nematode *S. abbasi*, were washed in distilled water, surface sterilised in 70% alcohol for 5 min and left to dry in a laminar flow cabinet. Sterilised larvae were opened carefully with a pair of sterile scissors and a needle, and a drop of the haemolymph was poured onto NBTA agar containing 37 g nutrient agar, 25 mg bromothymol blue powder, 4 ml of 1% 2,3,5 triphenyl-tetrazolium chloride, in 1 l of distilled water, (Akhurst, 1983).

The agar plates were incubated in the dark at 28 °C for 24 h and single colonies were selected for sub-culture onto NBTA agar plates.

The process was continued not more that

twice until uniform colonies of the bacteria were obtained. To test the purity of the colonies, bacteria were inoculated into *G. mellonella* larvae.

In all cases larvae were killed (the data are not presented) and the bacterium obtained from the haemolymph was the same as originally inoculated.

Preparation of bacterial suspensions

A pure colony of *P. oryzihabitans* was added in Nutrient broth No2 (NB2) and shaken for 24 h at 28 °C (150 rpm. min⁻¹ in the dark). Then the bacterial suspension was added in 250 ml tubes and was centrifuged at 3100 for 17 min.

After that procedure a bacterial pellet was formed at the bottom of the centrifuge tube. The supernatant solution was drained off until at least 30 ml of this suspension remained in the tube. Then sterile tap water was added to the pellet and mixed thoroughly to form a concentrated suspension of the bacteria cells.

Finally, to determine the required concentrations for the experiment, the concentrated suspension was diluted with sterile tap water and bacterial concentrations were determined by estimating the optical density (OD) of the suspension using a spectrophotometer adjusted to the 600-nm wavelength. The formula used to calculate the bacterial dose concentration for the experiments was $Y = 5237 X - 5609$;

where $X = OD_{600}$ values and

$Y = \text{cells/ml}$,

i.e. $X = OD_{280}$ so $Y = 1.4 \times 10^6 \text{ cells/ml}^{-1}$.

The bacterial concentration used in this study was 106 cells ml⁻¹ and prepared according to methods described before. In each treatment 100 μ l of the tested bacterial suspension was added.

Application of *P. oryzihabitans* to soil and tomato plants

Bacterial suspensions were applied either by making four 4 holes around the stem of the tomato plant to be inoculated and applying the inoculum with a pipette in a depth of 2-3 cm

or through soaking the root system of plants in the inoculum for 3 min. In both application methods care was taken to avoid over watering and flushing the inoculum in the first few days after inoculation.

Preparation of root tip exudates from tomato seedlings

For preparation/collection of root tip exudates and border cells from tomato seedlings the below method as described by Zhao et al., 2000 was used. Tomato seeds were surface sterilized in 95% ethanol for 10 min followed by 10 min in 1% sodium hypochlorite (NaOCl). Afterwards, seeds were rinsed in sterilized distilled water six times followed by immersion for about 2 h to remove any remains of the bleach. At that time of immersion, 1% water agar was prepared and imbibing seeds were transferred to a Petri dish laid with this agar. Each Petri dish contained about 20 tomato seeds to be germinated and was incubated at 24 °C for about 4 days. Before incubation, according to the method by Hawes and Lin (1990) the imbibed seeds were overlaid with a sterilized Whatman paper.

After 4 days, groups of 20 germinating seeds with root tips up to 25 mm long lengths were immersed in 1 ml of SDW for 2 min. Border cells and associated exudates were removed by agitating the water suspension gently using a pipette. Border cells were centrifuged and pelleted at 7000 rpm for 10 min and the supernatant solution used in this experiment is defined as the root tip exudates (Zhao et al., 2000).

However, some chemicals may have been secreted by cells of the root tip and some chemicals from border cells may have diffused into the germination paper or the water agar during the period of germination. Therefore, it is important to collect and process root seedlings as soon as they have germinated.

Soil type, application of root-knot nematodes, *P. oryzihabitans* and root tip exudates

Two different types of soil were used to de-

termine the effects of tomato root exudates on nematodes and *P. oryzihabitans*. A mixture of loam-sandy soil 3:1; v:v (pH 7.2) and pure sandy soil were sieved through a 2 mm mesh and air dried at 105 °C for 24 h. The matric potential was determined to be high (-0.03 MPa) and thus, known amounts of air-dried soil were mixed with the appropriate amount of sterile distilled water (18 g of SDW in 100 g of oven dried soil). Sterilised distilled water and soil placed in sealed plastic bags were massaged gently to mix the contents thoroughly and achieve the required matric potential. Afterwards, a soil with the appropriate amount of water was incorporated in a plastic oblong box

and was separated into three subplots within dish using 20-micron opening mesh screens. Each mesh screen was placed vertically with a 1.5-cm middle section and 2-cm wide sections on each side. The plastic oblong plate was separated into two main plots and each main plot was divided with mesh screens as described above in order to decrease numbers of plates needed for the experiment. Between two sites in each plate, there was an empty gap supported by a plastic piece of unused Petri dish. Nine treatments were used in this study to assess interactions of root-tip exudates, type of soil, *P. oryzihabitans* and root-knot nematodes.

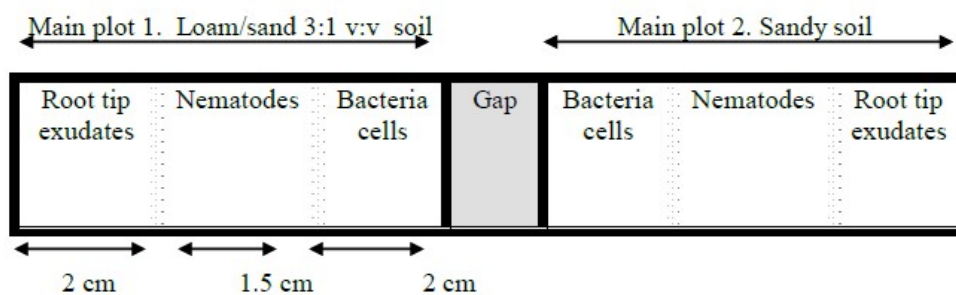
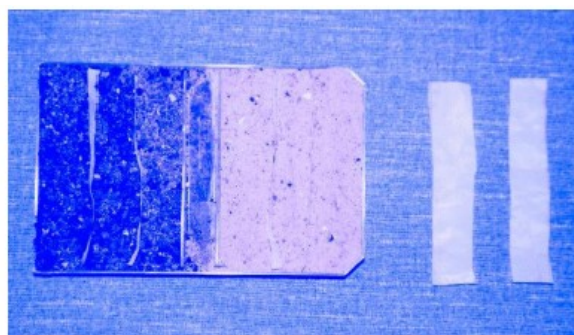


Figure 1. Oblong plastic box (12 x 6 x 1.5cm) used to determine the effects of tomato root exudates on root-knot nematodes and *P. oryzihabitans*. The plate was divided into 2 main plots with 2 different types of soil. Between the 2 main plots was a gap. The main plots were divided into sub plots using a 20-micron opening mesh screens (right of the picture).

The following treatments were applied:
Treatment 1. A 100 µl sample of root tip exudates (20 seedlings) was added to one side of the main plot and an equal volume of *P. oryzihabitans* was added on the other side. A 1 ml sample of 200 ± 18 /ml J₂s was added

in the middle sub-plot. The same amounts of root tip exudates, nematodes and bacteria cells were applied at the other side of plate (main plot 2.) where sandy soil was applied.

Treatment 2. Root tip exudates applied to one side of the main plot and bacteria cells on

the other side. The middle subplot inoculated with root-knot nematodes + 100 μ l of root tip exudates.

Treatment 3. Root tip exudates applied to both sides of the main plot and the middle section inoculated with root-knot nematodes + 100 μ l of bacterial cells.

Treatment 4. Root tip exudates applied to one side of the main plot and on the other side was applied a combination of an equal volume of root tip exudates and bacterial cells. The middle sub plot contained only the juveniles of root-knot nematodes.

Treatment 5. Root-knot nematode J₂ only added to middle sub-plot.

Treatment 6. A 100 μ l sample of root tip exudates was added in the sub-plot at the one side of the main plot and 200 J₂ in the middle one. The other side of the main plot remained untreated.

Treatment 7. 1 ml of 200 \pm 18 nematodes was added in both sides of the main-plot and 100 μ l of bacterial cells in the middle one

Treatment 8. A 100 μ l sample of root tip exudates was added to one side of the main plot and 1 ml sample of 200 \pm 14 /ml J₂s was added in sub-plot on the other side of the main plot. An equal volume to root tip exudates of bacterial cells was added on the middle sub-plot.

Treatment 9. Nematode suspension applied at the centre of the main plot and root tip exudates at both sides in equal volumes.

After 4 days of incubation at 28 °C, soil in each side of the treatments was removed separately and second stage juveniles of *M. javanica* in each subplot was collected into suspension by washing the soil in 50 ml of water three times. The nematode suspension was then passed through a 10-micron opening sieve and residues above the sieve were placed on glass slides. With this method, the number of J₂s could be counted directly in each section with the use of a light microscope and evaluation of possible effects of root tip exudates and bacteria cells on nematode behavior could be determined. The whole test was repeated twice and treatments were replicated ten times which

five were used to inoculate 20 plates of selective media of NA to assess the movement and the behaviour of *P. oryzihabitans* in the soil. Finally, the nematode J₂ treatments were substituted with egg masses or eggs to assess the cause of stimulation for *P. oryzihabitans* beside application of J₂ of *M. javanica*, five egg masses in subplots were applied. Root-knot egg suspension of 200 \pm 14 eggs in of SDW were used. The subplots where the egg masses and eggs of *M. javanica* applied were the same as in application of J₂.

The chemotaxis ratios were calculated based on the relative numbers of J₂s and colony forming units (cfu) of *P. oryzihabitans* in each sub plot of the plate. Thus, a 1:1 ratio represents a neutral response; a +4:1 ratio represents a positive chemotaxis response having four times more J₂ or cfu and finally a negative chemotaxis response when a ratio of -4:1 J₂s or cfu represented at subplots of the plate (Zhao et al., 2000)..

To isolate the bacterium from a soil sample and determine colonization of *P. oryzihabitans* in soil, 1 g of soil was diluted in 9 ml of a washing buffer (0.1 M phosphatase buffer, pH 7.0 supplemented with 0.1% w/v peptone). The suspension was then shaken vigorously for 30 sec and serially diluted twice. Studies by Andreoglou (2001) have shown that an increase in time of shaking did not increase the number of cells collected. Finally 50 μ l of the diluted suspension were streaked with a glass rod onto a semi selective selective medium. The inoculated plates were incubated for 72 h at 28 °C and the number of *P. oryzihabitans* colony forming units (cfu) appeared, were expressed as *P. oryzihabitans* cfu/g soil.

Effect of pre-inoculated soil with *P. oryzihabitans* on the movement and attraction of second stage juveniles of *M. javanica* to newly germinated tomato seedlings

Loam based compost soil was sieved to remove all big soil particles. The sieved soil was mixed thoroughly with sandy soil at v:v 3:1 and sterilised by autoclave. Afterwards, the sterilised soil was placed in a photographic tray, which

had been previously sprayed with alcohol in order to eliminate any possible contamination, by other microorganisms. The mixed soil was inoculated with cells of *P. oryzihabitans* at a concentration of 10^6 cells ml^{-1} and the tray was sealed with aluminium kitchen foil after application. The tray then was placed at room temperature and remained in this environment for about 4 months. After that period of time, 500 ml of 2% NA (3.71g/L of SDW) was autoclaved, allowed to cool and then mixed with 150 g of loam:sand soil (3:1) inoculated previously with bacterial cells of *P. oryzihabitans*. The soil, incorporated into the 2% NA and was shaken using a sterilised magnet in order to mix the two thoroughly before adding to the Petri dishes. As a control treatment, 150 g of soil without bacterium cells was used and mixed with another bottle containing 2% of NA. This untreated soil was first heated-sterilised in a microwave for 5 min before adding into the agar. In each Petri dish, 8 germinated tomato seedlings were placed after the mixture of agar and soil was added. The tomato seedlings were placed on the top of the agar surface. Four tomato seedlings were placed on one side of the Petri

dish and another four on the other side. The distance between them was 5 cm and 1 ml of approximately 130 J_2 of *M. javanica* was added between them (Plate 4.3.1). The tomato seeds used in this study, were previously surface sterilised in 95% ethanol for 10 minutes followed by 10 minutes in 1% sodium hypochlorite and finally they were rinsed in SDW 6 times, followed by immersion for about 2 h in order to remove bleach. Afterwards, the surface sterilised tomato seeds were germinated in 1% water agar (WA) according to the method described by Hawes and Lin (1990). The treatments were replicated 10 times and movement and number of J_2 collecting around the root tip were determined at 2, 12 and 24 h after nematode inoculation. All plates were placed in an incubator at 28 °C for the required period and nematode behaviour (positive or neutral) to the bacterium cells or tomato seedlings were examined. As positive nematode behaviour was defined as the attraction of J_2 to the tomato roots while neutral behaviour, was if the nematodes did not move. The number of nematodes around the root of tomato seedling was counted in each root separately.

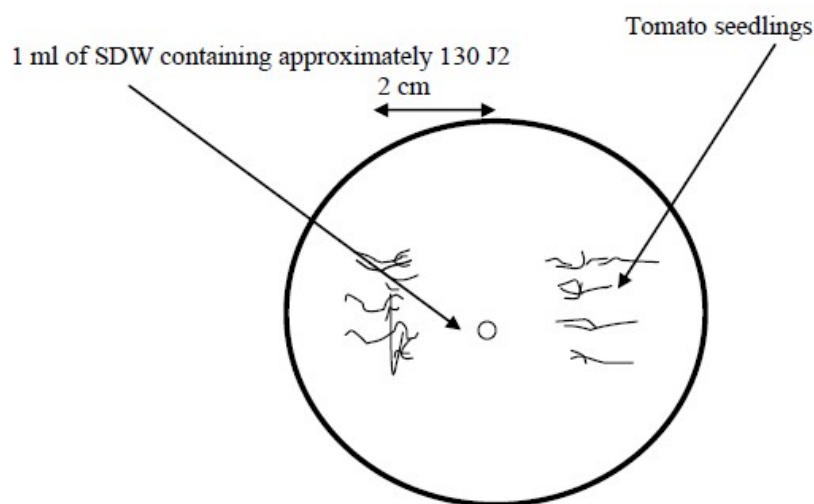


Figure 2. An 8 cm Petri dish filled with 2 % NA mixed with soil which had pre-inoculated with 10^6 cells ml^{-1} of *P. oryzihabitans* for 4 months. In the middle of the Petri dish a drop of SDW containing approximately 130 J_2 of *M. javanica* was applied. The tomato roots were placed about 2 cm from the nematodes.

Statistical analysis

Statistical analysis was performed using the software SPSS and Genstat statistical packages. Significant differences were determined at $P < 0.05$. The graphs were created in Excel using means and standard error of differences assessed from the SPSS. Mean separation was as-

essed when significant differences were found and was made using Tukey's multiple range test expressed the differences with different letters next to the presented values. In some cases the number of observations were $\log_{10}(x)$ transformed before analysis occurs.



Figure 3. Colonies of *Pseudomonas oryzihabitans* after 24 h of incubation on nutrient agar (NA) The colonies are circular, 1 mm in diameter, smooth shiny and vary in their degree of yellow pigmentation (Left column). Colonies of *Pseudomonas oryzihabitans* grown in NBTA agar for 24 h at 28 °C (Right column).



Figure 4. Instars larvae of *Galleria mellonella* inoculated with the entomopathogenic nematode *Steinernema abassi*. Some of the larvae (the middle one) have appeared to change color to dark brown after 14 h of exposition to the nematodes (Left column). Laminar flow cabinet used for all sterilised work (Right column).

III. RESULTS

Chemotactic responses of J₂ of *M. javanica* to tomato root tip exudates and cells of *P. oryzihabitans*

When the root tip exudates were applied as a stimulus in a chemotaxis assay on one side of the main plot and *P. oryzihabitans* applied at the other side in both soil types, loam/sand (3:1; v:v) and sandy soil (block), negative attraction of J₂ to root-tip exudates and bacterial cells was observed on both soil types with a ratio from -2.1 to -24.2 respectively. Near identical responses occurred at the second treatment, when root tip exudates applied at the same subplot with nematodes with a ratio of -30.9 (in loam/sand 3:1 v:v) nematodes repelled from *P. oryzihabitans*.

However, root tip exudates applied on other side of the main plot elicited no response from the nematodes applied in the middle one with a ration of -1.4 ($P < 0.05$). Similar results with lower ratio were observed when nematodes applied at the same subplot with bacteria cells surrounded with root-tip exudates in both soil types. In contrast, root tip exudates had a positive chemotaxis ratio of +2.1 when only root-tip exudates were applied on both sides of the main plot. Neutral nematode chemotaxis was observed when untreated soil was applied around the nematode subplot in both loam/sand 3:1 and sandy soil.. Moreover, no statistical differences were observed between the different types of soil and type of application ($P < 0.05$).

However, positive nematode chemotaxis to root tip exudates was observed while a negative chemotaxis response was detected on the other side where root tip exudates plus *P. oryzihabitans* cells was applied. Similarly, positive nematode chemotaxis was detected to root tip exudates in treatment six while a

neutral response was detected to that of untreated soil. Finally, root tip exudates elicited no response from the nematodes when bacterial cells were applied among them (Figure 5).

Bacterial cells response to root tip exudates and presence of second stage juveniles of *M.javanica*

It is a general observation that cells of *P. oryzihabitans* were found in all treatments, independent of the presence of stimuli such as root-tip exudates or J₂ of *M.javanica* in both soil types used. This observation can be explained as natural movement of bacterial cells due to the existence of flagellum; a natural movement for a few centimetres. In treatments where tomato root tip exudates or untreated soil was applied, the presence of *P. oryzihabitans* was neutral and it could be said that this caused its natural movement through the soil particles in time. Moreover, in treatments 5 and 6 there was no significant difference between soil type or in number of cfu from subplots inoculated to selective media.

Although the number of cfu observed in selective media when nematodes were applied to the bacteria cell subplot was statistically different to those with the initially inoculation point ($P < 0.05$).

Moreover, it could be said that the +1.4 chemotaxis ratio was not significantly different according to Zhao et al. (2000). However, the simultaneous presence of root tip exudates and nematodes caused a colligative stimulation of *P. oryzihabitans* cells to that source of food and the bacterium responses with a positive chemotaxis ratio of +20.1 and +18.1 at mixed loam/sand 3:1 v:v: and sandy soil respectively.

Finally, the occurrence of root tip exudates near nematodes cause positive chemotaxis but not as great as when they were applied at the same inoculation point (Figure 6).

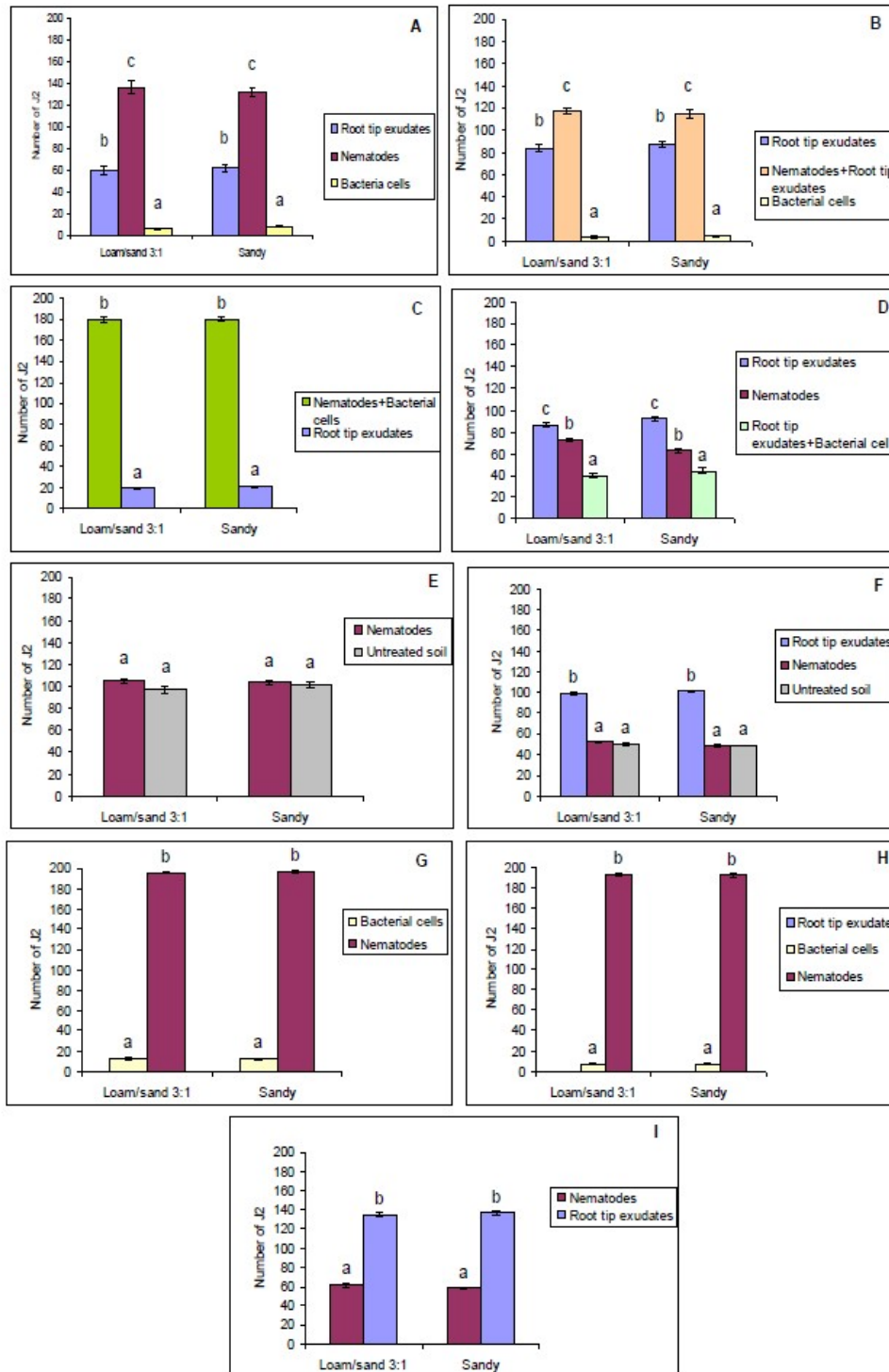


Figure 5. Different chemotactic responses in two soil types of J_2 of *M. javanica* to root tip exudates and cells of *P. oryzae*. A, treatment 1; B, treatment 2; C, treatment 3; D, treatment 4; E, treatment 5; F, treatment 6; G, treatment 7; H, treatment 8; I, treatment 9 as described in materials and methods. Values represent the means and the standard errors of ten replicates for each treatment. Values within each column followed by the same letter do not differ significantly ($P=0.05$) according to Tukey's multiple comparison test.

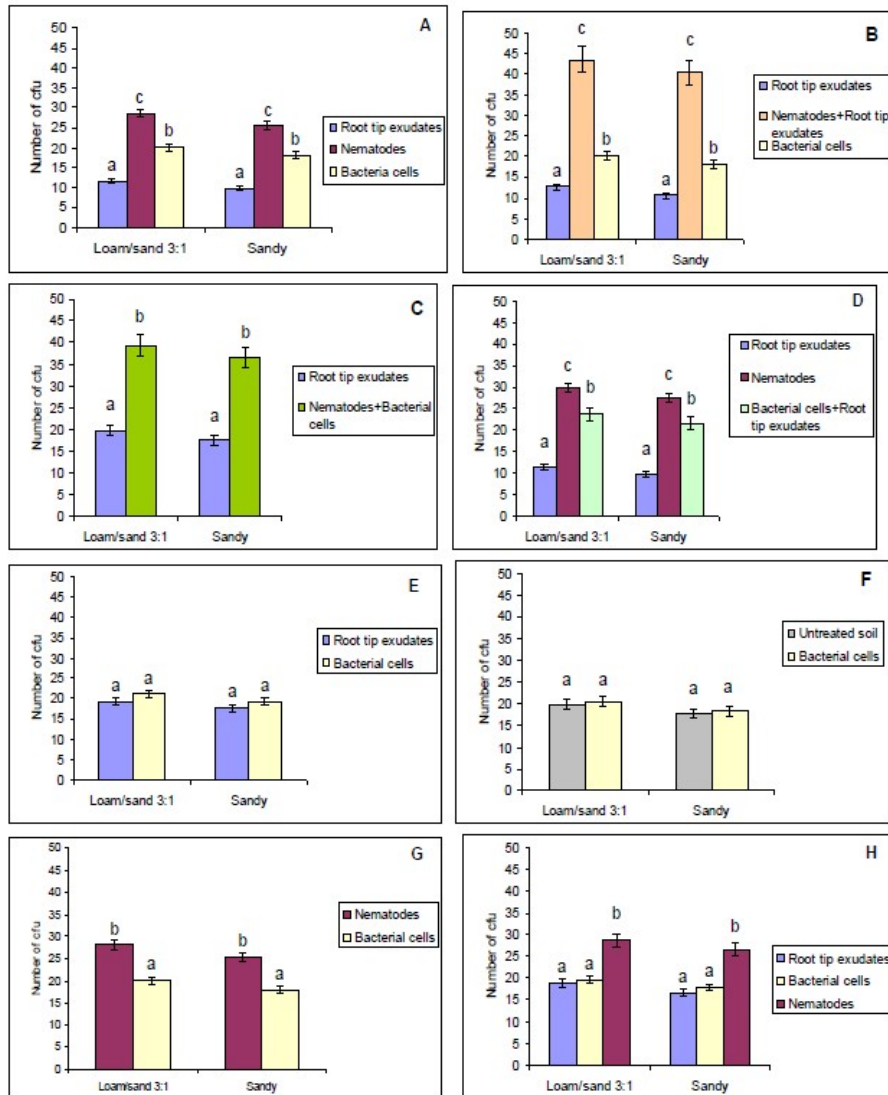


Figure 6. Number of cfu of *P.oryzihabitans* onto NA selective media after 72 h of incubation at 28 °C to assess the response of bacterial cells to root tip exudates and presence of J2 in two different types of soil. **A**, treatment 1; **B**, treatment 2; **C**, treatment 3; **D**, treatment 4; **E**, Root tip exudates at both sides and *P.oryzihabitans* in the middle; **F**, No root tip exudates, nematodes or bacterial cells applied at both sides of section. In the middle section only bacterial cells applied; **G**, treatment 7; **H**, treatment 8; as described in materials and methods. The values represent the means and the standard errors of twenty replicates for each treatment. The values within the column followed by the same letter do not differ significantly ($P=0.05$) according to Tukey's multiple comparison test.

Bacterial cells response to root tip exudates and presence of egg masses of *M. javanica*

Where egg masses were applied in subplots instead of J₂ of *M.javanica*, similar results as the application of J₂ were observed indicating

that there is no difference in different stimuli caused by root-knot nematode. However, in treatment 8 where, root tip exudates applied in one side of the main plot, egg masses of J₂ on the other side and the bacterial suspension in the middle subplot, statistical analysis show

differences in all type of application in sandy soil while in mixed loam/sand 3:1 soil differences were observed only in subplots applied with root tip exudates or inoculated with bac-

terial cells shown no difference among them in mixed soil but they differ form those inoculated with egg masses of *M.javanica* (Figure 7).

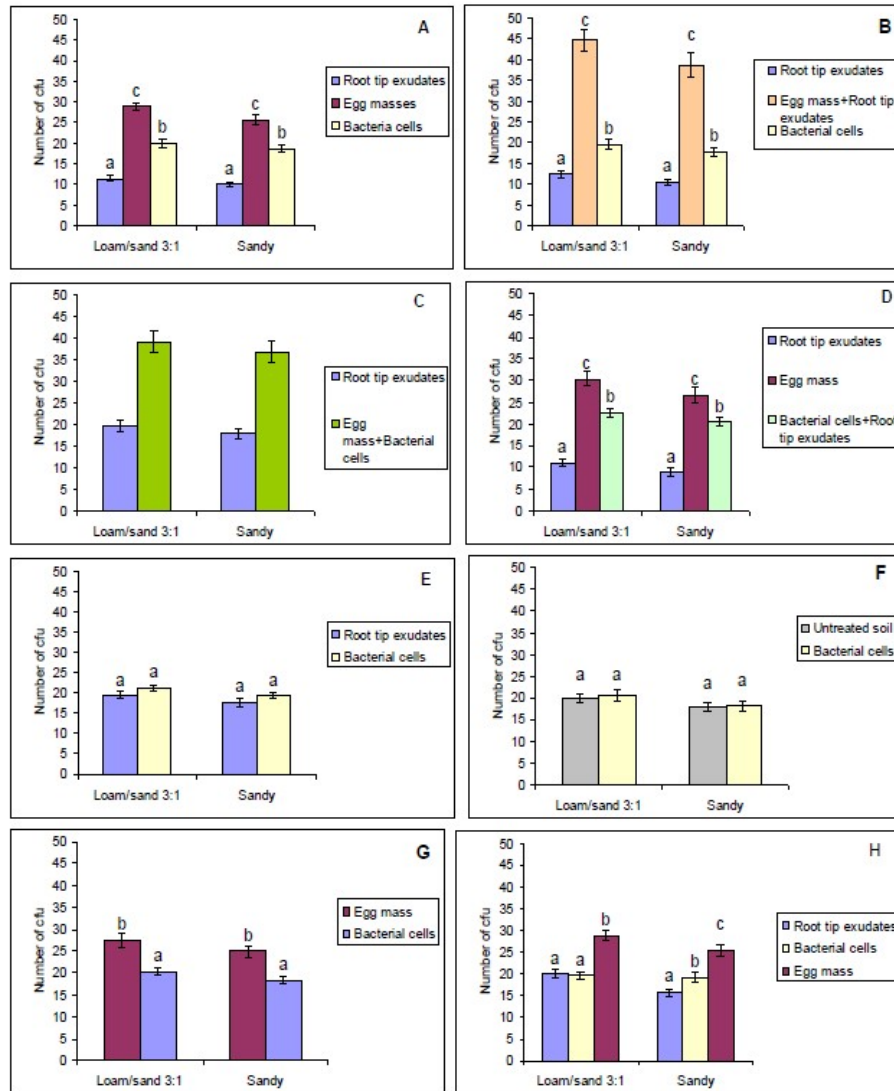


Figure 7. Number of cfu of *P.oryzihabitans* onto NA selective media after 72 h of incubation at 28 °C to assess the response of bacterial cells to root tip exudates and presence of egg masses of *M.javanica* in two different types of soil. A, treatment 1; B, treatment 2; C, treatment 3; D, treatment 4; E, root tip exudates at both sides and *P.oryzihabitans* in the middle; F, no root tip exudates, nematodes or bacterial cells applied at both sides of section. In the middle section only bacterial cells applied; G, treatment 7; H, treatment 8; as described in materials and methods. The values represent the means and the standard errors of twenty replicates for each treatment. Values within column followed by the same letter do not differ significantly ($P=0.05$) according to Tukey's multiple comparison test.

Bacterial cells response to root tip exudates and presence of eggs of *M.javanica*

When eggs of *M.javanica* were applied in subplots instead of J₂ or egg masses, there were slightly different observations in number of cfu counted in semi selective media after 3 days at 28 °C. In treatment 1 (A) and 2 (B) a highly significant difference was observed not only among the different applications in subplots

but among the soil types as well. However, in treatment 4 (D), 7 (G), and 8 (H) there was a statistical difference only between the application types and no difference at all between soil types. Finally, number of cfu counted in selective media did not differ statistically in soil types nor in types of application (Figure 8).

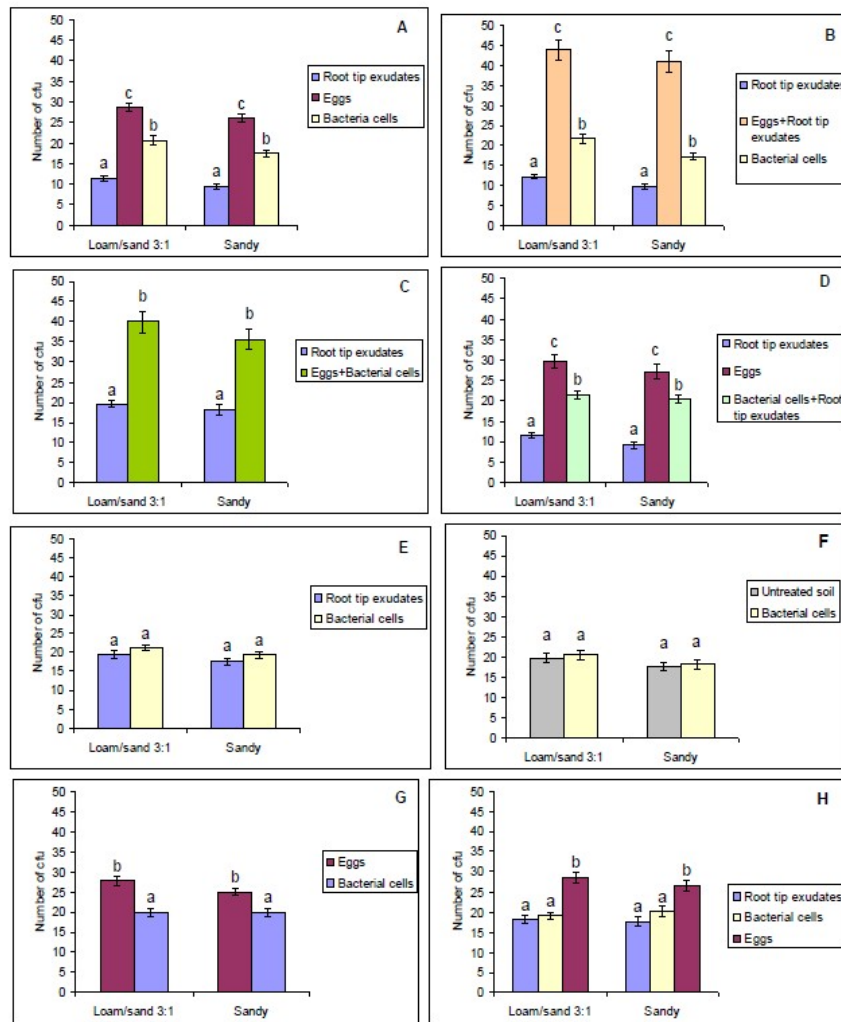


Figure 8. Number of cfu of *P.oryzihabitans* onto NA selective media after 72 h of incubation at 28 °C to assess the response of bacterial cells to root tip exudates and presence of eggs of *M.javanica* in two different types of soil. **A**, treatment 1; **B**, treatment 2; **C**, treatment 3; **D**, treatment 4; **E**, root tip exudates at both sides and *P.oryzihabitans* in the middle; **F**, no root tip exudates, nematodes or bacterial cells applied at both sides of section. In the middle section only bacterial cells applied; **G**, treatment 7; **H**, treatment 8; as described in materials and methods. The values represent the means and the standard errors of twenty replicates for each treatment. The values within the column followed by the same letter do not differ significantly ($P=0.05$) according to Tukey's multiple comparison test.

Effect of pre-inoculated soil with *P. oryzihabitans* on the movement and attraction of second stage juveniles of *M. javanica* to newly germinated tomato seedlings

It is clearly demonstrated from the plates showed below that the tomato seedling placed on the top of the Petri dish which contains 5% NA and loam:sand soil (3:1), previously inoculated with bacteria cells of *P. oryzihabitans* did not attract second stage juveniles of *M. javanica* even after 24 h of exposure. Moreover, in the soil inoculated with bacterium cells, nematode movement was convulsive and in most of the observations nematodes were paralysed after 24 h. However, J₂ were attracted by tomato seedlings in the control treatment where no bacterium cells had been applied in the soil.

The nematode response to the root of tomato seedlings was determined as positive and was observed even from the first observation, which took place 2 h after inoculation in the Petri dish. The J₂ were quite active searching the zone of root elongation and after 24 h many of them tried to penetrate it by repeating jabs of the stylet. Differences in number of J₂ surrounding the roots of tomato seedlings occurred during the time of observations. After 24 h of exposure there were about 12 second stage juveniles of *M. javanica* around roots of tomato seedlings in untreated soil. However, the number of J₂ at the same time of observation was only one, for the roots that have been placed on the top of the agar containing soil pre-inoculated with 10⁶ cells ml⁻¹ of *P. oryzihabitans*.

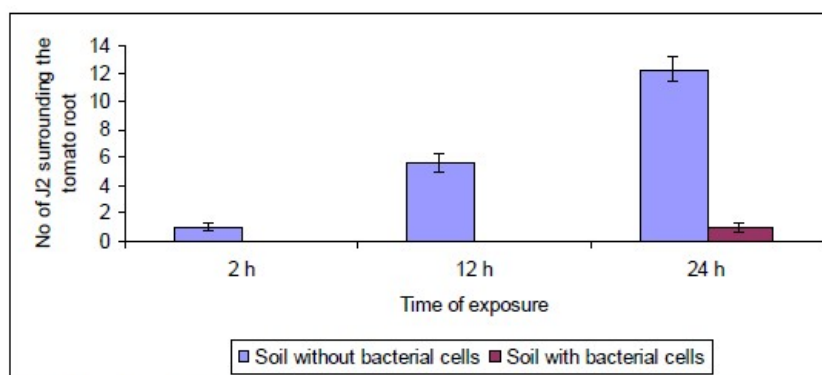


Figure 9. Number of J₂ attracted by root exudates of tomato seedlings in different time of exposure to the soil, pre-inoculated with cells of *P. oryzihabitans*.

Table 1. Levels of movement of second stage juveniles of *M. javanica* exposed at different time to soil pre-inoculated with 10⁶ cells ml⁻¹ of *P. oryzihabitans*.

	Time of exposure (h)		
	2	12	24
Soil pre-treated with 10 ⁶ cells ml ⁻¹ of <i>P. oryzihabitans</i>	+	•	•
Soil without bacterium cells	+++	+++	+++

Levels of movement: +++ High movement, ++ medium movement, + slight movement, • No movement (paralysis).



Figure 10. Attraction of J₂ nematodes of *M. javanica* from the root of tomato seedlings after 2 h of exposure in a clear from the bacterium soil mixture incorporated in 5 % NA (x20).



Figure 11. Attraction of J₂ nematodes of *M. javanica* from the root of tomato seedlings after 24 h of exposure in a clear from the bacterium soil mixture incorporated in 5 % NA (x20).



Figure 12. Attraction of J₂ nematodes of *M. javanica* from the root of tomato seedlings after 24 h of exposure in a pre-inoculated with *P. oryzihabitans* of 10^6 cells ml⁻¹ soil mixture which had been incorporated in a plate with 5 % NA (x20).



Figure 13. Paralysed J₂ of *M. javanica* after 24 of exposure in a soil pre-inoculated with cells of the bacterium *P. oryzihabitans* (x20).

IV. DISCUSSION

Over the last few decades considerable efforts have been undertaken to understand and identify the role of root exudates in nematode behaviour and thereby offer alternative avenues in crop protection. It is generally assumed that soil microorganisms use soluble compounds, which have been released into the rhizosphere by plant roots. Many bacteria such as those of the genus *Pseudomonas* are motile due to the possession of flagella, the importance of which has been studied and debated by many authors (Soby and Bergman, 1983; Weller, 1985). Under examination by light microscopy it was found that *P. oryzihabitans* is also motile by means of a single polar flagellum (Andreoglou et al., 2001; Elawad, 1998; Vagelas et al., 2000).

Components of plant root-exudates are not only complex, serve as a source of nutrients for microbial growth but also contain chemical molecules which attract and promote chemotactic effects to soil microbes to the rhizosphere. As the bacterium *P. oryzihabitans* is a soil microorganism, stimulation of root exudates or other organisms is not uninteresting and the occurrence of these nutrient sources is the basis of rhizosphere colonization. Nutrient sources like root exudates could result in positive, negative or neutral chemotaxis responses to an organism depending on the conditions of the assay (Griffin, 1977; Viglierchio, 1961). Although Zhao et al., (2000) demonstrate that a rapid attraction of J₂ to the root tip periphery occurred only when border cells were present. Observations in this study have shown that there was a positive chemotactic ratio to that points were root tip exudates occurred despite the fact that root tip exudates have usually repellent activity. This could be explained by different sources of root exudates produced by tomato plant which was used in this assay or due to alteration of root exudates by the bacterium *P. oryzihabitans*, making roots less attractive to nematodes (Oostendorp and Sikora, 1990). According to Lugtenberg et al., (1999) the major exudate, sugars, detected in tomato seeds, seedling and/or root exudate were glucose,

fructose, xylose, maltose, sucrose and ribose; sugars commonly found as major exudate components (Vancura and Hanzlicova, 1972). Over and above, chemical responses and production of antibiotics, hormones, siderophores etc., produced by pathogen-antagonistic bacteria may affect pathogen-host interactions.

Moreover, results from this study indicate that cells of *P. oryzihabitans* have a significant repulsive chemotactic effect on J₂ of *M. javanica* in loam/sand 3:1 and sandy soil. This observation may indicate that *P. oryzihabitans* produces toxic metabolites as a result of cellular metabolism, with nematostatic effects against hatched or unhatched J₂ of *M. javanica*. Some of the toxic metabolites produced by symbiotic bacteria from entomopathogenic nematodes, have been characterised (Bowen, et al., 1998) and has shown to have the ability to inhibit egg hatching and immobilise J₂ (Hu et al., 1999). However, hatch inhibition varies among nematode species which indicates that the bacterium might have a bimodal effect on the root-knot nematodes besides killing hatched J₂, it may attract substances produced by root tips or from the nematodes preventing subsequent hatching of root-knot nematodes. According to Andreoglou and Gowen (2000), temperature is a factor which limits this production of possible toxic metabolites as total hatching of nematodes exhibited comparatively slowly at 17°C than 25°C ± 1°C.

When J₂ of *M. javanica* was applied simultaneously at the same inoculation point with root tip exudates, the number of cfu of *P. oryzihabitans* grown in a selective media, was significantly greater than that at the initial inoculation point of the bacterium, showing an additive effect. That ability of *P. oryzihabitans* around root rhizosphere to allow the plant to tolerate to any subsequent invasion. Similar results were found when eggs or egg masses of *M. javanica* were applied instead of hatched J₂, indicating that the difference in source of nutrients such as eggs, egg masses or hatched J₂ did not affect bacterial chemotaxis. However, exudates from second stage juveniles, eggs or

egg masses may serve as energy sources for soil bacteria while exudates from fungal propagules have already been shown to affect bacterial movement (Dickinson and Coley Smith, 1970).

It is believed that *P. oryzihabitans* is able to attach to and colonise the root system due to its natural movement or stimulated by substances produced either by roots, like root tip exudates or by other soil microorganisms secretion. The production of these metabolites from the bacterium affect normal movement of nematodes and perhaps interfere with their orientation to host roots. Studies done by Andreoglou and Gowen (2000) have shown that the nematostatic/nematicidal effect appeared very soon after the plants were exposed to the nematodes and were longer than 24 days. This reaction is crucial, since root-knot nematodes are able to find a host and penetrate its roots within the first 1-2 days after invasion. Thereby to this effect, the presence and the good attractability of bacteria to the root system in an early stage could protect the plant from invasion. However, repulsion from root cells or bacteria in one region and attraction to another, could contribute to localised infection patterns. Studies of nematode behaviour that have been conducted during the last several decades have discovered many kinds of responses by highly diverse species to a wide range of environmental stimuli.

When soil was treated with bacterium cells for 4 months, studies in nematode behaviour show that the J₂ of *M. javanica* were not attracted by the tomato roots, possibly due to the high levels of bacterium cells that built up in the soil throughout this period. The results from incorporation of cells into the soil for 4 months suggest that the bacterium can remain for long periods even with the absence of possible source of nutrients provided by plants or other microorganisms and so be capable of affecting movement and behaviour of J₂ in the rhizosphere. This could be partially explained by studies made by Molina et al. (2000) in which that the metabolic versatility of pseudomonads species, was demonstrated through the use of organic compounds such as C-, N-,

P- and S- sourced.

Overall, the results indicate that *P. oryzihabitans* can have a nematicidal action *in vitro* and is effective in soil as well. The combination of bacterial cells with root tip exudates could give promising results to suppress nematode populations and increase the ability of *P. oryzihabitans* to colonize better the plant rhizosphere. However, longer times of exposure of nematodes in bacterium should be tested to reinforce these conclusions. Through its prolonged effect the bacterium could protect the plants from the invading juveniles when is applied near to rhizosphere and it also might provide protection against the nematode's second generation, thereby contributing to an even smaller overall infection of the plant. However, absolute control of the nematode is

very difficult since a small nematode infection could result in yield loss. Even a very small inoculum of around 200 J₂ may affect plant growth since a female can produce up to 2000 eggs (Tzortzakakis and Trudgill, 1996).

V. CONCLUSIONS

The pre-inoculated soil with cells of *P. oryzihabitans* affects movement and behaviour of J₂ even after 4 months from the initial bacterial inoculation into the soil. Tomato seedlings affected nematode behaviour possibly by secretion of root exudates where bacterium cells were not applied. Nematode chemotactic effects to the tomato root are limited by the presence of bacterium cells.

REFERENCES

- [1] Aballay, E., Prodan, S., Zamorano, A., Castaneda-Alvarez, C., 2017. Nematicidal effect of rhizobacteria on plant-parasitic nematodes associated with vineyards. *World Journal of Microbiology and Biotechnology*, 33: 131.
- [2] Abd-Elgawad, M.M.M., Vagelas, I.K., 2015. Nematophagous Bacteria: Field Application and Commercialization. CAB International. Biocontrol Agents of Phytonematodes.
- [3] Abd-Elgawad, M.M.M., 2015. Biological control agents of plant-parasitic nematodes. *Egyptian Journal of Biological Pest Control*, 26(2): 423-429.
- [4] Agrios, G.N., 1988. In: *Plant Pathology*. G.N. Agrios (ed) Third edition, pp. 713-746. Academic Press, London.
- [5] Akhurst, R.J. (1983). Neoaplectana species: Specificity of association with bacteria of the genus *Xenorhabdus*. *Experimental Parasitology*, 55: 258-263.
- [6] Andreoglou, F., Gowen, S.R., 2000. Temperature response of the bacterium *Pseudomonas oryzihabitans* from the entomopathogenic nematode *Steinernema abbasi*, on the potato cyst nematode *Globodera rostochiensis*. *Aspects of Applied Biology*, 59: 67-73.
- [7] Andreoglou, F., Samaliev, H., Elawad, S., Haque, N., Gowen, S.R., 2001. The susceptibility of the root-knot nematode *Meloidogyne javanica* to the bacterium *Pseudomonas oryzihabitans* isolated from the entomopathogenic nematode *Steinernema abbasi* (Steinernematidae: Nematoda). *Tritrophic interactions in the rhizosphere*, IOBC /wprs Bulletin 24: 5-8.
- [8] Baker, K.F., 1987. Evolving concepts of biological control of plant pathogens. *Annual Review of Phytopathology*, 25: 67-85.
- [9] Baiocchi, T., Lee, G., Choe, D.H., Dillman, A.R., 2017. Host seeking parasitic nematodes use specific odors to assess host resources. *Scientific reports*, (7): 1-13.

- [10] Bowen, D., Rocheleau, T.A., Blackburn, M., Andreev, O., Golubeva, E., Bhartia, R, French-Constant, R.H., 1998. Insecticidal toxins from the bacterium *Photorhabdus luminescens*. *Science*, 280: 2129-2132.
- [11] Bridge, J., Williams, J.D., 2001. Plant parasitic nematodes. In: *Plant Pathologist's pocketbook* 3rd edition. pp. 140-162. Waller, J.M., Lenne, J.M., and Waller S.J. (Eds). CABI Publishing, Wallingford, UK.
- [12] Chen, Z.X., Charnecki, J., Preston, J.F. and Dickson, D.W. (2000). Extraction and purification of *Pasteuria* spp. endospores. *Journal of Nematology*, 32: 78-84.
- [13] Chen, Z.X., Dickson, D.W., Freitas, L.G., Preston, J.F., 1996. Ultrastructure, morphology and sporogenesis of *Pasteuria penetrans*. *Phytopathology*, 87: 273-283.
- [14] Dash, M., Dutta, T.K., Phani, V., Papolu, P.K., Shivakumara, T.N., Rao, U., 2017. RNAi-mediated disruption of neuropeptide genes, nlp-3 and nlp-12, cause multiple behavioral defects in *Meloidogyne incognita*. *Biochemical and Biophysical Research Communications*, 490(3): 933-940.
- [15] Dickinson, D.J., Coley-Smith, J.R., 1970. Stimulation of soil bacteria by sclerotia of *Sclerotium cepivorum* Berk in relation to fungistasis. *Soil Biology and Biochemistry*, 2: 157-162.
- [16] Dyson, Z.A., Seviour, R.J., Tucci, J., Petrovski, S., 2016. Genome Sequences of *Pseudomonas oryzihabitans* Phage POR1 and *Pseudomonas aeruginosa* Phage PAE1. *Genome Announcements*, 4(3): 1515-15.
- [17] Elawad, S.A., 1998. Studies on the taxonomy and the biology of a newly isolated species of *Steinernema* (Steinernematidae:Nematoda) from the tropics and associated bacteria. PhD Thesis. The University of Reading, Reading, UK.
- [18] Elawad, S.A., Robson, R., Hague, N.G.M., 1999. Observations on the bacterial symbiont associate with the nematode *Steinernema abbasi* (Steinernematidae: Nematoda). In: COST 819 Entomopathogenic Nematodes-Taxonomy, Phylogeny and Gnotobiological Studies of Entomopathogenic Nematode Bacterium Complexes. pp. 105-111. Boemare, N.E., Richardson, P. and Coudert, F. (Eds). Office for official publications of the European communities, Luxembourg.
- [19] Freney, J., Hansen, W., Etienne, J., Vandenesch, F., Fleurette, J., 1988. Prospective infant septicemia caused by *Pseudomonas luteola* (CDC Group Ve-1) and *Pseudomonas oryzihabitans* (CDC Group Ve-2). *Journal of Clinical Microbiology*, 26: 1241-1243.
- [20] Gomez, G., Aguado, J.M., Fernandez-Clua, M.A., Soriano, F., 1986. *Pseudomonas* species Ve-2 septicaemia. *European Journal of Clinical Microbiology*, 5: 168-169.
- [21] Gravanis, F.T., Vagelas, I.K., Leontopoulos, S.V., Natsiopoulos, D., 2011. Nematicidal effects of *Azadirachta indica* seed extract on *Meloidogyne* spp. *Journal of Agricultural Science and Technology USA*, 1(1): 136-141.
- [22] Griffin, G.D., Elgin, J.H.J.R., 1977. Penetration and development of *Meloidogyne hapla* in resistant and susceptible alfalfa under different temperatures. *Journal of Nematology*, 9: 51-56.
- [23] Hamblin, A.P., 1981. Filter paper method for routine measurement of field water potential. *Journal of Hydrology*, 53: 355-360.

- [24] Hawes, M.C., Lin, H.J., 1990. Correlation of pectolytic enzyme activity with the programmed release of cells from root caps of pea (*Pisum sativum*). *Plant Physiology*, 95: 1855-1859.
- [25] Heald, C.M., 1987. Classical nematode management practices. In: *Vistas on Nematology*. Veech, J.A. and Dickson, D.W. (Eds). Society of Nematologists, Hayttsville.
- [26] Holmes, B., Steigerwelt, A.G., Weaver, R.E., Brenner, D.T., 1987. *Chryseomonas luteola* comb. Nov. and *Flavimonas oryzihabitans* gen. Nov., comb. Nov., Pseudomonas-like species from human clinical specimens and formerly know, respectively, as Groups Ve-1 and Ve-2. *International Journal of Systematic Bacteriology*, 37: 245-250.
- [27] Hooper, D.J., Evans, K., 1993. Extraction, identification and control of plant parasitic nematode. In: *Plant Parasitic Nematodes in Temperate Agriculture*. Evans, K., Trudgill, D.L. and Webster, J.M. (Eds). Wallingford: CABI, UK.
- [28] Howie, W.J., Cook, R.J., Weller, D.M., 1987. Effects of soil matric potential and cell motility on wheat root colonization by Fluorescent Pseudomonads suppressive to take-all. *Phytopathology*, 77: 286-292.
- [29] Hu, K., Li, J., Webster, J.M., 1999. Nematicidal metabolites produced by *Photorhabdus luminescens* (Enterobacteriaceae), bacterial symbiont of entomopathogenic nematodes. *Nematology*, 1: 457-469.
- [30] Hu, W., Samac, D.A., Liu, X., Chen, S., 2017. Microbial communities in the cysts of soybean cyst nematode affected by tillage and biocide in a suppressive soil. *Applied Soil Ecology*, 19: 396-406.
- [31] Jatala, P., 1986. Biological control of plant parasitic nematodes. *Annual Review of Phytopathology*, 24: 453-489.
- [32] Jones, J.B., 1999. In: *Tomato Plant Culture. In the field, greenhouse, and home garden*. CRC Press.
- [33] Jones, J.B., Stall, R.E., Zitter, T.A., 1991. In: *Compendium sp. of tomato diseases*. APS press.
- [34] Kamran, M., Javed, N., Khan, S.A., Jaskani, M.J., Ullah, I., 2014. Efficacy of *Pasteuria penetrans* on *Meloidogyne incognita* reproduction and growth of tomato. *Pakistan Journal of Zoology*, 46(6): 1651-1655.
- [35] Kavitha, K., Mathiyazhagan, S., Sendhilvel, V., Nakkeeran, S., Chandrasekar, G., Fernando, W.G.D., 2005. Broad spectrum action of phenazine against active and dormant structures of fungal pathogens and root knot nematode. *Archives of Phytopathology and Plant Protection*, 38(1): 69-76.
- [36] Kerry, B.R., Hominick, W.M., 2001. Biological control. In: *The Biology of Nematodes*. pp. 483-509. Lee, D.L. (ed). Taylor and Francis, London and New York.
- [37] Kokalis-Burelle, N., 2015. *Pasteuria penetrans* for control of *Meloidogyne incognita* on tomato and cucumber, and *M. arenaria* on snapdragon. *Journal of Nematology*, 47(3): 207-213.
- [38] Lamovsek, J., Geric Stare, B., Mavric Plesko, I., Sirca, S., Urek, G., 2017. Agrobacteria enhance plant defense against root-knot nematodes on tomato. *Phytopathology*, 107(6): 681-691.

- [39] Leontopoulos, S.V., Gowen, S.R., Vagelas, I.K., Gravanis, F.T., 2003. Influence of *Pseudomonas oryzihabitans* on growth of tomato plants and development of root-knot nematode *Meloidogyne javanica*. The BCPC International Congress-Crop Science and Technology 1: 635-638.
- [40] Leontopoulos, S.V., Vagelas, I.K., Gravanis, F.T., Gowen, S.R., 2004. The effect of certain bacteria and fungi on the biology of the root-knot nematode *Meloidogyne* sp. Mutitrophic Interactions in Soil and Integrated Control IOBC wprs Bulletin, 27(1): 165-169.
- [41] Leontopoulos, S.V., Gowen, S.R., Topalidou, E., Vagelas, I.K., Gravanis, F.T., 2011. *Pseudomonas oryzihabitans* suppresses damage caused by root-knot nematode *Meloidogyne javanica* on tomato. Journal of Agricultural Science and Technology USA, 5(4): 502-507.
- [42] Leontopoulos, S.V., Giavasis, I., Petrotos, K., Kokkora M., Makridis, Ch., 2015. Effect of Different Formulations of Polyphenolic Compounds Obtained from OMWW on the Growth of Several Fungal Plant and Food Borne Pathogens. Studies in vitro and in vivo. Agriculture and Agricultural Science Procedia, 4:327-337.
- [43] Leontopoulos S., Arabatzis G., Ntanos S., and Tsiantikoudis Ch., 2015. Acceptance of energy crops by farmers in Larissa's regional unit. A first approach. 7th International Conference on Information and Communication Technologies in Agriculture, Food and Environment (HAICTA), Kavala, 17-20/09/15, CEUR Workshop Proceedings, 1498:38-43.
- [44] Leontopoulos, S.V., Kokkora, M.I., Petrotos, K.B., 2016. *In vivo* evaluation of liquid polyphenols obtained from OMWW as natural bio-chemicals against several fungal pathogens on tomato plants. Desalination and Water Treatment 1-15.
- [45] Li, B., Xie, G.-L., Soad, A., Coosemans, J., 2005. Suppression of *Meloidogyne javanica* by antagonistic and plant growth-promoting rhizobacteria. Journal of Zhejiang University Science, 6 (6): 496-501.
- [46] Lugtenberg, B.J.J., Kravchenko, L.V., Simons, M., 1999. Tomato seed and root exudate sugars: composition, utilisation by *Pseudomonas* biocontrol strains and role in rhizosphere colonisation. Environmental Microbiology, 1: 439-446.
- [47] Molina, L., Ramos, C., Duque, E., Ronchel, M.C., Garcia, J.M., Wyke, L., Ramos, J.L., 2000. Survival of *Pseudomonas putida* KT2440 in soil and in the rhizosphere of plants under greenhouse and environmental conditions. Soil Biology and Biochemistry, 32: 315-321.
- [48] Nile, S.H., Nile, A.S., Keum, Y.S., Baskar, V., S., Ramalingam, 2017. *In vitro* and *in planta* nematocidal activity of black pepper (*Piper nigrum* L.) leaf extracts. Crop Protection, 100: 1-7.
- [49] Oostendorp, M., Sikora, R.A., 1990. *In-vitro* interrelationship between rhizosphere bacteria and *Heterodera schachtii*. Revue de Nematologie, 13: 269-274.
- [50] Rezzonico, F., Rupp, O., Fahrentrapp, J. 2017. Pathogen recognition in compatible plant-microbe interactions. Scientific Reports, 7(1): 6383
- [51] Rodriguez-Kabana, R., Morgan-Jones, G., 1988. Potential for nematode control by microfloras endemic in the tropics. Journal of Nematology, 20: 191-203.

- [52] Samaliev, H.Y., Andreoglou, F.I., Elawad, S.A., Hague, N.G.M. Gowen, S.R., 2000. The nematocidal effects of the bacteria *Pseudomonas oryzihabitans* and *Xenorhabdus nematophilus* on the root-knot nematode *Meloidogyne javanica*. *Nematology*, 2(5): 507-514.
- [53] Sawhney, R., Webster, J.M., 1975. The role of plant growth hormones in determining the resistance of tomato plants to the root-knot nematodes, *Meloidogyne incognita*. *Nematologica*, 21: 95-103.
- [54] Sayre, R.M., Starr, M.P., 1988. Bacterial diseases and antagonisms of nematodes. In: *Diseases of Nematodes vol 1*. pp.69-101. Poinar, G.O. and Jansson, H.B. (Eds). CRC Press, Boca Raton.
- [55] Skenderidis, P., Mitsagga, C., Giavasis, I., Hadjichristodoulou, C., Leontopoulos, S., Petrotos, K., Tsakalof, A., 2017. Assessment of antimicrobial properties of water and methanol UAE extracts of goji berry fruit and pomegranate fruit peels in vitro. 3rd I.C., FaBE 2017, Rhodes Island 01-04/06-17. FaBE Proceedings: 541-549.
- [56] Soby, S., Bergman, K., 1983. Motility and chemotaxis of *Rhizobium meliloti* in soil. *Applied Environmental Microbiology*, 46: 995-998.
- [57] Southey, J.F., 1986. In: *Laboratory methods for work with plant and soil nematodes*. pp 74. Ministry of Agriculture, Fisheries and Food.
- [58] Stevens, M.A., Rick, C.M., 1986. Genetics and breeding. In: *The Tomato Crop: A Scientific Basis of Improvement*. pp. 35-109. Atherton, J.G and Rudich, J. (Eds.). Chapman and Hall, New York.
- [59] Stirling, G.R., 1991. In: *Biological Control of Plant Parasitic Nematodes, progress, problems and prospects*. pp.22-49. CAB International, Wallingford, UK.
- [60] Thakur, S., Walia, R.K., 2016. Potential of bacterial parasite, *Pasteuria penetrans* application as nursery soil treatment and seed treatment in controlling *Meloidogyne graminicola* infecting rice. *Indian Journal of Nematology*, 46(1): 16-19.
- [61] Timper, P., Liu, C., Davis, R.F., Wu, T., 2016. Influence of crop production practices on *Pasteuria penetrans* and suppression of *Meloidogyne incognita*. *Biological Control*, 99: 64-71.
- [62] Tzean, S.S., Estey, R.H., 1981. Species of *Phytophthora* and *Pythium* as nematode destroying fungi. *Journal of Nematology*, 13: 160-163.
- [63] Tzortzakakis, E.A., Gowen, S.R., 1994. Evaluation of *Pasteuria penetrans* alone and in combination with oxamyl, plant resistance and solarization for control of *Meloidogyne* spp. on vegetables grown in greenhouses in Crete. *Crop Protection* 13: 455-461.
- [64] Tzortzakakis, E.A., Trudgill, D.L., 1996. A thermal time based method for determining the fecundity of *Meloidogyne javanica* in relation to modeling its population dynamics. *Nematologica*, 42: 347-353.
- [65] Tzortzakakis, E.A., Channer, A.G., Gowen, S.R., Ahmed, R., 1997. Studies on the potential use of *Pasteuria penetrans* as a biocontrol agent of root-knot nematodes (*Meloidogyne* spp.) *Plant Pathology*, 46: 44-55.
- [66] Vagelas, I.K., Andreoglou, F.I. Peters, J.C., Gravanis, F.T., Gowen, S.R., 2000. Testing the efficacy of microorganisms for antagonism to *Fusarium oxysporum*. *Brighton Crop Protection Conference-Pest and Diseases*, 3: 1049-1056.

- [67] Vagelas, I.K., Leontopoulos, S.V., Gravanis, F.T., 2007. *Pasteuria penetrans* as a commercial bio-nematicide. The XVI International Plant Protection Congress. Congress Proceedings 2: 456-457.
- [68] Vagelas, I. K., Pembroke, B., Gowen, S.R., Davies, K.G., 2007. The control of root-knot nematodes (*Meloidogyne* spp.) by *Pseudomonas oryzihabitans* and its immunological detection on tomato roots. *Nematology*, 9(3): 363-370.
- [69] Vagelas, I., Pembroke, B., Gowen, S.R., 2011a. Fitting discrete distributions to *Pasteuria penetrans* spore attachment data. *Pakistan Journal of Phytopathology*, 23(2): 88-91.
- [70] Vagelas, I., Pembroke, B., Gowen, S.R., 2011b. Modeling movements of root-knot nematodes *Meloidogyne* spp. juveniles when encumbered with spores of *Pasteuria penetrans*. HAICTA 2011.
- [71] Vagelas, I., Gowen, S.R., 2012. Control of *Fusarium oxysporum* and root-knot nematodes (*Meloidogyne* spp.) with *Pseudomonas oryzihabitans*. *Pakistan Journal of Phytopathology*, 24(1): 32-38.
- [72] Vagelas, I.K., Dennett, M.D., Pembroke, B., Gowen, S.R., 2012a. Adhering *Pasteuria penetrans* endospores affect movements of root knot nematode juveniles. *Phytopathologia Mediterranea*, 51(3): 618-624.
- [73] Vagelas, I.K., Leontopoulos, S.V., Pembroke, B., Gowen, S.R., 2012b. Poisson and Negative Binomial Modeling Techniques for Better Understanding *Pasteuria penetrans* Spore Attachment on Root-Knot Nematode Juveniles. *Journal of Agricultural Science and Technology USA*, 2 (2A): 273-277.
- [74] Vagelas, I., Leontopoulos, S., 2015. Cross-protection of cotton against *Verticillium* wilt by *Verticillium nigrescens*. *Emirates Journal of Food and Agriculture*, 27(9): 687-691.
- [75] Vancura, V., and Hanzlicova, A. (1972). Root exudates of plants IV. Difference in chemical composition of seed and seedlings exudates. *Plant Soil*, 36: 271-282.
- [76] Viglierchio, D.R., 1961. Attraction of parasitic nematodes by plant root emanations. *Phytopathology*, 51: 136-142.
- [77] Weller, D.M., 1985. Application of fluorescent pseudomonads to control root diseases. In: *Ecology and Management of Soilborne Plant Pathogens*. pp.137-140. Parker, C.A., Rovira, A.D., Moore, K.J. Wong, P.T.W. and Kollimorgen, J.F. (Eds.). American Phytopathological Society, St. Paul, MN.
- [78] Weller, D.M., 1988. Biological control of soil borne plant pathogens in the rhizosphere with bacteria. *Annual Review of Phytopathology*, 26: 379-407.
- [79] White, G.F., 1927. A method for obtaining infective juveniles from cultures. *Science*, 66: 302-303.
- [80] Yawson, D.O., Adu, M.O., Vanderpuije, G., Arthur, W.S., Aggrey, K.T., Boateng, E., 2017. Spatial distribution of nematodes at organic and conventional crop fields in Cape Coast, Ghana. *West African Journal of Applied Ecology*, 25(1): 57-67.
- [81] Zhao, X., Schmitt, M., Hawes, M.C., 2000. Species-dependent effects of border cell and root tip exudates on nematode behavior. *Phytopathology*, 90: 1239-1245.



Vol5 (1)

**International Journal of Foods and
Biosystems Engineering**

ISSN: 2408-0675